International Scientific-Technical and Production Journal

The Paton WELDING JOURNAL

November 2009 # 11

English translation of the monthly «Avtomaticheskaya Svarka» (Automatic Welding) journal published in Russian since 1948

Founders: *E.O. Paton Electric Welding Institute of the NAS of Ukraine*
International Association «Welding»

Publisher: *International Association «Welding»*

Address:
E.O. Paton Electric Welding Institute,
International Association «Welding»,
11, Bozhenko str., 03680, Kyiv, Ukraine
Tel.: (38044) 287 67 57
Fax: (38044) 528 04 86
E-mail: journal@paton.kiev.ua
http://www.nas.gov.ua/pwj

State Registration Certificate
KV 4790 of 09.01.2001

Subscriptions:
$324, 12 issues per year,
postage and packaging included.
Back issues available.

CONTENTS

Dear Readers 2
50 years of explosion welding 3

SCIENTIFIC AND TECHNICAL

Lysak V.I. and *Kuzmin S.V.* Development of concepts of the lower boundary of explosion welding of metals 6
Bondar M.P. Influence of deformation mechanism in the collision zone of material pairs on selection of optimum parameters of explosion welding 12
Dobrushin L.D., Fadeenko Yu.I., Illarionov S.Yu. and *Shlensky P.S.* Channel effect in explosion welding 16
Pervukhina O.L., Pervukhin L.B., Berdychenko A.A., Dobrushin L.D., Petushkov V.G. and *Fadeenko Yu.I.* Features of explosion welding of titanium to steel in a shielding atmosphere 18
Silchenko T.Sh., Kuzmin S.V., Lysak V.I. and *Dolgy Yu.G.* Peculiarities of instability of the process of explosion cladding of large-size billets 22
Smirnov G.V., Shuganov A.D., Stefanovich R.V., Yadevich A.I., Petrov I.V., Kamorny A.A., Konoplyanik V.A., Luchenok A.R., Toloshny A.A., Bogdanovich P.T. and *Dzichkovsky O.A.* Modelling and application of high-velocity explosion welding processes 28
Besshaposhnikov Yu.P., Kozhevnikov V.E., Chernukhin V.I. and *Paj V.V.* On the influence of shock wave on welding gap increase in production of large-sized sheet composites by explosion welding 36
Bondarenko S.Yu., Rikhter D.V., Pervukhina O.L. and *Pervukhin L.B.* Determination of the parameters of shock-compressed gas in the welding gap ahead of the contact point in explosion cladding 39

INDUSTRIAL

Banker J.G. Industrial applications of explosion clad (Review) 42
Lobanov L.M., Dobrushin L.D., Bryzgalin A.G., Illarionov S.Yu., Shlensky P.S., Volgin L.A., Lashkevich V.G. and *Grabar E.V.* Widening of technological capabilities of explosion treatment for reducing residual stresses in welded joints on up to 5000 m^3 decomposers 46
Carton E. and *Stuivinga M.* Explosive cladding for ITER components 49
Groeneveld H.D. Photogrammetry applications for explosive forming 52
Illarionov S.Yu., Dobrushin L.D. and *Fadeenko Yu.I.* New technology for production of joints on high-strength aluminium alloys by explosion welding 57
Silvestrov V.V., Plastinin A.V. and *Rafejchik S.I.* Application of emulsion explosives for explosion welding 61
Bogunov A.Z. and *Kuzovnikov A.A.* Production of aluminum–steel bimetal with profiled interface 65
Meshcheryakov Yu.P., Ogolikhin V.M. and *Yakovlev I.V.* Possibility of preservation of shape and size of cylindrical tubular billets of moulds in explosion cladding 68
Trykov Yu.P., Gurevich L.M. and *Shmorgun V.G.* Integrated technologies of producing multipurpose layered composite materials 71
List of main monographs on explosion welding 76

INFORMATION

Moscow Regional Shared Use Explosion Center of the Russian Academy of Sciences (SUEC) 77

Dear Readers!

This issue of «The Paton Welding Journal» offered to your attention is devoted to 50 years since the USA and USSR practically simultaneously launched systematic studies of the process of metal joining at a high-velocity collision.

By the mid of the 1960s, this welding method had already been used for mass production of bimetals and fabrication of critical metal structures.

The works on explosion welding were started at the E.O. Paton Electric Welding Institute in 1962. They gained particular development in the 1970s, when a specialized section was established, fitted with a shop for manufacture of charges of explosive materials and products, as well as sites for explosion welding operations. Later on this section transformed into the currently active Research and Engineering Center «Explosion Treatment of Materials». The explosion chamber of an original tubular structure with a 200 kg explosive capacity was built in 1973–1974. Since then, associates of the Scientific and Technical Complex «E.O. Paton Electric Welding Institute» have completed a significant work on investigation of the explosion welding process, development of the corresponding technologies and their application in the national economy. Noteworthy are such achievements as connection of branch pipes to pressurized gas pipelines by explosion welding, repair of a fuel tank of the «Buran–Energiya» rocket-space system, development of a welding method combined with simultaneous stamping, as well as a range of technologies for welding of adapters from dissimilar metals for high-current circuits used in electrometallurgy, electrical industry and in railway transport.

Along with explosion welding, other types of explosion treatment of materials were also studied. The Research and Engineering Center «Explosion Treatment of Materials» possesses the priority solutions for problems of explosion cutting of metals using elongated cumulative charges and explosion treatment of welded metal structures to reduce residual welding stresses.

Investigations of explosion welding and its practical application have gained acceptance in many developed countries. At the same time, the fundamental research efforts are concentrated mainly at the research centers of the CIS countries. Worthy of notice in this respect are achievements of the Volgograd school of explosion welding. The Volgograd State Technical University has a chair, which has been successfully functioning since 1962 and is the only chair in the CIS countries that trains engineers with the «Explosion Welding» specialization. This made it possible to provide the CIS countries with specialists, from whom a range of famous researchers and designers grew.

Up to now, the explosion welding has become one of the classic methods for producing permanent joints of metals, in particular, of dissimilar hard-to-weld combinations. The life confirmed that this unique process has not been exhausted as yet, and still has a great potential for development. A mass flow of the publications, mainly from the CIS countries, is indicative of emergence of the new research areas and widening of the field of technological application of explosion welding.

Much has been done, but much more is to be done.

Prof. B.E. Paton

50 YEARS OF EXPLOSION WELDING

The dynamic development and progress of many branches of industry (and in particular those science intensive ones as rocket-space, nuclear power engineering and other) are directly connected with development of new materials, combining high technical and service properties with a good manufacturability and low cost of production. Therefore, the problems of development of new challenging materials always related to the main scientific-technical priorities of industrialized countries. The composite materials and technologies of their producing are one of the most science intensive and promising directions of materials science with the prospect of effective application in practical purposes.

In general structure of modern production of structural materials the composites occupy still extremely poor position. Today the world production of composite materials of all kinds does not exceed 3 % and some decades ago their production was absent at all. However, with their application the mankind managed to solve many of the most difficult technical tasks, to create original machinery.

The explosion welding, celebrating its 50 years by the welding community, is one, due to its peculiarities, of the most effective and the only possible way in number of cases to develop high-quality bimetal and multi-layer composite materials. Outwardly simple, and in its physical sense very complicated, affecting many fundamental parts of sciences of materials, gas and hydrodynamics, strength physics and other, the process of explosion welding is very transient and peculiar and at first sight hardly similar to other methods of metal joining.

The high-velocity collision of bodies in explosion welding is accompanied by a number of noticeable effects: wave-formation phenomena, cumulation and bodies adhesion. In the collision area the intensive narrow-localised plastic deformations take place usually in the form of waves fixed on the interface of metals. The joining of bodies usually occurs without melting of metal, diffusion processes, and produced joints are characterized by exclusively high strength, even in welding of metals incompatible from the metallurgical point of view. Owing to the explosion welding it became possible for the first time to produce full strength joints of titanium with steel, zirconium with steel and other composites on practically unlimited areas.

Under the term «explosion welding» it is accepted to imply the phenomena of a sound joint of surfaces of metallic bodies, collided at some angle, at least one of which is accelerated up to the velocities of 150–1000 m/s by the detonation products of explosives. Here it is necessary to note that the explosion itself and namely the energy of expanding detonation products plays in the given process only the secondary role providing the acceleratory movement of the bodies relatively to each other and their collision.

Physical nature of sources of such acceleration of bodies can be very different: electromagnetic field (in magnetic-pulse welding), the energy of powder charge in gun barrel, the explosion energy of electric conductor at current passing through it and even shot energy of installation gun can provide spot welding. But in all cases the principle of processes and phenomena proceeding at high-velocity collision in solid bodies remains unchanged.

The history of discovery of explosion welding is interesting and instructive. The adhesion of bodies at their collision at high velocities was observed a long time ago. Already in the years of the World War I there were evidences of «sticking» of shells

to the metallic barriers. One of the first works, known to the scientific community, describing the phenomena of welding of two brass discs under the influence of detonation products, was a work of L.R. Carl[1] *published in the USA in 1944. In 1944–1946 in the USSR during studying a cumulative effect by the group of researchers headed by Prof. M.A. Lavrentiev the monolithic joint of two metallic cones co-axially assembled and cogged by the external charge was produced. On the surface of the joint the waves were observed, which are characteristic of the explosion welding. Unfortunately these works did not receive their further development by that time by different reasons. Moreover the industry of that period was not prepared to use unique possibilities of new welding method, i.e. producing of bimetallic and multi-layer composite materials.*

The second «birth» of explosion welding, for the moment not occasional, coincided with the intensive development of the new branches of industry, first of all, space, nuclear power engineering, chemical, which urgently needed high-quality bimetal and multi-layer materials combining high specific strength, manufacturability and sufficiently low cost. In 1958–1959 the reports on explosion welding were practically simultaneously made by J. Pearson[2] *and V. Philipchuk et al.*[3] *V. Philipchuk stated that he observed a partial welding of sheets to metallic matrix at explosion stamping already in 1957. However the welding scheme he offered and patented*[4] *using explosive charge blasting, immersed into the vessel with water fixed above the plates to be welded, appeared to be useless in practice. Nearly at the same time the research works on explosion welding began in the concern «Dupon de Nemur» (USA)*[5]*, and later, in 1961 at the Stanford Research Institute (USA)*[6]*.*

The works on explosion welding in the USSR began in 1961 at the Institute of Hydrodynamics of SD of AS USSR (Novosibirsk). The group of researchers in the membership of V.S. Sedykh, A.A. Deribas, E.I. Bichenkov, Yu.A. Trishin headed by the Prof. M.A. Lavrentiev, conducted the first experiments and was successful in producing quality welded joints[7]*. In the article the authors expressed assumptions about the possible nature of joint formation. V.S. Sedykh and also Prof. P.O. Pashkov working already since 1962 at the Volgograd Polytechnic Institute (now Volgograd State Technical University) laid grounds of scientific school on metal treatment using explosion. The wide research of new and challenging technological process began. Later the study of explosion welding continued and was actively developed by scientific groups of the E.O. Paton Electric Welding Institute (headed by Corr. Member of AS of Ukraine V.M. Kudinov), Belarussian Polytechnic Institute (headed by Prof. V.I. Belyaev), Altai Research Institutre of Engineering Technology (headed by Prof. B.D. Tsemakhovich), Moscow Institute of Steel and Alloys (Technical University), FUSE «Research Institute of Structural Materials «Prometej» and a number of other enterprises and organizations of the USSR and CIS countries.*

In the first scientific publications one could encounter the statements about the exclusiveness and even uniqueness of the new method of metal joining which does not fit to the famous welding methods according to the existent classification due to its outward exoticism. However, numerous research works of a big group of scientists and specialists of different world scientific centers proved that the process of explosion welding is not a kind of specific welding method, but relates to solid-phase, diffusion-free pressure welding method, in a coarse simplification to forging, related to welding, the most ancient method of metal joining. The differences consist in the values of pressure and

[1]Carl, L.R. (1944) Brass welds made by detonation impulse. *Metal Progress*, 46(**1**), 102, 103.
[2]Pearson, J. (1959) Recent advances in explosive pressing and welding. In: *Proc. of 2nd Metals Eng. Conf. of Explosive.* Chicago: ASM, 32–36.
[3](1959) Explosive welding is on the way. *Steel*, 145(**18**), 90–91.
[4]Philipchuk, V. et al. *Explosive welding*. Pat. 3024526 USA, Cl. 29-470. Publ. 1960.
[5]Cowan, G., Douglas, J., Holtzman, A. *Explosive bonding*. Pat. 3137937 USA, Cl. 29-486. Publ. 1960.
[6]Davenport, D.E., Duvall, G. (1961) *Creative manufacturing seminar*: Paper SP 60-161.
[7]Sedykh, V.S., Deribas, A.A., Bichenkov, E.I. et al. (1962) Explosion welding. *Svarochn. Proizvodstvo*, **2**, 6–9.

rates of proceeding of deformation processes in the zone of metals contact and, consequently, in the mechanisms of their realization.

50 years ago the humanity, it might be the first time in its history, saw explosion not as all-destroying power, but as a power source capable to create, i.e. to join metals and alloys, which cannot be joined using other welding methods, thus developing the composite materials.

Today the explosion welding, inherently supplementing other welding methods, allows the development of high-quality metallic composite materials of a wide nomenclature, dimension type and configuration. The methods of structural explosion welding are also improved providing the possibility of manufacturing of ready parts and structural elements of ever more complicated shapes. Using this process engineers and technologists can solve the most difficult technical problems of advanced engineering, metallurgy, power engineering, transport, rocket-space complex and many other industry branches.

In this issue of Journal the authors of the famous scientific schools tried to generalize accumulated experimental and theoretical material on fundamentals of the process of metal joining at their high-velocity collision, approaches and experimental data on the problems of welding and explosion metal treatment.

Prof. V.I. Lysak, Volgograd STU, Russia
Prof. L.D. Dobrushin, PWI, Ukraine

DEVELOPMENT OF CONCEPTS OF THE LOWER BOUNDARY OF EXPLOSION WELDING OF METALS

V.I. LYSAK and **S.V. KUZMIN**
Volgograd State Technical University, Volgograd, RF

The paper deals with subjects related to evolutionary development of concepts of the lower boundary of explosion welding of metals, interrelation of its position with parameters of high-velocity collision and mass characteristics of the colliding plates. Proceeding from analysis of the experimental and theoretical data accumulated so far, it is shown that the lower boundary can be presented in the space of «pressure–temperature–time» coordinates, which is not contradictory to the current concepts of the lower boundary of explosion welding.

Keywords: *explosion welding, plastic deformation, welded joint, welding boundary*

In explosion welding the joint forms as a result of deformation impact on the materials being joined, characterized by a high velocity of their collision at a short time of contact interaction. Numerous theoretical and experimental investigations of this process are indicative of the fact that it harmoniously fits into the line of solid-phase processes of metal joining, which proceed under the conditions of thermal-force impact by a common pattern of three-stage topochemical reaction with formation of physical contact at crushing of surface microroughnesses, activation of contact surfaces, realized mainly by the dislocation channel, and bulk interaction with coalescence of discrete interaction sites and stress relaxation. Such an interpretation of the nature of joint formation in the solid phase envisages, on the one hand, the discreteness of the process of formation of interaction sites (active centers), and on the other — collective nature of interaction of atoms in the field of these active centers. The process of adhesion — «bond stitching» — on the contact surfaces is assumed to be diffusionless [1–5], while the nature of joint formation is assumed to be the same, irrespective of the nature and intensity of the thermodeformational interaction. Differences consist in the kinetics of running of the individual stages of the process, which is determined by the temperature-velocity conditions of metal deformation, degree of localizing and deformation mechanisms.

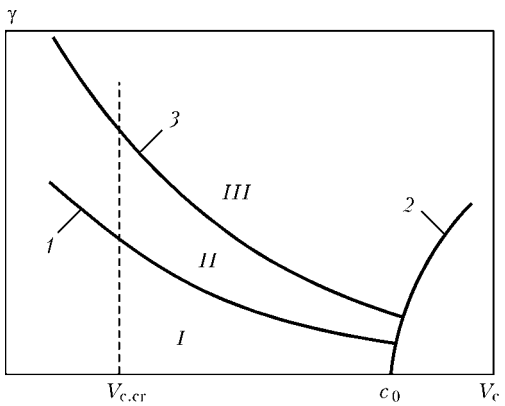

Figure 1. Characteristic regions and boundaries of explosion welding: *1, 3* — lower and upper boundary; *2* — supersonic boundary; *I* — region of «subcritical» modes (no welding); *II* — explosion welding region; *III* — region of «beyond-the-limit» modes

Similar to any other process of producing permanent pressure joints, the explosion welding process is characterized by a multitude of interrelated and interconnected distributed parameters [6, 7], the totality of which determines the deformational, temperature and time conditions of solid-phase joint formation. However, the approaches to evaluation of the role of these parameters in joint formation were different at different stages of investigations. Initially, proceeding from the fluid-dynamics concepts of explosion welding process, according to which the joint formation criteria are self-cleaning of the surface by the cumulative flow and wave formation, the main parameters of welding were angle of collision γ and velocity of contact point V_c.

R. Wittman [8] was the first to make an attempt, similar to cumulation studies [9, 10], to provide a theoretical description in γ–V_c coordinates of the characteristic regions and their boundaries (Figure 1), which were then precised several times in later works [11–21]. According to R. Wittman, welded joints can be produced in region *II*, limited by four lines. On the right it is limited by a curve, calculated from the critical conditions of structure jet [9, 10, 22]. To the right of boundary *2* there exist shock waves, associated with the contact point, but cumulation is absent. It is usually impossible to produce welded joints in this region. Position of curve *2* is determined by the dependence of critical angle of cumulative jet formation γ' on V_c, first established in [9, 10], where it is shown that the jet at supersonic collision modes can exist only, when γ' is exceeded.

On the left region *II* is limited by straight line $V_{c.cr}$, i.e. velocity, at which transition from the wavelike weld to a waveless one takes place, and which is calculated by the following formula from [8]:

$$V_{c.cr} = \left[\frac{2\mathrm{Re}(H V_1 + H V_2)}{\rho_1 + \rho_2}\right]^{1/2}, \quad (1)$$

where Re is the Reynolds number; HV_1, HV_2 is the Vickers hardness of the metals being welded; ρ_1, ρ_2 are the density of the metals being welded, respectively.

It is obvious that by a whole number of reasons this condition is beneath any serious criticism, as transition to waveless (equilvalent) weld at low contact velocities is determined not only by V_c, but also by angle of collision γ (or collision velocity V_{col}) [6, 23], and, on the other hand, the wave formation process is not at all obligatory for formation of a sound joint, so that this boundary is of no practical value.

From the top region *II* is limited by curve *3* (see Figure 1), the position of which is determined by the thermo-physical properties of the materials being welded, and can be calculated from the condition of melt solidification by the moment of rarefaction waves coming to the joint zone [8]:

$$V_{col\ max} = \frac{1}{N}\left(\frac{T_m c_0}{V_c}\right)^{1/2}\left(\frac{\lambda c c_0}{\rho_1 \delta_1}\right)^{1/4}, \quad (2)$$

where $N \approx 0.1$ is the coefficient; c_0 is the velocity of sound; λ is the heat conductivity; c is the heat content; $\rho_1\delta_1$ is the specific weight of the flyer plate.

Position of the lower boundary (see Figure 1, curve *1*) according to R. Wittman is determined by critical pressure of collision, providing plastic flow in the near-weld zone, and is calculated through the minimum collision velocity required for welding:

$$V_{col\ min} = \sqrt{\frac{\sigma_t}{\rho}} \quad \text{or} \quad \gamma_{cr} = \sqrt{\frac{\sigma_t}{\rho V_l^2}}. \quad (3)$$

Such a description and image in the coordinates characterizing mainly the «geometry» of plate collision in explosion welding, was pioneering work at the initial stage of studying this process, despite being based on purely «mechanistic» prerequisites of joint formation, thus forming the base and giving an impetus to concretization of process boundary position by other researchers, who suggested the respective dependencies correlating the critical value of the angle of collision γ_{cr} with Vickers hardness HV [12, 13], yield point σ_y [19, 20, 24], tensile strength σ_t [11], and deformation resistance S_k [18].

On the other hand, comparison of calculated data by these dependencies of positions of the lower welding boundary with experimental values showed a considerable discrepancy in a number of cases, which is noted, for instance in [12, 13]. Such a discrepancy is usually associated with ignored oxide films on the surfaces, their finish, etc., the role of which is, certainly, obvious. However, the common drawback of all the above models, which accounts for the discrepancy between the experimental and calculated data from the proposed dependencies, is the fact that much more «weighty» parameters were not included into them, and primarily mass characteristics of the colliding metals.

In their later work [25], the authors of [20], proceeding from the data of [26], made an attempt to determine the lower boundary, allowing for averaged mass $\tilde{m} = m_1 m_2/(m_1 + m_2)$ (here m_1 and m_2 are the unit masses, per a unit of surface area, of the flyer and fixed plates) and separating from the total energy consumed in plastic deformation of the near-contact layers of metal in explosion welding W_2 [27] the energy fraction localized in the zone of width equal to the range (two amplitudes) of waves formed in the joint $2a$:

$$V_{col.cr} = \sqrt{\frac{\sigma_{0.2}}{2\rho(1 - V_c^2/c_0^2)}}\left(1 + \sqrt{1 + \frac{4E_{st}}{\sigma_{0.2}\delta_1\delta_2/(\delta_1 + \delta_2)}}\right), \quad (4)$$

where $V_{col.cr}$ is the critical value (by analogy with the critical angle of collision, determined by the position of the lower welding boundary) of plate collision velocity; $E_{st} = 0.8 \cdot 2ac\rho T_m$ is the energy required in the opinion of the authors of [25] for joint formation; T_m is the melting temperature of metals being welded; δ_1, δ_2 are the thicknesses of the flyer and fixed plate, respectively.

Such an approach, unfortunately, is unjustified for quite a number of reasons. First, in explosion welding of absolute majority of dissimilar metals (Fe + Al; Ti + Al; Mg + Ti; Mg + Cu; Al + Cu, etc.) a sound joint is formed with a waveless boundary. Secondly, initial adhesion and welded joint formation even in welding of similar metals on the lower boundary proceeds under the conditions, when the wave formation process still does not yet exist [8, 13, 28]. More over, selection of the criterion proper, namely a zone of the width of two wave amplitudes, is not substantiated, either. It is obvious that the phenomenon of adhesion cannot be associated with the wave formation effect at high-velocity collision, as the latter just promotes intensification of plastic deformation, rather giving it, on the whole, an undesirable for welding periodical, essentially non-stationary nature with presence of eddy zones and partially melted regions.

A significant progress in this respect was promoted by establishing such fundamentally important factors as a considerable influence of averaged mass of layers, $\tilde{m}$, on the process of joint formation, existence of its critical $\tilde{m}_{cr}$ and limit $\tilde{m}_{lim}$ values (at specified V_{col}, V_c, γ), thus creating prerequisites for reconsidering the purely mechanistic interpretation of the critical conditions (boundaries) of welding, described only by fluid-dynamic phenomena in γ–V_c coordinates and a fundamental basis for formation of energy approach to the studied process. Concepts of the «process of formation of a metal jet from the point of contact as the necessary and sufficient physical process, determining the possibility of producing the joint» [13], are essentially identical to the concepts of the film

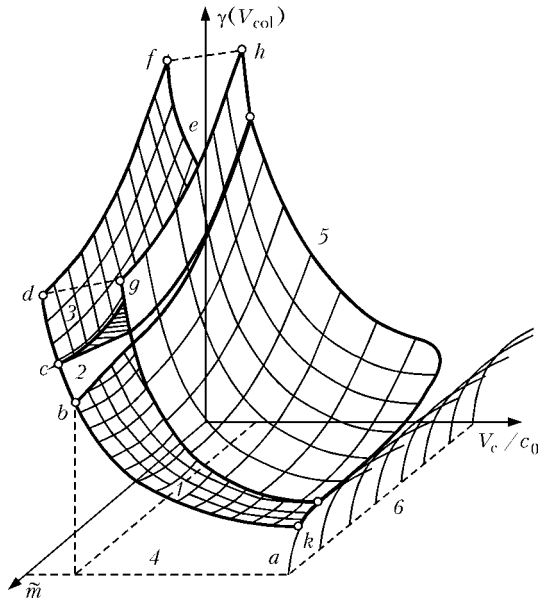

Figure 2. Position of the main characteristic regions of explosion welding of metals: *1, 2* — «traditional» and waveless modes, respectively; *3* — anomalous wave formation; *4* — subcritical modes; *5* — developed cumulation; *6* — supersonic modes

hypothesis, developed already in the 1950s by S.B. Ajnbinder with associates [29, 30] and proceeding from the fact that the thermodynamic probability of adhesion is due to reduction of the system free energy at disappearance of two free surfaces, thus eliminating the need for determination of thermodynamic permission of the process of interatomic bond formation.

Allowing for mass characteristics of the materials being welded, position of the main explosion welding regions can be transformed into parameter space (Figure 2). Such a transformation is of principal nature, as, first of all, according to [27], a certain value of energy W_2, consumed in plastic deformation of metal corresponds to any point of space in $\tilde{m}$–V_{col}–V_c coordinate system, and a quite concrete energy state of the system of colliding plates corresponds to characteristic surfaces given in Figure 2.

Secondly, establishing the interrelations of $\tilde{m}$ with the position of critical boundaries of the process served

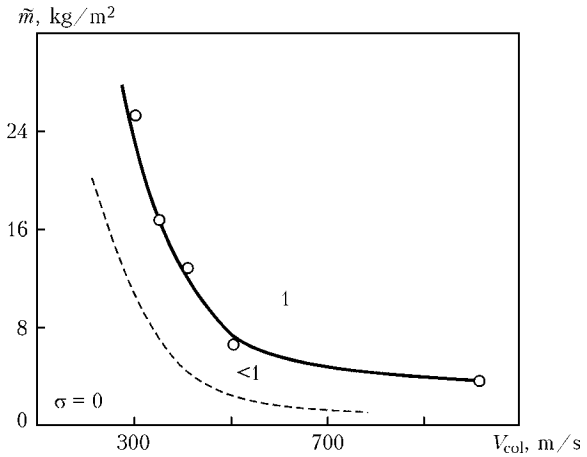

Figure 3. Position of the lower boundary of welding 12Kh18N10T steel to St3 steel depending on averaged mass $\tilde{m}$ of welded plates (dashed curve — adhesion boundary, marked conditionally)

as a real foundation for merging of the standpoints of the so-called metallophysical and fluid-dynamic scientific schools of researchers of this complex process, as addition of the mass axis to plane γ–V_c, describing the «external» fluid-dynamic phenomena at glancing collisions enables energy, «inner» interpretation of the process of metal adhesion without rejection of the current concepts.

Approach to description of the process of adhesion and formation of the welded joint in terms of energy organically follows out of the theory of solid-phase topochemical reactions [1–4], according to which running of the latter requires bringing the atoms on the metal interface into an activated state, imparting a certain amount of energy to them in explosion welding by localized and intensive plastic deformation.

The parameter space, in which welded joints can be produced, is schematically shown in Figure 2 by a closed figure, cut in its front part by a plane normal to axis $\tilde{m}$ and limited from the top and below by two surfaces *adf* (lower boundary) and *kgh* (upper boundary), located between which are three characteristic regions, differing in the phenomenology of plastic flow and the corresponding profile of residual deformations of metal in the near-weld zone. Joints of metals with close mechanical properties produced in the region of traditional welding modes (Figure 2, region *1*) feature a high strength and sinusoidal profile of the boundary line. In region *2* the plastic flow conditions are unfavourable for development of wave formation as a result of equality of the angle of collision and angle between the vector of velocity of deformation hump and plate surface [23], thus leading to production of a rectilinear interface at a high strength of layer adhesion. Welded joints with anomalous waves existing in region *3* also have high strength properties.

Located to the right of the welding region is region *6* studied in detail in works [9, 10, 12], in which shock waves associated with the point of contact are in place, and welded joints usually cannot be produced. The region of large collision angles (region *5*) corresponds to the modes of developed cumulation, and similar to region *6*, it does not have any practical importance for welding technologies.

Coming closer to surface *adf* from below (at constant mass characteristics of the welded system) energy W_2 [27] increases in proportion to V_{col}^2, leading to involvement of large volumes of metal adjacent to the contacting layer interface into plastic deformation, and when a certain critical level of energy consumption constant for each pair of materials being welded, has been reached [6, 7, 31], the joint becomes equivalent in terms of strength.

Position of the lower welding boundary, as seen from Figure 2, essentially depends on mass characteristics of the system being welded (averaged mass $\tilde{m}$) and shifts towards smaller values of dynamic angle γ or collision velocity V_{col} at $\tilde{m}$ increase (Figure 3).

Thus, in keeping with the existing energy concepts, a strong joint forms at exceeding a certain critical

level of energy consumption, depending, primarily, on the velocity of collision of the plates being welded and their mass (or thickness). However, the main parameter of energy group W_2 — energy or work consumed in plastic deformation of metal in the near-weld zone, — even though it is formally related to the conditions of collision and mass characteristics (i.e. thicknesses) of the elements being welded, describes the final result of their high-velocity interaction only in the generalized form, without disclosing the interrelations between other physical parameters of the process, namely pressure, its action time and temperature in the joint zone.

In [6, 32] a new parameter was proposed for correlation of pressure and time, namely deforming pressure pulse I_d, described in the general case by the following equation

$$I_d = \int_0^{\tau_0} p(\tau)d\tau = \int_0^{\tau_w} p_{max} e^{-\tau/\theta} d\tau, \quad (5)$$

where p_{max} is the peak pressure in the point of contact of the plates being welded; τ_w is the time of running of plastic deformations behind the contact point (or welding time); θ is the time constant characterizing the rate of pressure drop in the joint zone (for aluminium and steel St3, θ is approximately 0.565 and 0.96 μs, respectively).

Integral parameter I_d essentially determines the energy conditions of joint formation. So, pressure p acting on the near-contact layers of the joint for a certain time, performs certain work on plastic deformation of metal in them. The higher the pressure level and longer its impact, the greater is the fraction of kinetic energy of flyer element W consumed for plastic deformation of near-weld zone metal W_2, eventually determining the system energy balance.

Thus, deforming pressure pulse I_d is a certain «bridge» to «microlevel» parameters [33], linking the changing in time pressure in the joint zone (peak value of which is determined by collision velocity of elements being welded) and time of its action with process kinematics and energy, on the one hand, and degree of plastic deformation, completeness of running of activation processes in the contact zone and eventually, strength of layer bonding, on the other.

Generalization of a large number of experimental data allowed determination (by analogy with critical energy consumption [31]) of a certain critical value of the deforming pressure pulse, below which it is not possible to produce an equivalent joint. In the generalized form the established regularity, linking the strength of St3 + St3 welded joint with I_d value is given in Figure 4. Experimental points recalculated from the data of a number of other researchers are plotted in the same coordinate plane. It is seen that increase of welded joint strength starts approximately from 0.9–1.0 kN·s/m^2, whereas the above composition becomes equivalent in strength starting, approximately, from 3.5–3.7 kN·s/m^2, thus allowing in the first approximation this value to be regarded as critical value of the deforming pressure pulse $I_{d.cr}$ for a given pair of materials.

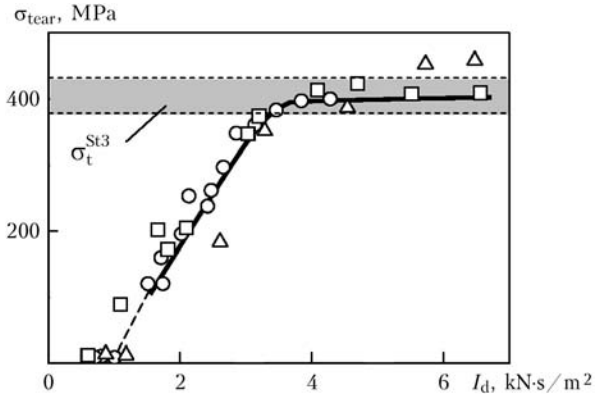

Figure 4. Influence of deforming pressure pulse I_d on strength σ_{tear} of low-carbon steel bimetal: ❐, Δ — data of A.N. Kriventsov [33, 34], V.G. Shmorgun [35], V.A. Pronin [36]; ❍ — of authors' data

In the general case deforming pulse value can be adjusted either by varying the thicknesses of the plates being welded, thus changing the duration of pressure impact in the joint zone, or by changing the peak pressure in the joint zone through collision rate V_{col}. When solving the practical tasks of explosion welding of specific compositions, when welded element thicknesses, as a rule, are strictly limited, the second path remains the only acceptable one. Nonetheless, from a purely hypothetical viewpoint, the lower boundary of explosion welding in «pressure p – time τ» coordinates can be presented by a hyperbolic dependence, shown in Figure 5. Here the axes of pressure and time are equivalent to a certain extent to the respective axes $\gamma(V_{col})$ and $\tilde{m}$ of the earlier plotted welding region (see Figure 2).

Third coordinate axis V_c (see Figure 2) can be compared with another important physical parameter of the process, namely metal temperature T in the joint zone, which, according to the theory of topochemical reactions, promotes joint formation in the solid phase, increasing, on the one hand, the frequency of dislocation exit into the joint zone (frequency of active center formation), and on the other hand — reducing the activation time, i.e. time during which

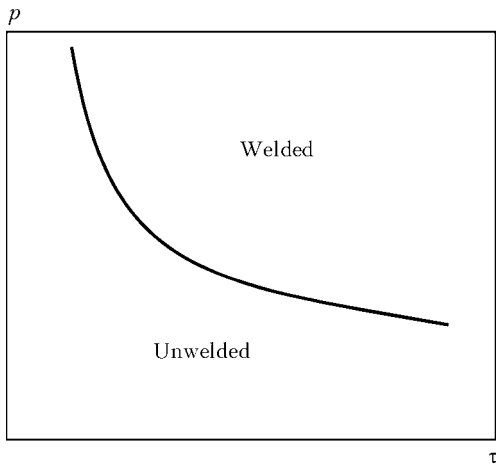

Figure 5. Hypothetical concept of lower welding boundary in «pressure p – time τ» coordinates

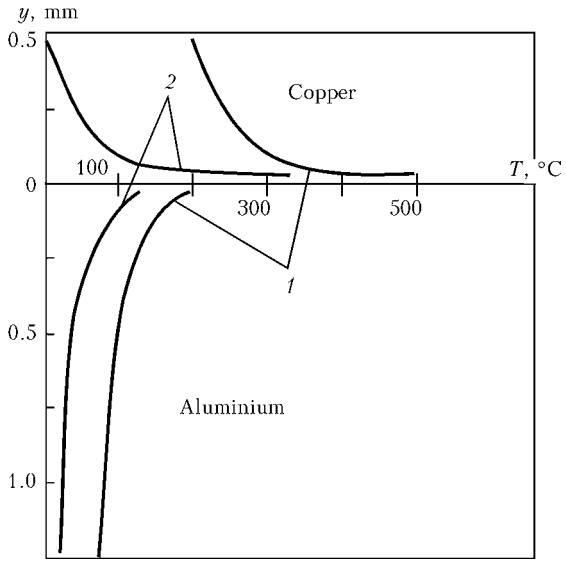

Figure 6. Temperature distribution in the section of explosion welded copper-aluminium composite: *1* — V_c = 2600; *2* — 2000 m/s

metal adhesion occurs within the active centers up to their natural relaxation.

Initial thermal situation in the joint zone in explosion welding is closely connected with the distribution of maximum shear plastic deformation across the welded element section [6, 37]. Here, in some arbitrary elementary metal layer of thickness dy, located at distance y from the joint line, the evolved heat is proportional to elementary work of deformation

$$\delta A_d = S_k g_{max}(y) dy, \qquad (6)$$

where S_k is the deformation resistance numerically equal to dynamic yield point σ_y^d; $g_{max}(y)$ is the current value of maximum shear plastic deformation.

Total specific (per a unit of welded sample area) work of deformation (or, which is the same, energy consumed in plastic deformation of near-weld zone metal) can be calculated by integration

$$A_d = S_k \int_0^{\delta} g_{max}(y) dy. \qquad (7)$$

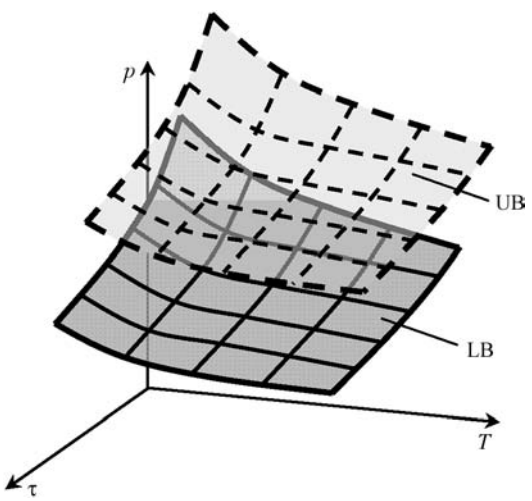

Figure 7. Region of explosion welding in «p–τ» coordinates (LB and UB are the lower and upper welding boundaries, respectively)

Assuming that heat evolves simultaneously in all the layers, it is easy to assess the thermal situation in the near-weld zone of the welded joint, i.e. calculate the initial temperature fields. For random layer y its temperature at the initial moment of time t = 0 allowing for expression (6) is equal to

$$T(y) = \frac{S_k g_{max}(y) dy}{c\rho dy} + T_0 = \frac{S_k g_{max}(y)}{c\rho} + T_0. \qquad (8)$$

Now, knowing the law of $g_{max}(y)$ variation across the plate thickness, the initial temperature fields can be plotted for an arbitrary section (Figure 6).

It should be noted that with increase of contact point velocity V_c temperature of near-contact layers of materials being welded rises considerably (in the limit case, when approaching the near-sonic speeds, their surface melting occurs in the joint zone, and a continuous interlayer of surface-melted metal is found in the joint), which according to the main principles of the theory of topochemical reactions «facilitates» the adhesion process, and the required levels of time-force factors of the joint formation can be lowered.

Thus, taking into account all the above considerations, we can move over to presentation of the lower boundary of explosion welding of metal in «pressure p–temperature T–time τ» coordinates (Figure 7), the outlines of which are not contradictory to the current concepts and positions of the welding boundaries plotted earlier.

It appears to be quite interesting to compare the location of parameter regions characteristic for different welding processes in the same coordinates (Figure 8). Explosion welding (similar to magnetic-pulse) welding with its characteristic quite short times of the joint formation and extremely high pressures takes up the upper corner of the coordinate domain.

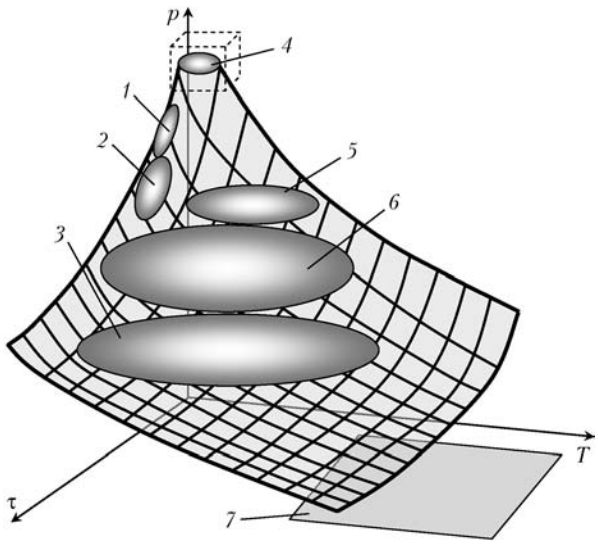

Figure 8. Parameter regions with various welding processes in «p–T–τ» coordinates (dash square is the region shown in Figure 7): *1* — cold welding (p, MPa; τ, ms; $T \sim 0.2T_m$); *2* — cold roll welding (p, MPa; τ, ms; $T \sim 0.2T_m$); *3* — diffusion welding (p, kPa; τ, s; $T \sim 0.9T_m$); *4* — explosion welding, magnetic pulse welding (p, GPa; τ, μs; $T \sim 0.6T_m$); *5* — roll welding (p, MPa; τ, ms; $T \sim 0.7T_m$); *6* — resistance welding (p, MPa; τ, μs; $T \sim 0.8T_m$); *7* — fusion welding (p, Pa; τ, s; $T > T_m$)

Other processes are located much lower. This is another proof of the fact that explosion welding is not some «exotic» isolated process of metal joining, but logically fits into the range of the known processes, organically complementing them.

The work was performed within the framework of Government Contract 02.523.12.3012.

1. Karakozov, E.S. (1976) *Solid phase bonding of metals*. Moscow: Metallurgiya.
2. Krasulin, Yu.L. (1971) *Interaction of metal with semiconductor in solid phase*. Moscow: Nauka.
3. Krasulin, Yu.L. (1967) Dislocations as the active centers in topochemical reactions. *Teoret. i Experim. Khimiya*, **III**, Issue 1, 58–65.
4. Krasulin, Yu.L., Shorshorov, M.Kh. (1967) About mechanism of dissimilar material joint formation in the solid state. *Fizika i Khimiya Obrab. Materialov*, **1**, 89–97.
5. Shorshorov, M.Kh., Karakozov, E.S., Fomenko, V.A. (1972) Specific methods of welding. In: *Results of science and technology*, Series Welding. Moscow: VINITI.
6. Lysak, V.I., Kuzmin, S.V. (2005) *Explosion welding*. Moscow: Mashinostroenie.
7. Lysak, V.I., Kuzmin, S.V. (2003) *Explosive welding of metal layered composite materials*. Ed. by B.E. Paton. Kiev: PWI.
8. Wittman, R.H. (1973) The influence of collision parameters on the strength and microstructure of an explosion welded aluminium alloy. In: *Proc. of 2nd Int. Symp. on Use of Explosive Energy in Manufacturing Metallic Materials of New Properties* (Marianske Lasne, 1973), 153–158.
9. Cowan, G., Holtzman, A. (1963) Flow configuration in colliding plates. *J. Appl. Phys.*, 34(**4**), 928–939.
10. Walsh, J.M., Shreffler, R.G., Willig, F.J. (1953) Limiting conditions for jet formation in high velocity conditions. *Ibid.*, 24(**3**), 349–359.
11. Belyaev, V.I., Devojno, D.G., Kasperovich, V.B. (1978) About lower boundary of explosion welding conditions. *Poroshk. Metallurgiya*, 51–56.
12. Deribas, A.A. (1980) *Physics of explosion strengthening and welding*. Novosibirsk: Nauka.
13. Zakharenko, I.D. (1990) *Explosion welding of metals*. Minsk: Navuka i Tekhnika.
14. Karpenter, S. (1976) *Explosion welding of metals*. Minsk: Belarus.
15. Petushkov, V.G., Fadeenko, Yu.I. (1998) About range boundaries of explosion welding of metals taking into account the toughness of metals: In: *Transact. of Higher Education Institutions on Explosion Welding and Properties of Welded Joints*. Volgograd: VolgGTU, 42–51.
16. Roman, O.V., Smirnov, G.V., Usherenko, S.M. (1998) Dynamics of high-velocity deformation and cumulative effects in explosion welding of metals. *Ibid.*, 51–64.
17. Sedykh, V.S., Sonnov, A.P. (1998) Determination of «lower boundary of weldability» in explosion welding of metals. *Ibid.*, 63–66.
18. Smelyansky, V.Ya., Ryskulov, M.T., Kozhevnikov, V.E. (1998) To problem of calculation of explosion welding conditions of dissimilar metals. *Ibid.*, 54–62.
19. Sonnov, A.P. (1998) Influence of initial strength of joined metals on the conditions of their explosion welding. *Ibid*.
20. Sonnov, A.P., Shmorgun, V.G. (1998) Calculation of lower boundary of explosion welding of similar metals. *Ibid*.
21. Deribas, A.A. (2006) Explosive welding: Weldability range. In: *Proc. of 7th Int. Symp. on Application of Explosion to Preparation of New Materials* (Sept. 11–14, 2006, Moscow). Moscow: TORUS PRESS, 28–34.
22. Kuzmin, G.E., Yakovlev, I.V. (1973) Study of collision of plates with supersonic contact point. *Fizika Goreniya i Vzryva*, 9(**5**), 746–753.
23. Kuzmin, S.V., Lysak, V.I. (1991) Main principles of transition to waveless conditions of joint formation in explosion welding. In: *Transact. Of Higher Education Institutions on Explosion Welding and Properties of Welded Joints*. Volgograd: VolgGTU.
24. Belyaev, V.I., Kovalevsky, V.N., Smirnov, G.V. et al. (1976) *High-velocity deformation of metals*. Minsk: Nauka i Tekhnika.
25. Shmorgun, V.G., Pronin, V.A., Zhdanov, V.D. (1988) To problem of theoretical evaluation of optimal conditions for explosion welding. In: *Transact. of Higher Education Institutions on Explosion Welding and Properties of Welded Joints*. Volgograd: VolgPI.
26. Lysak, V.I., Sedykh, V.S., Trykov, Yu.P. (1979) Energy parameters of explosion welding of multilayered composite joints. In: *Proc. of Int. Symp. on Use of Explosive Energy in Manufacturing Metallic Materials of New Properties* (Gotvaldov, ChSSR), 152–162.
27. Sedykh, V.S., Sonnov, A.P. (1970) Calculation of energy balance of explosion welding process. *Fizika i Khimiya Obrab. Materialov*, **2**, 6–13.
28. Dobrushin, L.D. (1979) About problem of lower boundary of explosion welding. *Avtomatich. Svarka*, **6**, 64–65.
29. Ajnbinder, S.B., Klokova, E.F. (1958) Some problems of metal cohesion theory in joint plastic deformation. *Izvestiya AN Latv. SSR.*, **12**, 141–154.
30. Ajnbinder, S.B. (1957) *Cold welding of metals*. Riga: AN Latv. SSR.
31. Lysak, V.I., Sedykh, V.S., Trykov, Yu.P. (1973) Determination of critical boundaries of explosion welding process. *Svarochn. Proizvodstvo*, **5**, 6–8.
32. Kuzmin, S.V., Lysak, V.I., Chuvichilov, V.A. (2008) Deformation-time conditions of joint formation in explosion welding. *Svarka i Diagnostika*, **1**, 6–13.
33. Kriventsov, A.N., Sedykh, V.S. (1969) On role of plastic deformation of metal in joint zone during explosion welding. *Fizika i Khimiya Obrabotki Materialov*, **1**, 132–141.
34. Vatnik, L.E., Kriventsov, A.N., Sedykh, V.S. (1974) Some peculiarities of joint formation in explosion welding of sheet bimetal. In: *Transact. of Higher Education Institutions on Explosion Welding and Properties of Welded Joints*. Issue 1. Volgograd: VolgPI.
35. Shmorgun, V.G. (1987) *Development of technology of explosion welding of titanium with steel based on energy input for plastic deformation in the joint zone*: Syn. of Thesis for Cand. of Techn. Sci. Degree. Volgograd: VolgPI.
36. Pronin, V.A. (1986) *Substantiation and development of technology of explosion welding of electrotechnical assembly units from plastic metals with lower power charges*: Syn. of Thesis for Cand. of Techn. Sci. Degree. Volgograd: VolgPI.
37. Peev, A.P., Kuzmin, S.V., Lysak, V.I. (2004) Distribution of temperature in the near-weld zone in explosion welding of dissimilar metals. *The Paton Welding J.*, **4**, 8–11.

INFLUENCE OF DEFORMATION MECHANISM IN THE COLLISION ZONE OF MATERIAL PAIRS ON SELECTION OF OPTIMUM PARAMETERS OF EXPLOSION WELDING

M.P. BONDAR
M.A. Lavrentiev Institute of Hydrodynamics, RAS SD, Novosibirsk, RF

The necessary condition for providing a strong joint between the bodies in a region of the lower boundary of explosion welding is formation of a zone of intensive plastic deformation with a localization band along the joint interface. The mechanisms of formation of bands of plastic deformation localization (BPDL) under high-velocity loading depend on grain size of initial materials. It is shown that initiation of BPDL in a coarse-grained material occurs at $\varepsilon = 0.2–0.3$ and is related to loss of shear stability. There is a certain critical grain size d_{cr}, starting from which the prevailing deformation mechanism is slipping along the grain boundaries, like in a nanocrystalline material. Being a result of rotation instability, in a fine-grained material BPDL are formed at high velocities and deformations of $\varepsilon > 10^4$ s^{-1} and $\varepsilon \geq 2$.

Keywords: *explosion welding, grain size, high-rate deformation of metals, deformation mechanism, plastic deformation, slipping*

Successful application of explosion welding is determined by a correct combination of three groups of parameters, namely technological, kinematic and physical. The first two groups have been quite well studied [1, 2]. The third parameter group related to determination of processes responsible for realization of the bond between the surfaces being joined, has been studied to a smaller degree. Work [3] deals with fundamentals of formation of a bond of a large number of metal pairs in the case of explosion welding. Bond strength is expressed in terms of bond energy calculated by the model of interatomic interaction on the contact surfaces. It is assumed in particular in [3] that the inner surface bonds form at interaction of volume atoms, rather than those of them, which were present on the initial surfaces. This interaction is realized at high-velocity collisions, where «opening» of volume atoms occurs due to high plastic deformations of the colliding surfaces, accompanied by stripping of surface layers, i.e. «self-cleaning». Thus, the process of joint formation in explosion welding essentially is a volume process, similar to development of grain boundaries. In [3] it is shown that the energy of grain boundaries is by 5–6 orders of magnitude lower than the energy consumed in formation of a strong joint in explosion welding. Therefore, the mechanical energy, applied in dynamic methods of bond formation, is mainly required to create conditions, leading to interaction of volume atoms determining the bond strength. This problem is solved by selection of loading parameters. So, in explosion welding a «welding window» in $\gamma - v_c$ coordinates (where γ is the angle of collision; v_c is the contact point velocity) is experimentally determined for each pair of materials being welded. Derived in [4, 5] expressions for the lower boundary of welding somewhat lower the region of γ, v_c values. The lower boundary is characterized by minimum velocity of acceleration $V_{0\,\min}$ ($V_{0\,\min} = (\sigma_b/\rho)^{1/2}$, where σ_b is the ultimate strength; ρ is the material density), at which a strong joint forms without liquid melts in the contact.

Further optimization of collision parameters in the vicinity of the lower boundary requires knowledge of the nature of physical processes determined by these parameters. In [6] it is shown that formation of a strong joint in explosion welding is associated with a certain width of the zone of intensive plastic deformation R, including the joint boundary. Value R is in the same functional dependence on γ, as thickness of cumulative jet δ and wave length λ in the case of a wave-like joint boundary. Expressing each of parameters λ, R, δ in the form of a functional dependence on γ is natural, as they characterize one deformation process at different levels of its intensity [7]. In interval $\gamma = 7–12°$, optimized experimentally by value R, practically all the conditions providing formation of a strong joint are satisfied in the vicinity of the lower boundary. Self-cleaning of the surfaces being welded is characterized by value δ [5]. Dimension R and the corresponding structural state, in which the volume interaction of the atoms of materials being welded is realized, determine formation of a strong joint [6], whereas value λ is related to deformation of surface layers of the colliding plates resulting in their physical contact. A rather wide interval of γ variation is related, primarily, to the quality of the surfaces being welded (roughness, presence of contamination, etc.) [5].

The purpose of this work is studying the dependencies of deformation mechanisms in the zone of a strong joint formation both on the initial material structure, and on its modification during loading. It is also of interest to study the dependence of parameters $\gamma - v_c$ of optimum welding mode on the deforma-

tion mechanism, which will promote understanding of the physical nature of the processes determined by the collision parameters.

It was shown earlier [8, 9] that a strong joint in explosion welding is related to formation of a band of plastic deformation localization (BPDL) along the welding line, which is characterized by a qualitatively new structure. There is a difference between the zone of intensive plastic deformation R, on the boundary of which shear deformation $\varepsilon_{sh} \geq 0.1$, and BPDL. Value ε_{sh} in BPDL is higher than 3 (logarithmic values are used) [7].

Type of deformation, which is shear with compression, is characteristic for explosion welding and for axisymmetrical explosive loading of hollow thick-walled cylinders (TWC) [7–9]. This allows taking into account in explosion welding the physical regularities of BPDL development established at TWC collapse. This provides a broader physical insight into the processes occurring in the joint zone.

Method of TWC collapse has its advantages for studying the nature of the processes at BPDL development. During TWC compression different layers of the cylinder are exposed to different radial deformations ε_r with different velocities $\dot{\varepsilon}_r$. This allows studying in one experiment the change of material structure depending on deformation and its velocity. Characteristic values of deformation velocities are equal to about 10^4–10^5 s^{-1} [8].

It should be noted that a common feature for explosion welding and explosive collapse of TWC is the found abrupt change of material properties with grain size $d \leq 50$ μm. So, in earlier work of the author [7–9] it was established that:

- critical value of deformation ε_{cr} determining BPDL appearance at TWC collapse, varies between 0.2 and 0.3 up to value $\varepsilon > 2$ at transition from coarse- ($d > 100$ μm) to fine-grained ($d \leq 50$ μm) materials [9];
- formation of a strong bond in the region of the lower boundary in explosion welding of fine-grained materials ($d \leq 50$ μm) occurs at a significantly higher velocity of the contact point v_c than for the coarse-grained materials [7].

In both the cases high deformations $\varepsilon > 2$ and high deformation velocities $\dot{\varepsilon} > 10^4$ s^{-1} are created. In addition, in the above processes the grain size causing a jump in the change of the properties, is the same and does not exceed value $d = 50$ μm, taken further on as d_{cr}. This determined the problem of investigation of physical processes causing an abrupt change of material properties.

Influence of grain size on material properties in dynamic deformation is the most clearly manifested in the regions with changing deformation fields. Regions with such deformations are the radial plane of explosion-collapsed TWC and vicinity of the weld in explosion-welded samples.

Conducted studies of evolution of microstructure and properties in fine- and coarse-grained copper samples with deformation increase at explosive collapse of TWC allowed establishing the following: at ε = = 0.2–0.3 BPDL aimed along cylinder radius, form in coarse-grained samples. In these samples the dislocation mechanism of deformation is the main one and BPDL appearance is associated with a loss of shear stability [10]. Initially the grains with a favourable orientation for dislocation movement (highest value of Schmidt factor) determine the sites for development of concentrated shifts, along which BPDL develop. With increase of deformation and development of texture in coarse-grained samples, the number of sites with a favourable orientation increases and the number of BPDL also rises [9].

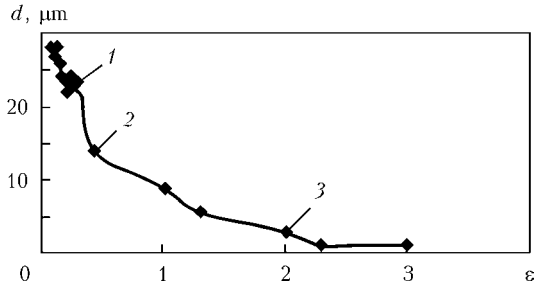

Figure 1. Dependence of the size of structural fragments on relative deformation: *1* — $\varepsilon = 0.08$; *2* — 0.43; *3* — 2.3

In fine-grained samples at $\varepsilon = 0.2$–0.3 a homogeneous texture is observed, the start of formation of which is seen already at $\varepsilon \approx 0.07$. With deformation increase, microstructure fragmentation along cylinder radius is increased.

Change of the dimensions of fragments in fine-grained samples, depending on value ε, is given in Figure 1, d (ε) curve which demonstrates a stable tendency of fragment size refinement with three clear-cut sections. The most intensive refinement of the fragments occurs in the range of variation of deformation ε from 0.08 to 0.43. Furtheron at ε change from 0.43 to 2 the degree of refinement of fragment dimensions becomes lower, and at BPDL and crack formation, it practically stops. The nature of $d(\varepsilon)$ change points to different nature of the processes, which determined d decrease.

An abrupt refinement of fragments (*1*, *2* in Figure 1) is determined, primarily, by development of texture and reduction of grain cross-section, respectively. At $\varepsilon = 0.43$ an intragranular fragmentation starts developing in a fine-grained material (Figure 2, *a*). Fragment arrangement in the sample volume shows that their initiation starts at grain boundaries, while

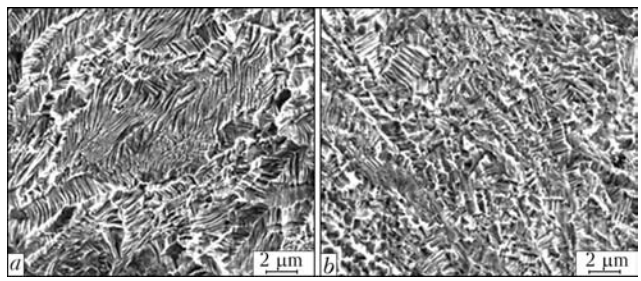

Figure 2. Microstructures of the collapsed region of a fine-grained sample corresponding to $\varepsilon = 0.43$ (*a*) and $\varepsilon > 1$ (*b*)

elongated fragments of textured grains are preserved in the grain center. With ε increase, the fragmentation process develops and spreads to the entire grain volume (Figure 2, *b*), fragment size reaching 3–5 μm. In fine-grained samples BPDL form at ε ≈ 2 and at a slight increment of ε they are transformed into cracks. Unlike the coarse-grained samples, in fine-grained ones BPDL form at the same deformation value in a greater number and their quantity does not change with ε increase [9].

Texturing of fine-grained samples during deformation is related to grain rotation. This increases the number of grains with a high value of Schmidt factor and lowers the probability of the process of concentrated shifts in individual grains. It is obvious that such a mode of deformation of fine-grained materials increases the uniformity of the process of energy dissipation and uniformity of sample deformation to high ε values, respectively.

For fine-grained samples value ε = 0.43 (point *2* in Figure 1) corresponds to the start of appearance of a fragmented microstructure at the initial grain boundaries (see Figure 2, *a*). Initiation of the start of microstructure fragmentation at grain boundaries points to a greater role of intergranular boundaries with deformation increase. As is shown in [11], the intergranular boundary becomes a source of dislocations (disclinations) released into the grains. With increase of deformation, dislocation multiplication and nonconservative motion is enhanced. Processes of stress relaxation are accelerated by transformation of linear defects into boundaries of fragments and grains, the dimensions of which become smaller with stress increase. Development of a fragmented microstructure and change of fragment dimensions with ε increase is given in Figure 2, *b*.

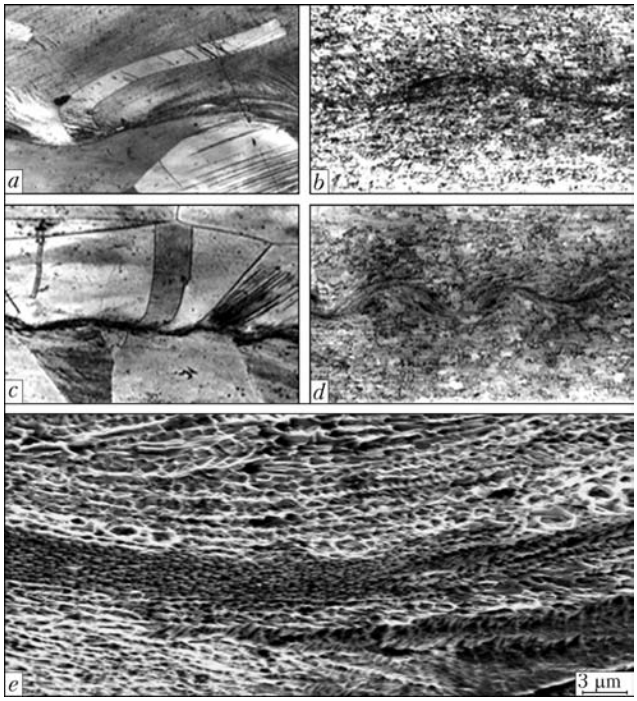

Figure 3. Microstructure (×70) of explosion-welded samples in the region of the lower boundary $V_{0\ min}$: *a, b* — mode I (*a* — σ_t = = 230 MPa, *d* = 300 μm; *b* — σ_t = 50 MPa, *d* = 30 μm); *c, d* — mode II (*c* — σ_t = 90 MPa, *d* = 300 μm; *d* — σ_t = 250 MPa, *d* = = 30 μm); *e* — band of intensive plastic deformation in the zone of bond formation

Thus, appearance of a fragmented structure at grain boundaries, similar to grain rotation, which determined the uniformity of deformation through the sample bulk up to high values of ε, points to a greater contribution of grain boundary slipping into the deformation. At ε ≈ 2 fragmentation is performed in the full volume of grains, and fragment size corresponds to $d \approx 5$ μm. Material properties completely correspond to those which characterize it as a nanocrystalline one. One of the main deformation mechanisms, specific to nanomaterials, is grain-boundary slipping [12]. BPDL appear in the formed structure, which then develop into cracks. Structure homogeneity in BPDL vicinity and the accompanying cracking are indicative of the fact that BPDL result from a loss of rotation stability due to an abrupt lowering of resistance to fragment rotation relative to each other. The given experimental factors demonstrate that grain-boundary slipping is the main deformation mechanism in that part of samples, where fragment size $d \approx 5$ μm. This also indicates that grain size ($d \approx 5$ μm), in which the material demonstrates nanocrystalline properties, depends on its deformation velocity. Under static loading conditions this dimension corresponds to 10–250 nm, at $\dot{\varepsilon} \sim 10^4$–$10^5$ s^{-1} — 5 μm.

A similar development of the processes of BPDL appearance, accompanying the deformation processes, is found in explosion welding in the lower boundary region. Structure of deformation field of the near-weld zone in explosion welded samples is determined by shear deformation gradient, which is readily revealed by the change of the shape of twins entering the weld (Figure 3, *a, c*). Distance from the weld to the site of twin abrupt bending determines the size of the region of intensive plastic flow *R*. Lower boundary of explosion welding is a line in plane γ–V_k (V_k is the deformation velocity), characterized by a constant value of minimum acceleration velocity $V_{0\ min}$. Collision parameters γ and V_k are linked by the following relationship [4]:

$$\gamma = \sqrt{(HV/\rho V_k)},$$

where *HV* is the microhardness.

Angle γ defines the width of the region of intensive plastic flow. It follows from the above expression and Figure 3 that reduction of the collision angle leads to narrowing of intensive deformation region and increase of contact point velocity and deformation velocity in the zone of bond formation ($\dot{\varepsilon} = V_k/R$), respectively.

Figure 3 gives the microstructures of the joint zones and the respective strength characteristics of explosion-welded copper samples. Two selected welding modes allow the most accurate determination of the influence of grain size *d* on the deformation mechanism at the change of stresses in the joint zone. Mode I — V_{k1} = 1060 m/s, γ_1 = 11°; II — V_{k2} = 1680 m/s, γ_2 =

= 7°. When mode I is used, an equivalent joint (σ_t = = 230 MPa) is produced in samples with $d \approx 300$–1000 μm at $R_1 = 100$–120 μm. When mode II is used, $d \approx 30$ μm ($\sigma_t = 250$ MPa), $R_2 = 50$–60 μm. In the work it is shown that formation of a strong bond in explosion welding occurs at formation of BPDL in the region of contact of the plates being welded. A combination of parameters $\gamma_1 = 11°$, $V_{k1} = 1060$ m/s provides the conditions for formation of a strong joint in coarse-grained samples, and BPDL forms in the contact zone. In a fine-grained sample at these collision parameters a homogeneously textured microstructure is observed in the zone of intensive plastic flow without BPDL formation (Figure 3, *b*). Development of deformation in the fine-grained material requires higher stresses for BPDL formation than in the coarse-grained ones.

Variation of collision parameters at transition to mode II led to narrowing of the zone of intensive plastic flow R_2 by approximately 2 times and respective increase of stress in the joint zone. Ratio V_{k2}^2/V_{k1}^2, which is equal to approximately 2.5, can be a measure of energy changes at R narrowing. Deformation velocity $\dot{\varepsilon}$ increases 3 times (from $10.6 \cdot 10^6$ up to $33.6 \cdot 10^6$ s^{-1}). Figure 3, *d* gives the microstructure of a fine-grained sample welded by mode II. Intensive plastic flow with BPDL formation, where a strong bond is in place, can be seen in the narrow joint zone. BPDL microstructure observed in a scanning electron microscope features a high uniformity (Figure 3, *e*). This points to the fact that in mode II the deformation conditions, characteristic for nanomaterials, are realized completely. High stresses and the respective high deformation velocites determined the loss of rotation stability, which was due to an abrupt lowering of the resistance to rotation of fragments of 30 μm size relative to each other. Deformation velocity in the used modes is higher than 10^7 s^{-1}. It is obvious that at deformation velocity $\dot{\varepsilon} \approx 10^7$ s^{-1} manifestation of nanocrystalline properties is found in materials with grain size of 30 μm.

Under the conditions of mode II in a coarse-grained material, where the deformation process is realized by the dislocation (shear) mechanism, melt formation on the contact boundary and lowering of joint strlocity are found.

In conclusion it should be noted that a condition of producing a strong joint in the region of the lower boundary of explosion welding, is formation of the zone of intensive plastic deformation with a band of localization along the joint boundary.

Deformation mechanisms, nature of microstructure evolution at large high-velocity deformations and the determined by them critical deformations ε_{cr} of BPDL initiation, essentially depend on the initial grain size. The established dependence for ε_{cr} of BPDL initiation in a coarse-grained material on Schmidt factor in specific grains reveals the determinant role of the dislocation mechanism of deformation. BPDL initiation in a coarse-grained material is related to the loss of material shear stability with increase of deformation.

There is a certain critical grain size d_{cr}, starting from which slipping along the grain boundaries becomes the mechanism of high-velocity deformation, similar to nanocrystalline materials.

Identical nature of deformation types at TWC collapse and in the zone of intensive plastic deformation in explosion welding is shown. This widened the range of the studied deformation velocities $\dot{\varepsilon}$ and allowed showing that value d_{cr} depends on $\dot{\varepsilon}$. It is established that BPDL formation at explosive collapse of TWC in a fine-grained material occurs as a result of the loss of rotation stability at $\dot{\varepsilon} \approx 10^4$–$10^5$ s^{-1} in areas, where fragment size $d = 3$–5 μm. In explosion welding of materials with grain size $d \le 50$ μm, BPDL formation as a result of the loss of rotation stability occurs at $\dot{\varepsilon} = 33 \cdot 10^6$ s^{-1} ($\dot{\varepsilon} > 10^7$ s^{-1}).

Regularities of manifestation of plastic flow instability in the form of BPDL for TWC to a certain extent allow controlling parameter selection in explosion welding.

It is obvious that threshold value of grain size at material transition into the nanocrystalline state in explosion welding depends on the contact point velocity, which determines the deformation velocity in the collision zone ($\dot{\varepsilon} = v_c/R$).

Such interrelated parameters, as the velocity of the contact point v_c and angle of collision γ in explosion welding of materials with different grains sizes, are determined by the change of deformation mechanism in BPDL formation.

1. Sedykh, V.S. (1985) Classification, evaluation and interrelation of the main parameters of explosion welding. In: *Transact. of Higher Education Institutions on Explosion Welding and Properties of Welded Joints*. Volgograd: VolgPI.
2. Lysak, V.I., Kuzmin, S.V. (2005) *Explosion welding*. Moscow: Mashinostroenie.
3. Oberg, A., Martensoon, N., Shweitz, J.A. (1985) Fundamental aspects of formation and stability of explosive welds. *Metallurgical Transact. A*, **16**, 841–851.
4. Deribas, A.A., Zakharenko, I.D. (1973) On surface effects at glancing collisions of metal plates. *Fizika Goreniya i Vzryva*, 10(**3**), 409–423.
5. Zakharenko, I.D. (1979) On prerequisites for explosion welding. *Ibid*., 8(**3**), 422–428.
6. Bondar, M.P., Ogolikhin, V.M. (1985) About plastic deformation in explosion welding joint zone. *Ibid*., 21(**2**), 147–151.
7. Bondar, M.P. (1995) Type of localization of plastic deformation on contacts determining the formation of bonding. *Ibid*., 31(**5**), 122–128.
8. Bondar, M.P., Nesterenko, V.F. (1991) Deformation on contacts and criteria of joint formation in pulse actions. *Ibid*., 27(**3**), 103–117.
9. Nesterenko, V.F., Bondar, M.P. (1994) Localization of deformation at collapse of thick-wall cylinder. *Ibid*., 30(**4**), 99–111.
10. Bondar, M.P., Merzhievsky, L.A. (2006) Evolution of metal microstructure and conditions of deformation localization at high-rate loading. *Ibid*., 42(**3**), 121–131.
11. Tyumentsev, A.N., Ditenberg, I.A., Pinzhin, Yu.P. et al. (2003) Peculiarities of microstructure and mechanisms of formation of submicrocrystalline copper made by methods of intensive plastic deformation. *Fizika Metallov i Metallovedenie*, 96(**4**), 33–43.
12. Gleiter, H. (1981) Materials with ultrafine grain size. In: *Proc. of 2nd Int. Symp. on Metallurgy and Materials Science* (Denmark), 15–21.

CHANNEL EFFECT IN EXPLOSION WELDING

L.D. DOBRUSHIN, Yu.I. FADEENKO, S.Yu. ILLARIONOV and **P.S. SHLENSKY**
E.O. Paton Electric Welding Institute, NASU, Kiev, Ukraine

A significant influence of «channel processes» propagating at superdetonation velocity in the welding gap (cumulative jets, shock waves in gas, bending vibrations of plates and other) is manifested in explosion welding of long items. The paper presents the known data and results of authors' experiments which allowed clarifying the mechanism of pre-welding erosion of the surfaces of long steel parts being joined. The main element of this mechanism is heating and loss of the surface layer material at ricocheting collisions with the cumulative jet particles.

Keywords: *explosion welding, channel effect, erosion of surface being joined*

The problem of deterioration of quality of a welded joint during its removal from initiation point of welding detonation [1] exists in application practice of explosion welding in manufacturing of long-length bimetal items (bimetal sheets, pipes with channel protective coatings). At the distance of about 1 m and more from the point of detonation initiation the deterioration of mechanical properties of a welded joint and even a fracture of a cladding layer occurs. The increase of size of eddy zones («pockets») up to the formation of a solid interlayer of a fused metal takes place, which is predetermined by a complex effect of several factors, one of which is the so-called channel effect.

The welding of large-size sheets is performed according to the parallel scheme: joining plates (or cylindrical shells) are fixed with a small gap of constant width along the entire surface being welded. The channel effect is a formation in the gap of a flow of cumulative ejections of metal and gas, filling the gap, moving at the superdetonation velocity. As compared with its analogue, i.e. the detonation channel effect thoroughly studied a long time ago [2], welding channel effect has been studied insufficiently.

The calculation of parameters of a shock wave exciting in a gas by flapping of a welding gap is not definitely itself a problem. The application of numerical modelling allows describing this process even in the case when necessary to account for plates displacement ahead of a detonation front, revealed in the work [3], and able to change greatly the geometry of a gap. There is also a general conception of velocity [4], mass and energy of cumulative particles flow [5] in a gap. However the combined examining of a shock wave in gas and cumulative particles flow represents insuperable difficulties. They are aggravated in case of long items, as far as with moving of the explosion welding process from the point of initiation the mass of flow of metallic particles is gradually increased due to erosion of its surface by particles of initial flow. In this connection the effect of channel effect should be evaluated using direct experiments.

To evaluate the carrying of mass of metallic particles flow away from the surfaces being joined and their state before joining, the special experiment was held [6]. In experiment the assembly (Figure) of steel rod of 25 mm diameter and steel tube, coaxial to it, of 3.5 mm wall thickness (material — steel 20) was used. The width of welding gap was 1.5 mm. The full length of assembly was 750 mm; the first 600 mm belonged to test area welded by the external charge of explosive. The cumulative flow, forming in welding, passed to a gap of the final assembly section of 150 mm length without explosive and having the role of a specimen under investigation.

To evaluate the state of gap surfaces being joined directly before passing the front of detonation wave, the thickness of metal layer carried away from the metal layer surface was measured and the change in height of irregularities of rough surface was evaluated. The thickness of metal layer, carried away from the rod surface, was 30 μm and the height of relief irregularities increased from 3 up to 6–12 μm, which is far less than height of welding wave.

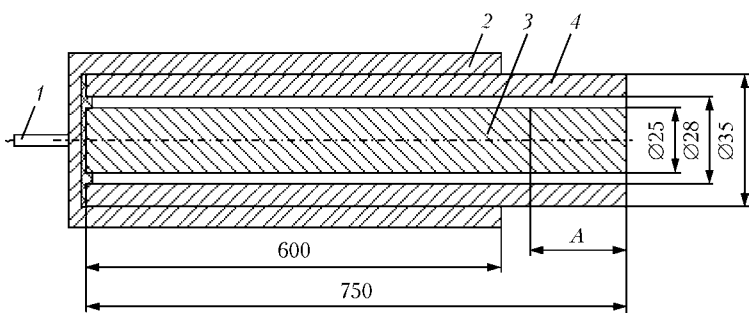

Scheme of experiment on study of channel effect: *1* — detonator; *2* — charge of explosives (ammonite 6ZhV + ammonium nitrate); *3* — steel cylinder; *4* — cladding steel shell; *A* — measuring area (ratio of gap length to height is 400)

The obtained results give a possibility to compare the contributions of primary and secondary particles to the general flow of cumulative ejections. Having applied the formula from the work [7] $d_{c.j}/d_{sh} = \text{tg}^2(\alpha/2)$ (here, $d_{c.j}$ is the half-thickness of cumulative jet; d_{sh} is the thickness of flying shell; α is the dynamic angle of collision), it is found that at the ideal cumulation the jet thickness should be 40–50 μm. However, according to data of [5], at the low velocity of contact point (in our case — 2300 m/s) the value $d_{c.j}$ can be 3–5 times lower than ideal one. Thus, the thickness of metal layer being carried away into the cumulative jet from each surface being joined could be 4–8 μm that is 4–7 times lower than carried away one, observed at the measuring area. The increase in total mass of cumulative jet by 5–8 times as compared with the primary jet results in considerable reduction in its velocity which becomes less than the rate of line of contact and detonation. As a result the contact point overruns the delayed channel flow and traps it into the pockets. Even if to suppose that channel flow has a radial structure (high-velocity primary flow in a near-axial area and slow secondary flow in a near-surface layer), the main part of gap contents should be subjected to trapping.

In case of detonation channel effect the accumulation of mass in the pre-detonation area results in periodicity of process of detonation or its disruption. It is obvious that the same occurs also in explosion welding.

The problem of definite mechanism of erosion of surfaces requires separate discussion. According to the work [4] the velocity of primary flow of cumulative particles under the given conditions can be estimated as 3.0–3.5 km/s. From the investigations of high-velocity collisions it is known that in this range of velocity the glancing collisions of particles with the surface of solid bodies are accompanied by considerable deformations (dents formation) and conversion of kinetic energy of particles into heat energy of colliding bodies. However, the ejections of mass of flow of metallic particles into the flow of secondary particles are negligible at this velocity of collision. Therefore, the observed erosion of the surfaces being joined can be explained only by their heating up to the temperature at which the strength of surface layer is very low. According to [8] at quick deformation of low-carbon steels the decrease in value of yield strength by one order is observed at the temperature of 800 °C and higher. At the typical condition of explosion welding the kinetic energy of the primary cumulative flow is nearly equal to the energy required for heating of eroding layer up to 800 °C and even higher. The energy, generated in the air shock wave in the welding gap, is 10 times lower than this value. Thus, the main reason of erosion is heating and carrying-away of material of the near-surface metal layer due to collisions with cumulative flow particles. As far as conversion of kinetic energy of cumulative particles into heat energy of surface metal layers is performed in sequence of ricocheting collisions the large period of time is required for development of the erosion process. Thus, the significant erosion occurs only in welding of long items.

The mass of primary particles exceeds the mass of air in the gap by tens of times and the total mass of metallic particles flows on the measuring area exceeds by hundreds of times. The multiplication of secondary particles increases contact area of their surface with gas, however, decreases the mean contact temperature, which obviously delays the proceeding of metal–gas reactions which are finalized in the pockets at the crests and troughs of welding wave.

The pockets content is naturally solidified melts formed at intensive plastic deformation. However, the latter is capable itself to provide heating of metal only till the pre-melting temperature at which the deformation resistance is negligibly small. The further heating up to the melting temperature and providing the metal with a latent heat of melting is possible, but it should be provided by other mechanisms. It can be dynamic pressing of porous content of pockets in the zone of the joint formation. In this process the volumetric density of energy pm can be additionally imparted to a substance (here p is the average pressure during reduction; m is the initial porosity). The question about mechanisms of pockets formation and their content is little studied. The measurements of pockets volume, investigations of composition and structure of their content are the sources of information about channel processes and their effect on the quality of produced joints.

Thus, the conception about cleaning of surfaces being joined and metal carrying away only in the vicinities of contact point can be considered applicable to the angular scheme of explosion welding and to the initial its stage by the parallel scheme. After the completion of initial stage a sufficiently dense flow of metallic particles is accumulated in the gap which performs the cleaning of surface and carrying away of surface layer far ahead the contact line.

1. Kudinov, V.M., Koroteev, A.Ya. (1978) *Explosion welding in metallurgy*. Moscow: Mashinostroenie.
2. Dubnov, A.V., Khotina, L.D. (1966) On mechanism of channel effect in detonation of condensed explosive. *Fizika Goreniya i Vzryva*, **4**, 97–104.
3. Silchenko, T.Sh., Kuzmin, S.V., Lysak, V.I. et al. (2008) Estimation of vertical displacement of flyer metal plates before contact point in explosion welding. *The Paton Welding J.*, **4**, 20–23.
4. Deribas, A.A., Zakharenko, I.D. (1974) About surface effects at glancing collisions of metal plates. *Fizika Goreniya i Vzryva*, 10(**3**), 409–423.
5. Lysak, V.I., Kuzmin, S.V. (2005) *Explosion welding*. Moscow: Mashinostroenie.
6. Fadeenko, Yu.I., Illarionov, S.Yu., Dobrushin, L.D. et al. (2006) Channel effect in parallel-scheme explosive welding of long-length parts. In: *Shock-assisted synthesis and modification of materials*. Ed. by A.A. Deribas, Yu.B. Scheck. Moscow: TORUS PRESS.
7. Trishin, Yu.A. (2005) *Physics of cumulative processes*. Novosibirsk: RAS SD M.A. Lavrentiev HI.
8. Gulyaev, A.P. (1978) *Metals science*. Moscow: Metallurgiya.

FEATURES OF EXPLOSION WELDING OF TITANIUM TO STEEL IN A SHIELDING ATMOSPHERE

O.L. PERVUKHINA[1], L.B. PERVUKHIN[1], A.A. BERDYCHENKO[2], L.D. DOBRUSHIN[3], V.G. PETUSHKOV[3] and Yu.I. FADEENKO[3]

[1]Institute of Structural Macrokinetics and Problems of Materials Sciences, RAS, Chernogolovka, RF
[2]Altai State Technical University, Barnaul, RF
[3]E.O. Paton Electric Welding Institute, NASU, Kiev, Ukraine

As proved by investigations, to produce a sound joint between steel and titanium on large-sized blanks by explosion welding, it is necessary to perform this process in a shielding gas atmosphere. The use of the trap method made it possible to establish that, when performing explosion welding in air, burning of particles and surface of titanium in the shock-compressed gas in the welding gap ahead of the contact point causes preferential heating of the titanium surface, which is attributable to low thermal conductivity of titanium. This leads to non-uniform variations in hardness of the materials welded ahead of the contact point, as well as to a change of the high-velocity collision mechanism from the solid–solid state to the soft–solid one. Adding an inert gas into the welding gap prevents burning of titanium and provides quality welding on unlimited surfaces. Properties of the produced steel–titanium bimetal in argon atmosphere are given.

Keywords: *explosion welding, steel, titanium, inert gas, intermetallics, welding gap, contact point, particles burning*

In application of explosion welding for manufacturing large-sized bimetal plates with titanium cladding layer a deterioration of welded joint quality is found with increase of the distance from the start of the welding process — point of the charge initiation [1]. At more than 1 m distance from this point a lowering of mechanical properties of the welded joint and even breaking up of the cladding layer are found. These changes are accompanied by increase of the dimensions of eddy zones right up to formation of a continuous interlayer of surface-melted metal. As follows from [2], one of the reasons for the revealed instability is formation of Fe–Ti intermetallics on the contact surface. Improvement of the quality of welded surface treatment and change of the welding mode somewhat improved the situation, but the scale effect could not be completely eliminated.

Work [3] proceeding from experimental data obtained in explosion welding of titanium plates to titanium, demonstrates the theoretical possibility of inflammation and burning of finely-dispersed titanium particles due to interaction with oxygen and nitrogen of the air. In this zone high temperatures and pressure are created, and complex physico-chemical processes proceed, direct observation of which is difficult because of the presence of an air shock wave and detonation products. In this case, indirect methods, i.e. studying the final reaction products, have the main role in investigation of the processes running in the welding gap.

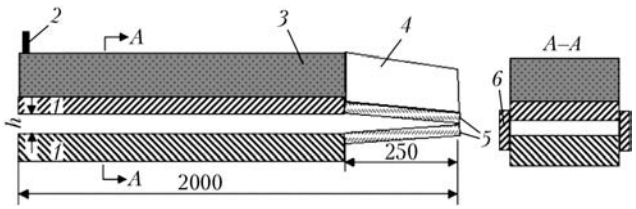

Figure 1. Schematic of explosion welding with a trap: *1* — welded plates from steel and titanium; *2* — detonator; *3* — explosive charge; *4* — sand; *5* — trap; *6* — side plates

In [4] the trap method, which allows fixing on the trap surface the products which are removed from the welding gap by the shock-compressed gas, was applied to study the processes proceeding ahead of the contact point.

In this study an upgraded variant of the traps was used (Figure 1), which allowed mounting them at explosion welding of large-sized plates, without disturbing the bimetal manufacturing technology, and changing the atmosphere in the welding gap. Plates *1* (cladding layer is titanium, base layer is steel) were positioned with gap h on a sand bed. The gap was sealed along the long sides of the plates to be welded by welding on plates *6*; trap *5* consisting of plates welded together at an angle, was mounted from the end face opposite to the charge initiation point. Explosive charge *3* in a required layer and detonator *2* were placed on the upper plate. Trap was protected by a layer of sand *4* from direct impact of the detonation products. If required, the welding gap was filled with argon. Presence of plates *6* eliminates unloading into the plate sides or flying of the reaction products out of the gap. A long trap allows not only intercepting particles flying out of the gap, but also following the dynamics of their deposition on the trap surface.

At plate collision in explosion welding mode shock-compressed gas forms in the welding gap ahead of the contact point, which is saturated with finely-dispersed particles removed from the surface of the colliding materials.

After the explosion, the thickness of the deposited layer was measured on the trap plates, its configuration was recorded, then samples were cut out, on which

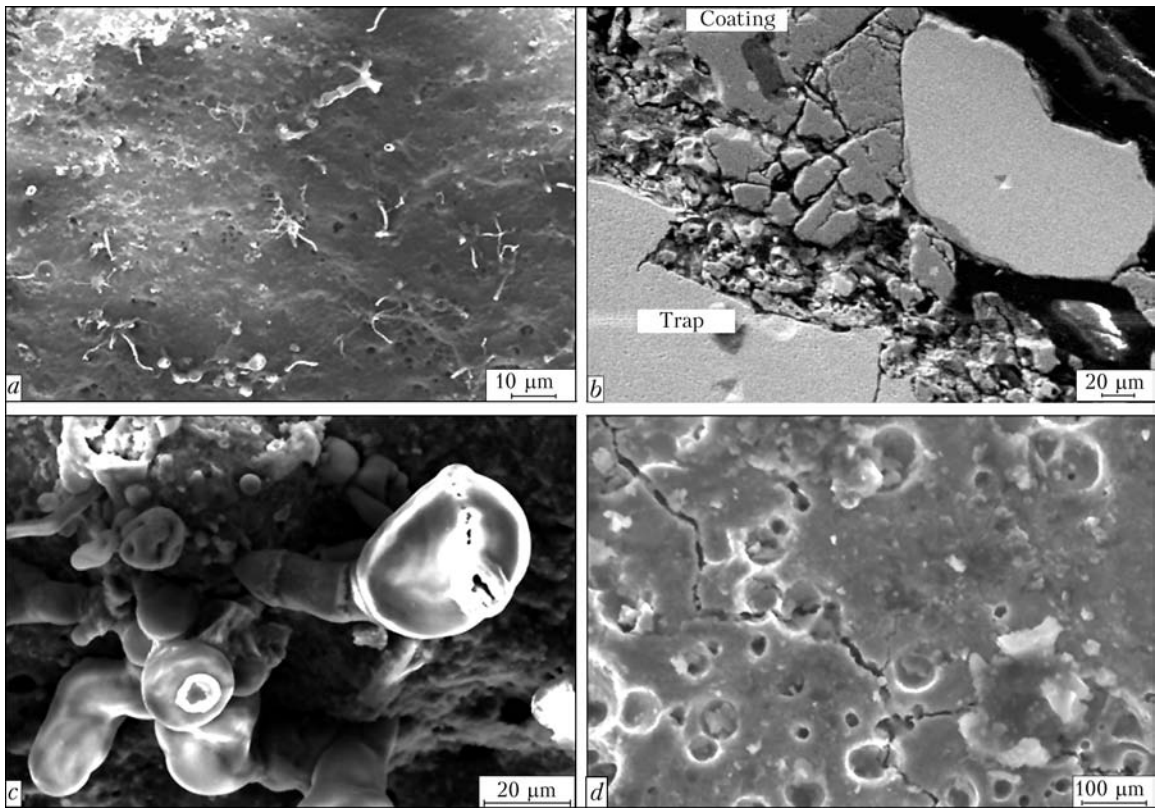

Figure 2. Characteristic surface of the trap (*a*, *d*), same with individual inclusions in the form of jets and globules (*c*) and cross-sectional microstructure of the interface (*b*) in steel–titanium samples produced by explosion welding in air atmosphere

the composition and structure of products on the trap surface as well as the plate joint structure were determined by means of optical and electron microscopy, X-ray microprobe analysis and microhardness measurements.

The trap method allowed studying the composition of the deposited layer on the trap plate surface, determined by the process of avalanche-like burning of dispersed titanium particles in the welding gap, which leads to disturbance of the thermodynamic equilibrium and the joint formation process. Feeding inert gas into the welding gap eliminates the process of titanium particle burning, thus ensuring stable conditions of welding over the entire surface of the plates being joined.

In explosion welding in air, a continuous mat porous coating with a net of microcracks (Figure 2, *a, d*) 40–50 μm wide, developing into individual jets, was found on the surface of both the trap plates. The thickness of this coating is non-uniform and is equal to 20–50 μm. The interface between the coating and trap material is clear-cut, and its structure is porous (Figure 2, *b*). Coating material has the microhardness of 5000–7000 MPa (titanium microhardness is *HV* 1800 MPa, that of steel is *HV* 1200 MPa).

Chemical and X-ray microprobe analyses of the coating composition showed that it consists of various TiO, Ti_3O, Ti_2O titanium oxides (Figure 3, *a*). Individual inclusions in the form of solidified jets of iron carbooxides and globules consisting of titanium oxides, are found on the coating surface (see Figure 2, *a* and *c*). No presence of pure iron or titanium phases, or their solid solutions and compounds was found in the coating structure.

Investigation of the mechanical properties of the produced welded joint showed that with greater distance from the explosive charge initiation point the

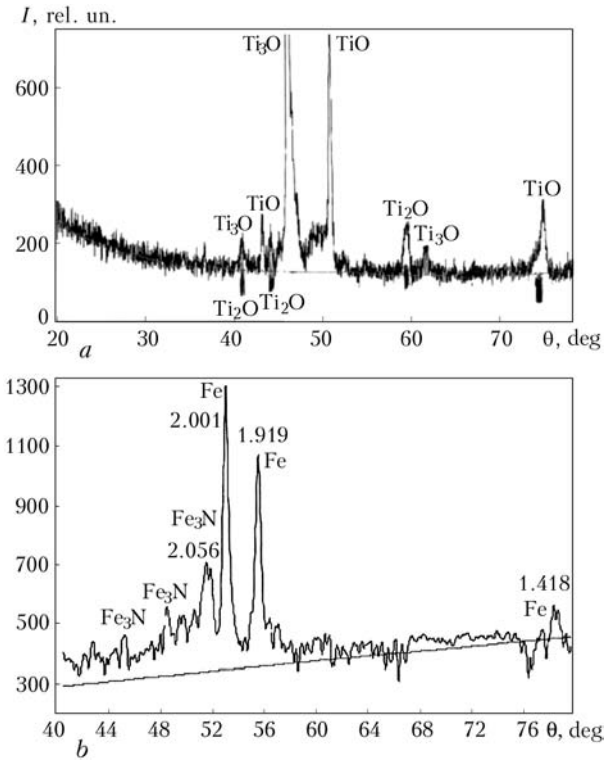

Figure 3. Roentgenogram of the trap surface after welding titanium to steel in air (*a*) and in argon (*b*)

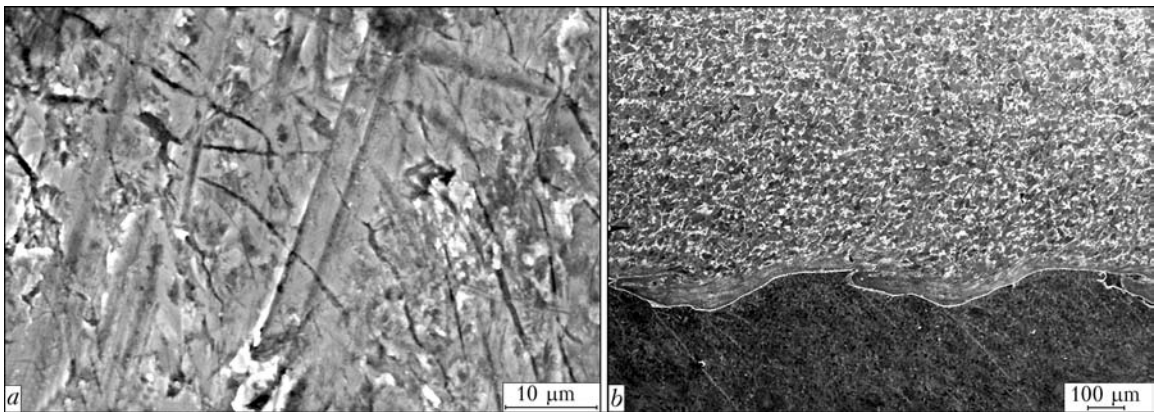

Figure 4. Microstructure of trap surface (*a*), and steel to titanium joint (*b*) welded in argon

pull strength of the bimetal drops from 300 to 1 MPa, and wave amplitude and number of surface-melted regions in the joint zone become greater. Moreover, chaotically located regions of lack-of-penetration looking like bulging, as well as cladding layer damage in the form of ruptures and blowholes, are found. Weld microstructure develops intermetallic interlayers.

In explosion welding of steel–titanium plates in an argon atmosphere visual inspection of the trap surface did not reveal any changes. Metallographic studies showed only traces of initial machining (Figure 4, *a*). Chemical analysis did not reveal presence of a surface layer of a composition differing from that of the trap metal. X-ray microprobe analysis registered iron and its compounds with nitrogen Fe_3N (Figure 3, *b*) on the trap surface. Shear strength of the joint is equal to 190–250 MPa, pull strength is 250–350 MPa. No intermetallic phases, inclusions of titanium oxides or nitrides were found in the joint structure in the initial and final sections (Figure 4, *b*).

At present extensive experimental and theoretical material has been accumulated on the subject of joint formation in explosion welding and production of the characteristic wave-like joint. At explosion welding high pressure is achieved and intensive plastic deformation develops in the collision zone, which is accompanied by a considerable increase of metal temperature in this zone.

In order to analyze the obtained experimental data, let us consider the processes, occurring at explosion welding. Metal adhesion is considered as a particular case of topochemical reactions in pressure welding, which are characterized by three-stage nature of the process of formation of strong bonds between the atoms of the metals being joined, namely formation of physical contact, activation of contact surfaces, and volume development of the interaction. In joint formation at explosion welding three characteristic zones can be singled out (Figure 5): *I* — contact point zone; *II* — zone located ahead of the contact point; *III* — zone of joint formation behind the contact point.

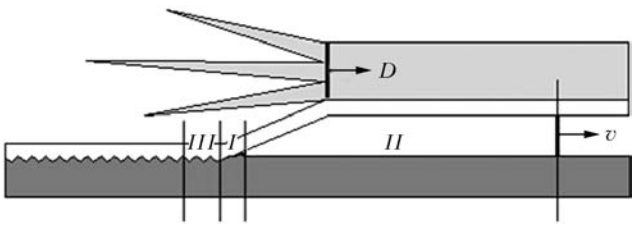

Figure 5. Schematic of joint formation in explosion welding: *I*–*III* — see in the text; *D* — explosive detonation velocity; *v* — shock wave velocity

Zone *II* is the most important in terms of production of a strong joint. Heat sources here are gas compression in the gap at acceleration of the cladding plate q_1, aerodynamic braking of particles in the shock-compressed gas q_2, as well as burning of dispersed particles and titanium surface layers in the shock-compressed gas q_3. Assessment of these values is given in [3]. Variation of joint strength along the length of the plates being joined shows that thermodynamic equilibrium sets in at a certain distance from the start of the process of welding of most of the metal pairs, i.e. the evolving heat is removed from the joint zone even in welding in very stringent modes. One part of heat q_4 is removed from the joint zone by shock-compressed gas saturated with dispersed metal particles, and the other part of heat q_5 goes into the joint in the form of cast inclusions or eddy zones. Values q_4 and q_5 can be assessed in the first approximation by the data of [5] for the specified welding mode. Heat from the shock-compressed gas q_6 consumed in heating of surfaces ahead of the contact point, is removed into the materials being welded.

Thus, presence of thermodynamic equilibrium ahead of the contact point, i.e. in zone *II*, is necessary to ensure the welding process:

$$q_1 + q_2 + q_3 - q_4 - q_5 - q_6 = 0.$$

In titanium welding this equilibrium is disturbed because of an abrupt increase of value q_3 due to burning of particles and surface of titanium in shock-compressed gas. Increase of the mode rigidity increases the heat flow with + sign, but at the same time, according to [5], q_4 rises, i.e. heat removal due to increase of the quantity of cast inclusions in the joint increases, thus providing the process stability at large areas of the plates being welded.

Consideration of thermal processes ahead of the contact point shows that in the steady-state mode of

explosion welding, surfaces heated up to a certain temperature (about 500–700 °C for steel [6]), come into contact (zone *I*). This fact should be taken into account in welding of different metal pairs. It should be noted that deformation level in the joint zone, which is evaluated by its metal structure, apparently, does not influence the adhesion process, but influences joint formation.

Comparing the derived results with those obtained in welding titanium to titanium [7] we can anticipate lowering of the negative influence of burning of finely-dispersed particles in the welding gap ahead on the contact point, as replacement of one of the titanium plates being welded by steel should reduce titanium content in the shock-compressed gas 2 times. However, the nature of the coating, composition and quantitative characteristics of the trap coating turned out to be identical to coating obtained in welding titanium to titanium [7]. This is attributed to the fact that the surface layer of titanium, participating in the joint formation, is characterized by a much lower heat conductivity compared to steel, and is heated up to much higher temperature than steel. Evaluation by the procedure of [6] of metal heating behind the front of shock-compressed gas, in which burning of finely-dispersed titanium particles proceeds, showed that a layer of steel 10 μm thick at 1 m distance from the start of the welding process at 2500 m/s velocity of the contact point can heat up to approximately the temperature of 500 °C, that of titanium — up to 900 °C. Allowing for the heat from burning of finely-dispersed titanium particles in the welding gap, titanium surface temperature can reach titanium melting temperature, leading to lowering of titanium hardness and strength, as well as its melting. Increase of titanium content in the region of shock-compressed gas leads to its avalanche-like burning. In this connection, at explosion welding in air a continuous coating of titanium oxides forms on the trap surface (see Figure 2, *a, b*) with just individual inclusions of iron compounds (see Figure 2, *c, d*). No intermetallics or dispersed mixture of titanium with iron are found on the trap surface.

Thus, in explosion welding of titanium to steel the welding mechanism changes (conditions in the region of welded joint formation) at greater distance from the start of the welding process. While in the initial regions the process can be characterized as explosion welding of two «solid» metals, as the process moves on burning of titanium particles present in the region of shock-compressed gas, leads to increase of the temperature of shock-compressed gas and temperature of heating of surfaces to be joined ahead of the contact point right up to their melting, as a result of the cumulative effect. More intensive heating of titanium leads to a considerable lowering of its hardness, and further process of explosion welding can be regarded already as joining of the soft and solid metal [8]. Here, a liquid titanium phase forms, which even further increases the concentration of finely-dispersed titanium particles in the region of shock-compressed gas, and increases its temperature and heat evolution. Such a development of the welding process leads to an even greater heating of metal ahead of the contact point, its considerable surface melting and violation of welding conditions.

It should be noted that we have not established the role of nitrogen in the process of titanium and iron particle burning in the welding gap — nitrogen compounds were not found in the traps. However, rounded pores form on the trap coating surface and in the cast inclusions in the joint. This can be associated with the fact that nitrogen dissolves in the metal at high temperatures and pressures. At pressure lowering behind the contact point, when nitrogen solubility decreases, it precipitates with formation of rounded pores on the coating surface. Replacement of active gas by inert gas in the welding gap eliminates direct burning of dispersed particles, thus lowering their temperature and possibility of burning initiation due to the gases dissolved in the particle. In this case, the explosion welding process runs in the mode of welding «solid» metal, thus allowing elimination of defects in large-sized titanium–steel bimetal plates.

Proceeding from the conducted studies, a technology of steel–titanium bimetal production was developed, and specification TU 27.81.09.009–2005 «Explosion Welded Steel–Titanium Bilayer Blanks» was prepared and approved. Steel–titanium bimetal is certified by testing center «TsNIITMASh-Analitika-Prochnost» (Certificate of Compliance 16 of 01.03.2005). Results obtained in bimetal production showed that the used technology provides zero class continuity of the joint, i.e. joint discontinuity defects the area of which is more than 1 cm^2 are absent. Bi-

Mechanical properties of steel–titanium bimetal

Bimetal grade (dimensions, mm)	Joint strength, MPa		Angle for bending/side bending tests, deg
	Pull	Shear	
09G2S + VT1-0 (35 (30 + 5) × 1000 × 2000)	390–490	155–215	130–135
12Kh18N10T + VT1-0 (55 (50 + 5) × 1100 × 1750)	305–335	180–350	130–135
St20 + VT1-0 (38 (30 + 8) × 2700 × 2900)	250–350	190–250	Above 80
St20 + VT1-0 (48 (40 + 8) × 1800 × 3500)	250–350	190–250	Above 80

metal quality meets the requirements of the international standards and specifications, in particular, AD Merkblatt W8, Iuli 1987, specification 1264 (Germany), NC-501 (France). Continuity of layer joining is 100 % by zero class. Shear strength of the joint determined in different plate zones is not lower than 150 MPa, pull strength is higher than 250 MPa (Table). Joint zone structure is wave-like without any brittle inclusions.

1. Kudinov, V.M., Koroteev, A.Ya. (1978) *Explosion welding in metallurgy*. Moscow: Metallurgiya.
2. Deribas, A.A. (1980) *Physics of explosion strengthening and welding*. Novosibirsk: Nauka.
3. Berdychenko, A.A., Pervukhin, L.B., Shtertser, A.A. et al. (2003) About possible inflammation of metal particles ejected into the gap during explosion welding of titanium. *Fizika Goreniya i Vzryva*, 39(**2**), 128–136.
4. Pervukhina, O.L., Berdychenko, A.A., Pervukhin, L.B. et al. (2006) Effect of atmosphere composition on formation of titanium-steel joint in explosion welding. In: *Transact. of Higher Education Institutions on Explosion Welding and Properties of Welded Joints*. Volgograd: VolgGTU.
5. Konon, Yu.A., Pervukhin, L.B., Chudnovsky, A.D. (1987) *Explosion welding*. Moscow: Mashinostroenie.
6. Ishutkin, S.N., Kirko, V.I., Simonov, V.A. (1980) Study of heat effect of shock-compressed gas on the surface of colliding plates. *Fizika Goreniya i Vzryva*, 16(**6**), 69–73.
7. Berdychenko, A.A., Pervukhin, L.B. (2000) Principles of change of the structure of welded joints made by explosion welding with increase of its overall dimensions in the case of titanium. In: *Transact. of Higher Education Institutions on Explosion Welding and Properties of Welded Joints*. Volgograd: VolGTU.
8. Dobrushin, L.D. (2003) Precision explosion welding of structures. *The Paton Welding J.*, **4**, 29–32.

PECULIARITIES OF INSTABILITY OF THE PROCESS OF EXPLOSION CLADDING OF LARGE-SIZE BILLETS

T.Sh. SILCHENKO, S.V. KUZMIN, V.I. LYSAK and **Yu.G. DOLGY**
Volgograd State Technical University, Volgograd, RF

The most probable causes of instability of properties of the joining zone in explosion clad large-size billets are revealed on the basis of analysis. Results of experimental studies of variations in temperature of the mating surfaces with increase in length of the plates, as well as peculiarities of violation of the geometry of position al relationship of long plates ahead of the detonation front are presented.

Keywords: *explosion cladding, large-size billets, detonation velocity, temperature of mating surfaces, flyer plate, vertical displacement, detonation front, collision velocity and angle*

Explosion welding of metals is a controllable process resulting in formation of a joint in the solid state. In this process, the distributed parameters (parameters of the kinematic and energy sub-groups) can be varied by varying in a certain way the technological (design) parameters, through affecting the deformation and temperature-time welding cycles that determine properties of the welded joints [1]. Theoretically (in accordance with one- and two-dimensional models of acceleration [2–4]), providing constant size of the gap, h, between the plates welded over the entire welding area, as well as constant height of the captive charge, H, should lead to constant values of collision velocity V_{col}, contact point velocity V_c and collision angle γ and, therefore, guarantee stability of the process and properties of the joining zone of an explosion welded composite. However, this is not the case in practice of explosion cladding of large-size billets [5–14].

The purpose of this study is to analyse causes and experimentally investigate peculiarities of instability of the process of explosion cladding of large-size billets.

Analysis of literature data allows distinguishing at least three most probable causes that lead to fluctuations of the wave profile and increase in the amount of the fused metal along the length of the resulting bimetal [5–12].

In principle, increase in wave parameters in the end part of the billets welded could be related to enhancement of parameters of a high-velocity collision of the plates, taking place because of increase in detonation velocity D of an explosive along the length of the charge. However, this hypothesis put forward as early as in 1974 in study [8] found no experimental verification.

In particular, study [15], where detonation velocity D of explosives 4 m long was measured by the Dotrisch method [2] every 200 mm, shows that absolute deviations from the mean value of D are not in excess of ±3 %, which, according to [2], corresponds to the accuracy of the measurement method used and, therefore, evidences a high stability of detonation properties of long explosive charges.

A number of researchers [5–7, 13, 16, 17 etc.] put forward a more convincing assumption that variations in properties of the joint along the length of the large-size billets welded is a result of preheating of the colliding surfaces under the impact by a high-temperature flow of particles of the shock-compressed gas of a cumulative origin, moving ahead of the contact point.

If, according to [5], we assume for simplification that the compression of air in the gap between the plates is caused by a flat piston moving along the detonation front at contact velocity V_c, the state of the shock-compressed air ahead of the contact point

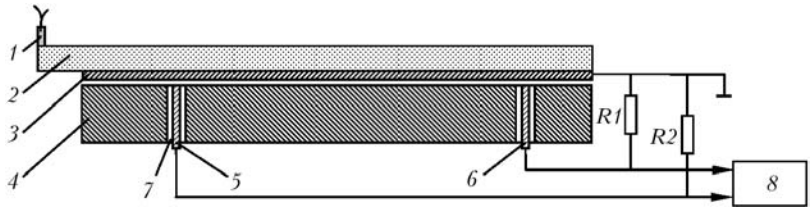

Figure 1. Scheme of experiments on investigation of variations in temperature of surfaces of the explosion welded metal plates in the initial and end sections of a pack: *1* — electric detonator; *2* — explosive charge; *3* — flyer copper plate; *4* — target plate; *5, 6* — constantan rods; *7* — insulator; *8* — digital memory oscillograph

can be written down in the form of the following equation system [18]:

$$\begin{cases} p_w = \dfrac{2\rho_0 V_w^2}{k+1}, \\ u_w = \dfrac{2V_w}{k+1}, \\ T_w = \dfrac{T_0 p_w (k-1)}{p_0 (k+1)}, \end{cases} \quad (1)$$

where V_w is the velocity of the shock wave front; p_w and T_w are the pressure and temperature of air behind the shock wave front, respectively; k is the polytropic exponent; ρ_0, T_0 and p_0 are the initial density, temperature and pressure of air; and $u_w = V_c$ is the mass velocity behind the shock wave front.

The calculations from (1) show that temperature of the shock-compressed air at V_c = 1800–4000 m/s amounts to 2300–6300 °C [16] under a pressure of 5–20 MPa, which agrees with the experimental data [17].

As the contact point moves along the billet welded, because the former lags behind the shock wave front, the time of the effect of a heated air on the mating surfaces grows obeying the following dependence [16]:

$$t = L\,\frac{V_w - V_c}{V_w V_c}, \quad (2)$$

where L is the distance from the sensor to the point of the beginning of welding.

According to study [16], at distance L = 1–2 m this time may exceed 100 μs, increasing with decrease in V_c.

Study [17] suggests using the following dependence to calculate heat flow q from the shock-compressed air inside the surface of the plates welded:

$$q = \mathrm{St}\cdot\rho u c_p (T^* - T_{col}), \quad (3)$$

where $T^* = T\left(1 + \dfrac{k+1}{2}\,\mathrm{M}^2\right)$ is the deceleration temperature [17]; St and M are the Stanton and Mach numbers, respectively; T, c_p and ρ are the temperature, heat capacity and density of gas, respectively; u is the mass velocity; and χ is the adiabatic exponent.

As follows from estimation (in rough approximation for the model of an instantaneous flat heat source) of the process of heating the near-contact volumes of the plates welded during time t (2), made by the authors of [16], thickness of the metal heated to several hundreds of degrees at L = 1 mm is 10–20 μm, which, in their opinion, does influence the general thermal situation in the near-weld zone and, hence, formation of the joint.

According to the calculations made in study [7], power of the heat flow from gas to metal at V_c = = 4.0–4.5 km/s is approximately 10^3–10^4 MJ/(m^2·s), which, for a time of its effect equal to t ~ 100 μs from formula (2), gives an increment of energy input to the joining zone (in the form of heat) equal to about 0.1–1.0 MJ/m^2. Such energy inputs become commensurable with the values of energy consumed for plastic deformation of metal in the near-weld zone. However, they are localised in a narrower zone and can lead to fusion of metal of the near-contact metal layers up to 100 μm thick.

Many methods are available now for measurement of temperature in the bulk of metal under pulse loading [3]. The most promising of them is the method of dynamic thermocouples that form during the explosion welding process at collision of two dissimilar elements (e.g. copper and constantan). Key drawback of the method is the presence of baroEMF, which introduces a significant error to the experiment. At the same time, assuming that the value of baroEMF of a specific thermocouple for identical experimental assemblies is constant, investigation of changes in thermal situation in the joining zone with distance from the beginning of the pack welded can be reduced to qualitative comparison of temperatures in different sections on the basis of a value of the pulse signal (in the form of a voltage jump) fixed by an oscillograph (at the moment

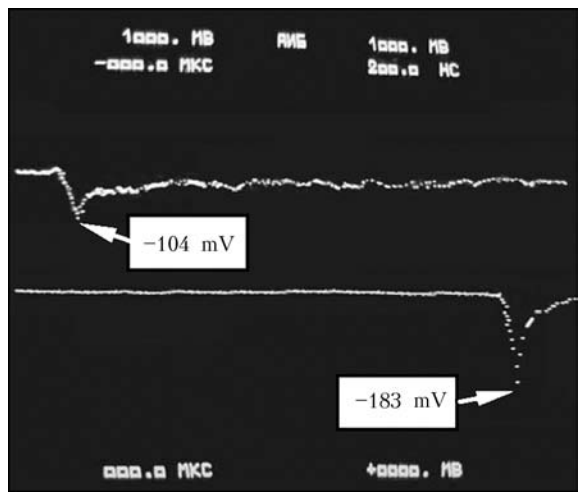

Figure 2. Oscillogram of the temperature mode fixed in one of the experiments: upper curve — sensor located in the initial section of the plates welded (100 mm from the beginning of welding); lower curve — sensor located in the end section of the plates welded (550 mm from the beginning of welding)

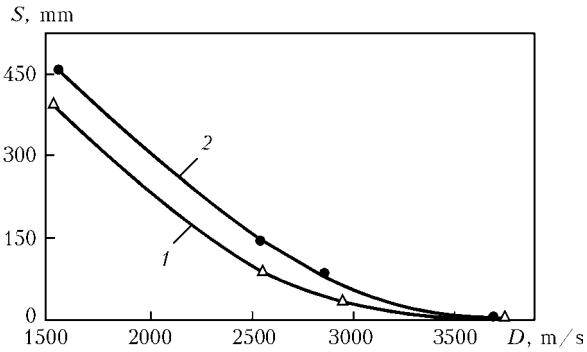

Figure 3. Dependence of distance S between the investigated section of the 2 mm flyer plate and detonation front upon the explosive charge detonation velocity under explosion welding conditions (*1*) and at the absence of the target element (*2*); distance from the beginning of welding to the investigated section is x_i = 750 mm, minimal value of vertical displacement of the investigated section is Δ = 4 mm

of touching the thermocouple elements), characterising an almost instantaneous growth of temperature.

Variations in temperature of the mating surfaces with distance from the explosive charge initiation point were qualitatively assessed by conducting a series of experiments based on the method of local dynamic thermocouples [3, 19, 20]. The point of the experiments was as follows (Figure 1). Long copper plate *3* accelerated by explosive charge *2* was caused to collide in series with constantan rods *5* and *6* located in fixed (target) steel plate *4* at different distances from the beginning of welding. Insulator *7* was placed between the constantan rod and steel plate to eliminate their electric contact. The thermoEMF signal was registered by using digital oscillographs C9-8 and GDS-820C. Velocity of the contact point during the experiments was maintained within a range of 2100 to 2200 m/s.

As a result, a substantial difference in amplitudes of the electric signals was detected, this reflecting formation of the maximal instantaneous thermoEMF + baroEMF in the copper–constantan joint at a distance of 100 and 550 mm from the beginning of welding. A typical oscillogram fixed in one of the experiments is shown in Figure 2.

Therefore, the effect of preheating the mating surfaces of the plates to be explosion welded, which shows up in cladding of large-size billets, will certainly foster fluctuations of the wave profile and increase in the amount of the fused metal over the joining surface in bimetal.

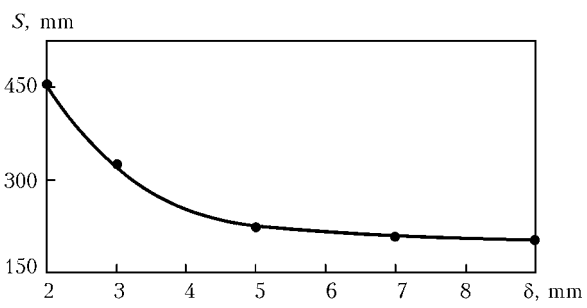

Figure 4. Dependence of distance S between the investigated section of the plate upon its thickness δ at the absence of the target plate (x_i = 750 mm, Δ = 4 mm, D = 1500–1550 m/s)

In our opinion, the most significant factors leading to instability of structure and properties of the joining zone in explosion welding of long plates are vertical displacements of sections of the flyer plate ahead of the contact point under the explosive charge that has not yet detonated. This causes changes in the initial size of the setting gap, h, during explosion welding, thus resulting in deviation of the values of collision angle γ and collision velocity V_{col} from the calculated ones. This violation of the geometry of positional relationship of long elements, which was experimentally proved in studies [7, 9, 21, 22], may occur both due to the pressure of the shock-compressed gas (air) present between the plates welded [5], and due to the effect of inertia forces of a shock-wave origin [12, 23]. In our opinion, investigation of peculiarities of violation of the geometry of positional relationship of long elements being explosion welded is of a high scientific and practical interest, as this phenomenon, firstly, allows explaining non-uniform elongation deformation of the long plates, in addition to fluctuations of waves and increase in the amount of the fused metal along the length of the plates [14], and, secondly, outlining the new, scientifically justified ways of stabilising their properties, which is an important task, as the technological approaches known by now are of low technical feasibility and low efficiency.

Several series of experiments, the parameters of which are given in the Table, were carried out to investigate the character of vertical displacements of sections of the flyer metal plate by using the specially developed procedure described in detail in [22]. Distance S between the detonation front in an explosive charge and section of the flyer plate located ahead of the front and moved vertically to a distance of not less than Δ (gap between the needle sensor and surface of the flyer plate) was determined in the experiments using different input conditions and parameters of explosive loading.

Experiments 1–6 were conducted by the parallel scheme of explosion welding, and in experiments 7–15 the target plate was not used to exclude the effect of the shock-compressed gas present between the elements welded. In experiments 1––10, 14 and 15 the detonation velocity was varied over a wide range (1500–3800 m/s) and thickness of the flyer plate was kept constant, whereas in experiments 11–13 (as well as 7 and 14), on the contrary, thickness of the flyer element was varied from 2 to 9 mm and parameters of the explosive charge (H, ρ_{ex}) providing the detonation velocity of about 1500 m/s were kept constant. In addition, in experiments 1, 4–7, 10 and 14, the size of the setting gap, Δ, was varied from 2 to 5 mm along a vertical between the surface of the flyer plate and contact displacement sensors, and two lines of the sensors were installed at distances of 600 and 750 mm from the beginning of the flyer plate.

Conditions of explosive loading of plates in experimental study of the character of violation of the geometry of positional relationship of long elements ahead of the contact point

Experiment No.	Material of plates welded	Sizes of plates, mm	Detonation velocity D, m/s	Setting parameters			Distance S between section and detonation front at the time moment of needle sensor short-circuiting, mm
				Welding gap h, mm	Coordinate of installation of needle sensors x_i, mm	Gap Δ between needle sensor and plate surface, mm	
1	Steel St.3 / Steel St.3	2×200×800 / 9×200×760	1510	3	600/750	2 4 5	236/386 236/386 236/386
2			2560		750	4	91
3			2860		750	4	33
4			3750		600/750	2 4 5	7/0 0/0 0/0
5		2×200×800 / 9×200×760	1540		600/750	2 4 5	151/301 151/301 117/297
6			3740		600/750	2 4 5	0/0 0/0 0/0
7	Steel St.3 / –	2×200×800 / –	1550	–	600/750	2 4 5	304/454 304/454 304/454
8			2550		750	4	152
9			2760		750	4	107
10			3700		600/750	2 4 5	0/0 0/0 0/0
11		3×200×800 / –	1530		750	4	336
12		5×200×800 / –	1560		750	4	220
13		7×200×800 / –	1520		750	4	209
14		9×200×800 / –	1510		600/750	2 4 5	341/201 329//201 51/201
15			3800		600/750	2 4 5	3/2 2/0 0/0

Note. Numerator gives values for the flyer plate, and denominator — values for the target plate.

As follows from analysis of the results obtained in experiments 1–4, size S decreased non-linearly (Figure 3, curve *1*), approximately from 420 mm at a mean value of V_c = 1510 m/s (experiment 1) and detonation velocity D ~ 3750 m/s (experiment 4) with increase in the detonation velocity. In this case, no vertical displacements of sections of the flyer plate ahead of the contact point were observed (the time fixed by the displacement sensors strictly corresponded to the moment at which the detonation front passed through their location plane). Similar changes in the S value were noted in the case of the 2 mm flyer plate (experiments 7–10) and absence of the target (fixed) element (Figure 3, curve *2*), as well as in investigation of the geometry of positional relationship of sufficiently thick and massive plates in experiments 5, 6, 14 and 15.

Increase in thickness of the flyer element in experiments 7, 11–14 at a relatively low value of detonation velocity D, equal to 1510–1550 m/s, leads to decrease in a value of S (Figure 4), approximately from 450 mm in the case of using the 2 mm flyer plate (experiment 7) to about 200 mm at plate thickness δ = 9 mm (experiment 14).

The results of experiments 5 and 14, where the contact sensors with different values of Δ were in-

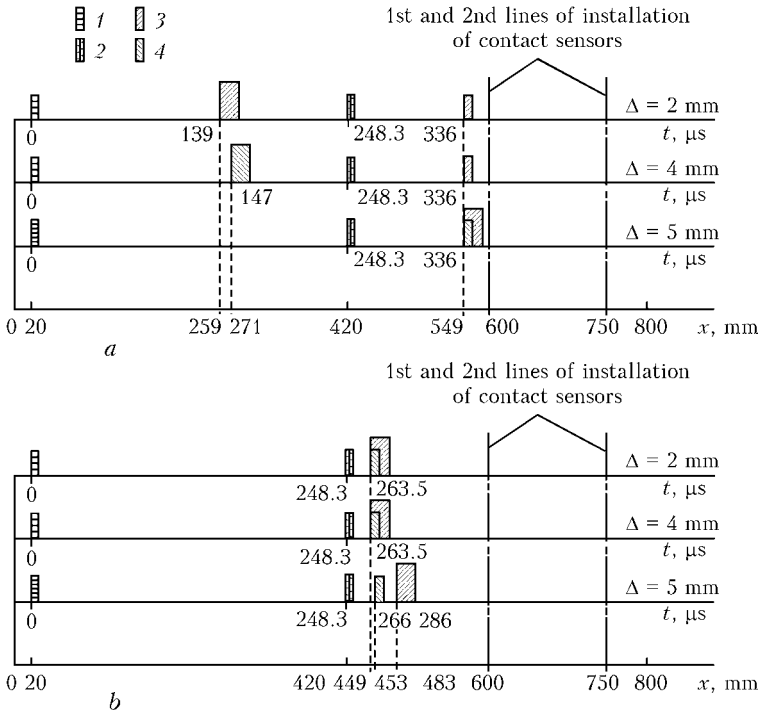

Figure 5. Diagrams plotted on the basis of the results of experiments 14 (*a*) and 5 (*b*) for positions x of the detonation front at the moments when investigated sections of the plate make vertical displacements D: *1* — pulse signal triggering scanning of oscillographs; *2* — pulse signal fixing that the detonation front has passed a distance of 420 mm; *3, 4* — pulse signal fixing displacement Δ of sensors of the 1st and 2nd lines, respectively

stalled in two lines, also allow an unambiguous conclusion that violation of the geometry of positional relationship of long elements ahead of the detonation front, at the absence of the target plate and under explosion welding conditions, may occur in different ways. This conclusion follows from analysis of the diagrams (Figure 5) plotted on the basis of the results of experiments 5 and 14, the only and fundamental difference in which was the presence of the target plate (see the Table).

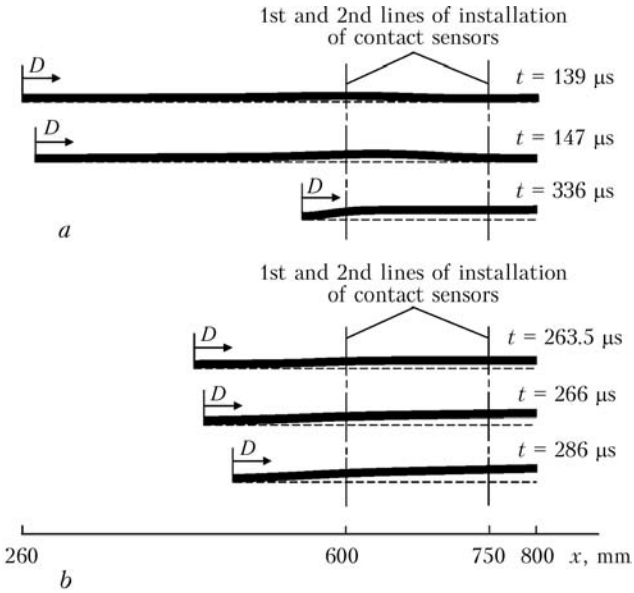

Figure 6. Hypothetical representation of changes in shape of the long flyer metal plate 9 mm thick ahead of the detonation front at time moments t, corresponding to short-circuiting of the contact sensors, according to the results of experiments 14 (*a*) and 5 (*b*): dashed line — initial position of internal surface of the long flyer plate; the explosive charge and target plate present in experiment 5 are not shown

It can be easily seen from the diagram plotted on the basis of the results of experiment 14 (Figure 5, *a*) that contact sensors of the 1st and 2nd lines, having a gap of 2 and 4 mm, short-circuited in series. Displacements of both investigated sections to 5 mm occur synchronously. Therefore, it can be assumed (Figure 6, *a*) that initially the displacement of the first section is of a local character, and then the situation changes because of acceleration of the right end of the plate, leading to simultaneous short-circuiting of all the sensors of the 2nd line and displacement of the first section at least to 5 mm. The presence of the target plate in experiment 5 leads to a substantial change in the situation (Figure 5, *b*). At the beginning, the displacement of both sections to 4 mm occurs synchronously and is characterised by an intensive acceleration, this being evidenced by simultaneous short-circuiting of the sensors having a gap of 2 and 4 mm. It took extra 22.5 μs for the first section of the plate to cause short-circuiting of the sensor with gap Δ = = 5 mm (i.e. for further upward displacement to 1 mm), and no more than 2.5 μs for the second section. Therefore, the initial stage of vertical displacements (to 4 mm) is characterised by a dramatic acceleration of both first and second investigated sections, after which a substantial difference can be seen in changes of the velocities of the latter (the second section moves at a much higher velocity, compared with the first section, this being evidenced by a difference in time of short-circuiting of the contact sensors with a value of the setting gap equal to 5 mm). Therefore, it can be assumed (Figure 6, *b*) that under explosion welding

conditions the parallel welding scheme is transformed into the angular one with some variable angle α. In this case, violation of the geometry of positional relationship of the elements welded is of a non-local character, this explaining some «congestion» of pulses within a narrow time range (see Figure 5, *b*).

CONCLUSIONS

1. It was established that violations of the geometry of positional relationship of the elements being explosion welded ahead of the detonation front and effect of preheating of the colliding surfaces are the main causes of changes in properties of the joint along the length of the billets welded, which show up in increase in sizes of the waves and amount of the fused metal.

2. It was experimentally determined that in the case of vertical displacements outpacing the detonation front (in a number of cases, comparable with welding gap size h), outpacing value S decreases with increase in the detonation velocity of the captive explosive charge (up to complete termination of the vertical displacements of the flyer element sections) and thickness of the flyer element.

3. It was reliably proved that the flyer metal plate accelerated by a sliding detonation wave (at the absence of the target plate) is characterised by the disturbances occurring in it, which are the result of action of the inertia forces of a shock-wave origin, while under conditions of explosion welding of long elements arranged by the parallel scheme the latter can be transformed into the angular one due to the dominating effect of the shock-compressed air moving in the gap between the plates.

The study was completed under State Contract 02.523.12.3012.

1. Kuzmin, S.V., Lysak, V.I., Khaustov, S.V. et al. (2006) Main principles of designing parameters for explosion welding of layered composites. In: *Transact. of Higher Education Institutions on Explosion Welding and Properties of Welded Joints*. Issue 2(**9**). Volgograd: VolgGTU, 4–17.
2. (1975) *Physics of explosion*. Ed. by K.P. Stanyukovich. Moscow: Nauka.
3. Kuzmin, G.E. (2002) *Experimental-analytical methods in problems of dynamic loading of materials*. Novosibirsk: SO RAN.
4. Deribas, A.A., Kuzmin, G.E. (1970) Two-dimensional problem on acceleration of plates by sliding detonation wave. *Prikladn. Mekhanika i Tekhn. Fizika*, **1**, 1977–1981.
5. Kudinov, V.M., Koroteev, A.Ya. (1978) *Explosion welding in metallurgy*. Moscow: Metallurgiya.
6. Konon, Yu.A., Pervukhin, Yu.A., Chudnovsky, A.D. (1987) *Explosion welding*. Ed. by V.M. Kudinov. Moscow: Mashinostroenie.
7. Zakharenko, I.D. (1990) *Explosion welding of metals*. Minsk: Navuka i Tekhnika.
8. Vatnik, L.E., Kriventsov, A.N., Sedykh, V.S. (1974) Some peculiarities of formation of joint in explosion welding of sheet bimetal. In: *Transact. of Higher Education Institutions on Explosion Welding and Properties of Welded Joints*. Issue 1. Volgograd: VolgPI, 35–45.
9. Gelman, A.S., Chudnovsky, A.D., Tsemakhovich, B.D. et al. (1978) *Explosion cladding of steel*. Moscow: Mashino–stroenie.
10. Lysak, V.I., Kuzmin, S.V. (2005) *Explosion welding*. Moscow: Mashinostroenie.
11. Kuzmin, S.V., Lysak, V.I., Dolgy, Yu.G. (2002) Formation of joint in explosion welding of large-size layered metal composites. *Svarochn. Proizvodstvo*, **5**, 48–53.
12. Tarabrin, G.T., Trykov, Yu.P. Effect of elastic waves on nature of plate movement under the effect of explosion products. In: *Transatc. of Higher Education Institutions on Metals Science and Strength of Materials*. Volgograd: VolgGTU, 5–13.
13. Berdychenko, A.A., Pervukhin, L.B. (2000) Principles of changes in structure of the explosion welded joint with increase in its dimensions by an example of titanium. In: *Transact. of Higher Education Institutions on Explosion Welding and Properties of Welded Joints*. Volgograd: VolgGTU, 102–114.
14. Bersenev, P.V., Trykov, Yu.P., Kuzmin, S.V. et al. (1985) Principles of deformation of plates in explosion welding. *Ibid*., 84–93.
15. Lysak, V.I., Shmorgun, V.G. (1987) Detonation characteristics of mixed explosives for welding, based on ammonite № 6ZhV + filling material. *Ibid*., 105–114.
16. Berdychenko, A.A., Pervukhin, L.B. (2002) Theoretical principles of gas-shielded explosion welding. *Ibid*., 134–151.
17. Ishutkin, S.N., Kirko, V.I., Simonov, V.A. (1980) Investigation of the thermal effect of shock-compressed gas on surfaces of the colliding plates. *Fizika Goreniya i Vzryva*, **6**, 69–73.
18. Zeldovich, Ya.B., Rajzer, Yu.P. (1966) *Physics of shock waves and high-temperature hydrodynamic phenomena*. Moscow: Nauka.
19. Besshaposhnikov, Yu.P. (1990) On the role of residual pressure and detonation products in explosion welding of titanium to steel. In: *Subj. Transact. of AS USSR SD on Material Processing by Pulse Loads*. Novosibirsk.
20. Ishutkin, S.N., Kuzmin, G.E., Paj, V.V. et al. (1992) On measurement of temperature field in steady-state plane metal flow. *Prikladn. Mekhanika i Tekhn. Fizika*, **2**, 157–165.
21. Silchenko, T.Sh., Kuzmin, S.V., Lysak, V.I. et al. (2006) Infringement of collision geometry during explosive cladding of long-sized plates. In: *Shock-assisted synthesis and modification of materials*. Ed. by A.A. Deribas, Yu.B. Scheck. Moscow.
22. Silchenko, T.Sh., Kuzmin, S.V., Lysak, V.I. et al. (2008) Estimation of vertical displacement of flyer metal plates ahead of contact point in explosion welding. *The Paton Welding J*., **4**, 20–23.
23. Gorobtsov, A.S., Silchenko, T.Sh., Kuzmin, S.V. et al. (2006) Mathematical model of interaction between flyer plate and pulse load in explosion welding conditions of metals. In: *Izvestiya VolgGTU*: Transact. of Higher Education Institutions on Explosion Welding and Properties of Welded Joints Series. Issue 2(**9**). Volgograd: VolgGTU, 93–101.

MODELLING AND APPLICATION OF HIGH-VELOCITY EXPLOSION WELDING PROCESSES

G.V. SMIRNOV, A.D. SHUGANOV, R.V. STEFANOVICH, A.I. YADEVICH, I.V. PETROV, A.A. KAMORNY, V.A. KONOPLYANIK, A.R. LUCHENOK, A.A. TOLOSHNY, P.T. BOGDANOVICH and **O.A. DZICHKOVSKY**
Research Institute of Pulsed Processes, Minsk, Belarus

Studies of Belarus researchers in theory of explosion welding are reviewed. Physical concepts underlying the mathematical model are described, and capabilities of numerical modelling of the joint formation process at subsonic oblique collision are demonstrated. Simple semi-empirical calculation methods are presented, and examples of practical applications of explosion welding and treatment are given.

Keywords: *explosion welding, high-rate deformation, shock, dynamics*

Utilisation of the energy of explosives and effects of dynamic cumulation for production of new composite materials is still a topical area of research. Dynamic methods hold promise for formation of meta-stable structures with special properties or chemical compositions, for joining of phases that cannot be formed by traditional methods, and for development of new superhard composites based on nanocrystalline powders of refractory compounds. Unique physical-mechanical characteristics of materials can be achieved owing to a short time process and high-energy pulse effect exerted on a material by high pressures, which lead to substructural changes and phase transformations.

Studies in the field of dynamics of the explosion processes conducted lately at the Belarus State Research and Production Association for Powder Metallurgy have been aimed at advancement of these priority areas of materials science. Known studies by O.V. Roman, P.A. Vityaz, V.I. Belyaev et al. give phenomenological quantitative description of the mechanisms of metal flow, evolution of continuum and porous medium at an explosion collapse, under conditions of explosion consolidation and welding, and impact thermo-mechanical treatment. Critical parameters of the processes and their relationship with structure and properties of a material were identified. Numerical modelling was used to substantiate process parameters and develop procedures for engineering calculations of shock-wave pulsed loading of materials under high-rate deformation conditions.

Widening of the range of process parameters by using high-temperature equipment and new schemes for cumulation of energy in the dynamic experiment made it possible to generalise the results obtained for a case of welding of cermet compositions. Layered composites based on metals with substantially different physical-mechanical properties, including materials based on refractory metals and structural materials, as well as powder composites based on superhard materials, were produced by explosion welding and commercially applied. A topical research and practical task is to further develop important applied aspects of high-rate deformation of metals, improve experimental methods for investigation of the processes of explosion welding, impact thermo-mechanical treatment and consolidation at high-temperatures, and, on this base, address the problem of production of new composite materials by the methods of high-energy pulsed technologies.

Specific character of impact interactions. Traditionally, explosion welding is regarded as a process of joining materials in the solid state, which takes place at a high-velocity oblique collision of billets being welded. The problem relates to different aspects of metal physics, but, first of all, it is the problem of mechanics. This is evidenced by the fact that the greatest advances in the theory of this phenomenon are associated with investigations conducted by a large number of scholars belonging to the scientific school of the M.A. Lavrentiev Institute of Hydrodynamics of the Siberian Division of the Russian Academy of Sciences.

Improvement of the explosion treatment methods put forward a number of new problems related to modelling and calculation of high-velocity contact interaction and dynamic cumulation processes. Characteristic peculiarity of welding at a high-velocity oblique collision is generation of a jet and formation of a wavy surface within the contact zone. The range of parameters, wherein this phenomenon takes place, coincides, as a rule, with the range of optimal conditions or is close to it, as wave formation causes self-cleaning and activation of the mating surfaces, and collision becomes of a substantially inelastic type. Considerable portion of the initial kinetic energy transforms into the thermal energy, rather than in the elastic compression energy, while the intensive plastic deformation of contact layers, characteristic even of refractory materials (Figure 1), excludes formation of tensile stresses during unloading, which may lead to fracture of a joint.

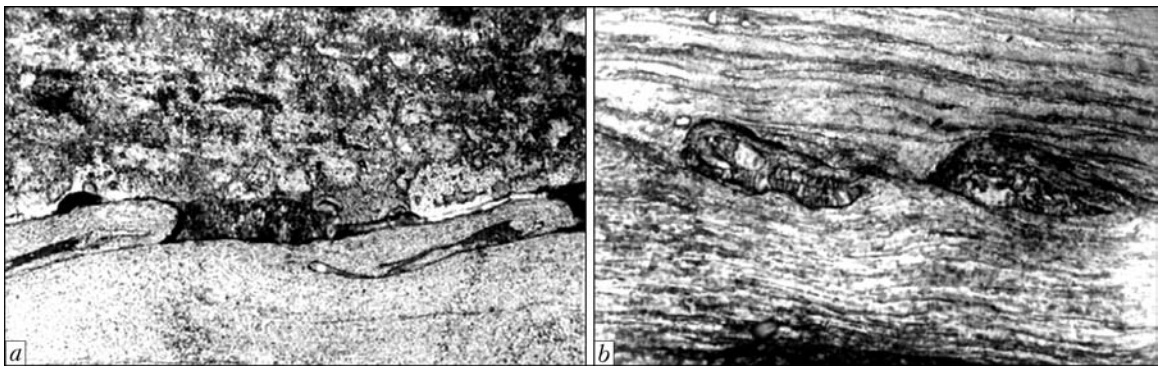

Figure 1. Microstructures (×200) of contact zones at oblique collision of refractory metal pairs Mo–W (*a*) and Ti–W (*b*)

Reported are the attempts to explain wave formation at a high-velocity oblique collision in terms of hydrodynamics, ignoring strength properties of metals and important technological aspects. From this point of view it is impossible to describe limitations on the nucleation effect by a back jet under moderate loads, the formation and instability of which, as experimentally proved, is a real cause of formation of a wavy path on the interface and condition of self-cleaning of the metal surfaces.

For example, studies [1–6] analyse the phenomenon on the basis of a model of incompressible liquid and relate it to different forms of hydrodynamic instability. Thus, conditions of formation of a back jet ahead of the contact line under excessive loading became clear from the positions of physics of shock waves and cumulation theory, according to which the back jet is formed in the subsonic flow region behind the oblique shock waves coming out from the flow deceleration zone.

The latter circumstance, which can be understood from the positions of the compressible medium model, as well as simple practical considerations were indicative of the necessity to use such explosives for welding, the detonation velocity of which is known to be lower than the velocity of sound in metals. However, the pressure of detonation of low-velocity explosives is much lower than that of high explosives, and it was found out that the character of the phenomenon is determined by strength properties of materials, this making it necessary to develop models that would allow for their real strength properties.

The attempts to establish criteria and develop principles of the theory of the explosion welding process were made as more and more experimental data were accumulated and analysed in detail [7–13]. Many of the above studies shared four requirements for identification of optimal welding parameters (Figure 2). Let us make a brief mention of each of these requirements.

1. Critical conditions of wave formation that set the upper limit of the range of parameters, wherein the phenomenon takes place, were strictly defined only for homogeneous metals in classical cumulation studies. The known modes of jet formation for dissimilar metals were adjusted on the basis of two-dimensional calculations for the pairs of materials having contrast properties. The critical angle of jet formation determines the right limit if the contact point in Figure 2, behind which, as noted earlier, the collision occurs without formation of a cumulative jet and welding is impossible. In this case, critical collision angle γ^* for materials characterised by a linear dependence of the shock wave velocity on the mass velocity is evaluated as follows:

$$\theta = \varphi - \text{arctg}\,[\text{tg}\,\varphi - \text{tg}\,\varphi/s + c/(sV_c c\cos\varphi)], \quad (1)$$

$$\varphi = \arcsin[(-b - \sqrt{b^2 - 4ad})/(2a)], \quad (2)$$

were $a = (1 - 2s)/s$; $b = (s - 2)c/(sV_{c)}$; $d = \frac{c^2}{sV_c^2} + 1$; c and s are the impact adiabatic coefficients of a material; φ is the angle of incidence of the shock wave in a material with high compressibility; θ is the flow rotation angle in the shock wave; and $\gamma = \alpha + \beta$ is the collision angle equal to the sum of a setting angle between the plates and a flying angle. For similar materials

$$\gamma^* = 2\theta. \quad (3)$$

The exact formula for this limit is significant only in welding of compositions with dramatically differing physical-mechanical properties (e.g. titanium and lead), as welding is performed at a subsonic velocity

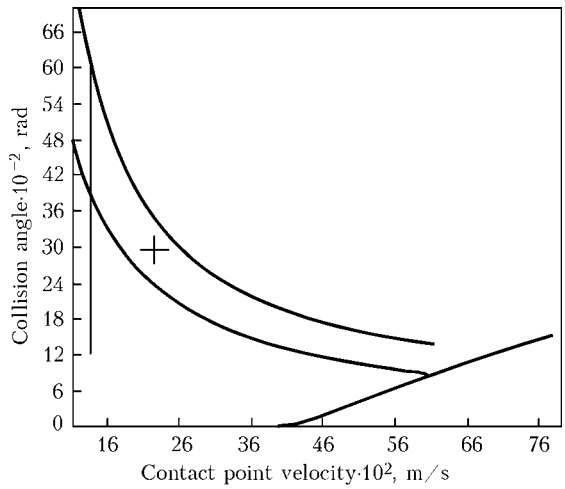

Figure 2. Graphic presentation of four conditions that limit the range of optimal welding parameters for the titanium (Ti B265-GR2)–steel (A516-70) pair 6 and 30 mm thick, respectively (results of the calculations made by using WMASTER software)

of the contact point for a material with a lower volumetric compressibility. In this case

$$\gamma^* = \frac{\rho_1\delta_1 + \rho_2\delta_2}{\rho_2\delta_2}\,\theta, \qquad (4)$$

where $\rho_{1,\,2}$ and $\delta_{1,\,2}$ are the densities and thicknesses of the plates.

2. Minimal velocity of impact of a flyer plate should be sufficient to ensure plastic deformation of a material ahead of the contact line. The stress at collision is calculated, as a rule, according to a model of elastic impact. Strictly speaking, this calculation is applicable only for the initial stage of impact, and it yields an overestimated value of flow stress. For this reason, Wittman and the author of [7] conclude that the calculated pressure at collision should be not less than 5 times in excess of the Gugonio elasticity limit.

Another estimation of flow stress according to the model of inelastic impact gives an expression for determination of a minimal velocity of impact and lower welding limit $v = V_c\gamma$ (Figure 2), which was derived in studies [8, 10]:

$$v = \sqrt{\frac{2\sigma_y(\rho_1\delta_1 + \rho_2\delta_2)}{\rho_1\rho_2(\delta_1 + \delta_2)}}. \qquad (5)$$

It was suggested using the dynamic rather than technical value of yield stress at a set deformation rate, pressure and temperature.

3. It is the opinion of a number of authors that transition from the waveless structure of interface of the joint to the wave one occurs at a strictly determined flow rate for each pair of metals. Using the hydrodynamic model, the authors of [5] determined the critical transition velocity in a range of relatively low velocities as a transition from the laminar flow to the turbulent one. Wittman [7] suggested the following relationship to determine the transition velocity:

$$V_c = \left[\frac{2\mathrm{Re}(HV_1 + HV_2)}{\rho_1 + \rho_2}\right]^{1/2}, \qquad (6)$$

where Re is the Reynolds number having a specific value for a given pair of metals. The mean value of this parameter for a number of metals is 10.6. However, if Vickers hardness values are replaced by Gugonio elasticity limit values, then Re = 12.6 ± 1.0 for all metals and alloys. The best quality of the joint, as claimed by the authors, is achieved in the case where the contact velocity is just a bit higher than the transition velocity (by 50–200 m/s).

We think these and other similar studies are important, because they directly indicate what detonation velocity (i.e. type of an explosive) is optimal for joining a specific pair of materials. If detonation velocity D is much in excess of V_c, the use is made of the angular welding scheme and the setting angle

$$\alpha = \frac{v}{V_c} - \frac{v}{D}.$$

However, of notice is the fact that relationship (6), which follows from comparison of the Bernoulli hydrodynamic pressure at a point of deceleration of the flow and the Gugonio yield stress, is similar to equation (5) in its idea, but it yields a different estimate of impact pressure.

It was noted later on [10] that the transition velocity suggested by Wittman is related to the velocity of propagation of a non-linear surface wave in a more rigid material, and to the resonance with a contact load that overtakes it:

$$V_c \le \frac{2\mu_2(1-\nu_1) + 2\mu_1(1-\nu_2)}{\mu_2(2-\nu_1) + \mu_1(2-\nu_2)} \times \max\left(\sqrt{\mu_1/\rho_1},\, \sqrt{\mu_2/\rho_2}\right), \qquad (7)$$

were μ_j and ν_j are the shear moduli and Poisson's ratios of materials. For a case of contact of metal and fluid, in the extreme we have that $V_c = 2/3\sqrt{\mu/\rho}$.

4. Maximum permissible velocity of a flyer plate sets the so-called upper limit of welding for a specific pair of materials. Fracture is related to increase in the deformation temperature and formation of fused regions, which have no time to solidify by the moment of arrival of the unloading waves to the joining zone. The ratio that determines interrelation between the maximal impact velocity and thermal-physical parameters of the materials welded was proposed by Wittman, and a similar ratio was suggested by I.D. Zakharenko [8, 12]:

$$\nu_{\max} = \frac{1}{N}\left(\frac{T_m c_V}{V_c}\right)^{0.5}\left(\frac{\zeta\chi c_V}{\rho_1\delta_1 V_c}\right)^{0.25}, \qquad (8)$$

where N is the constant that is approximately equal to 0.1; T_m is the melting temperature of a low-melting point material; c_V is the volumetric velocity of sound; ζ is the thermal conductivity; and χ is the specific heat.

For dissimilar materials, the values for a material that is the first to melt should be used as parameters without indices.

An essential detail of analysis by Wittman et al. is a groundless statement that tensile stresses are always formed due to impact loading at the interface of the joint, and that the amount of the heat released within the joining zone is determined by a fixed portion of the impact energy. In this case, the larger the thickness of a flyer plate, the lower is the maximum permissible velocity at a required impact velocity set by criterion 2. Welding of the plates whose thickness is larger than some critical value becomes impossible, as the maximum permissible velocity (7) is lower than the minimal required one (5). The absence of parameters characterising the material melting heat, probable phase transformations and chemical reactions in the above formulae reduces substantially their significance.

Thorough calculations show that a big part of the deformation energy is concentrated directly in the deformation zone, and the heat released in the weld zone is much in excess of the dissipated impact energy used for the calculations. If we assume that the entire absorbed energy is released within the wave formation zone, estimation of the critical flow rate, at which the zone can be completely fused, yields another, approximately constant limitation of the contact point velocity, which is equal to

$$V_c = \sqrt{\frac{4\pi}{\omega} \frac{(\psi\rho_1(\xi_1 + \chi_1 T_m) + \rho_2(\xi_2 + \chi_2 T_m))}{(1 + \psi)(\rho_1 + \rho_2)}}, \quad (9)$$

where $\psi = \sqrt{\frac{\max(\rho_1, \rho_2)}{\min(\rho_1, \rho_2)}}$; $\xi_{1,2}$ is the melting heat of materials; and ω is the portion of the kinetic energy consumed for wave formation. For similar materials

$$V_c = \sqrt{2\pi(\xi + \chi T_m)/\omega}. \quad (10)$$

This fact, which was experimentally noted by R.V. Stefanovich, is determined by an evident interrelationship of the value of the kinetic energy absorbed by the deformation processes and wave formation parameters (amplitude and length):

$$a \sim \frac{\lambda}{2\psi}, \quad \lambda = 2\pi\delta_1 \frac{\rho_1}{\rho_1 + \rho_2} \frac{\rho_2\delta_2}{\rho_1\delta_1 + \rho_2\delta_2} \sin^2 \gamma. \quad (11)$$

The internal region is a region where welding is probable. However, it should be noted that the attempts to limit the zone of weldability of materials by lines in coordinates (γ, V_c) result from the hydrodynamic approach to the welding theory, and do not quite reflect the point of the phenomenon.

A few notes about the calculation of the dynamic process parameters and acceleration parameters should be added to the above-said. The process of detonation of explosives is described by a simplified Chapman–Jouguet model of the steady-state detonation wave, which allows only for the state of an initial explosive and final reaction products, whereas width of the reaction zone is neglected. Solutions of the gas-dynamic equations combined with the Chapman–Jouguet boundary and initial conditions are adequate only at a sufficiently large size of the charge, when the shock wave and chemical reaction region can be regarded as an explosion. Examples of such calculations are shown in Figures 3 and 4, and described in detail in [6, 8, 13].

Practical calculations are made by using formulae that determine the acceleration velocity or angle as function of the load coefficient [3, 8], as well as formulae for estimation of the acceleration phase of the flyer plate, e.g.:

$$v = 0.8D\sqrt{3R^2/(R^2 + 5R + 4)/(k^2 - 1)}, \quad (12)$$

$$D = D_{max}(1 - x)(1 - e^{-H/H_{min}})^{2(1-x)}, \quad (13)$$

$$h = \sqrt{R}H/5, \quad (14)$$

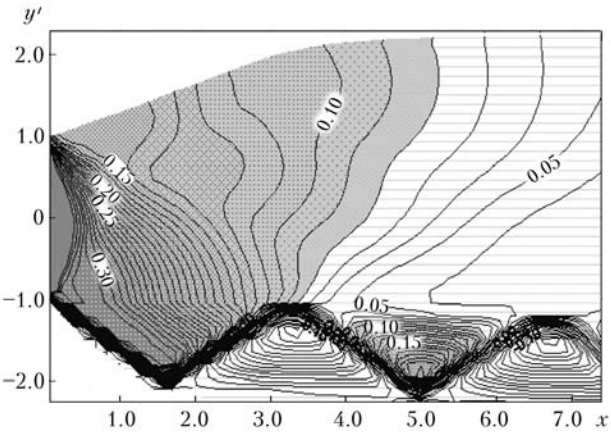

Figure 3. Acceleration of a lead plate by detonation wave at D = = 4000 m/s sliding over its surface. Flow isobars behind the detonation front [13]. Flow isobars in coordinate system related to detonation front $x' = x/H/2$, $y' = y/H/2$, where H is the charge size. Pressure in isobars is related to value kP_D, where k is the adiabatic exponent, $P_D = \rho_0 D^2/(k + 1)$ is the pressure at the detonation front

where R is the explosive to flyer plate weight ratio; k is the experimental adiabatic exponent of the explosion products; D_{max} is the ultimate detonation velocity; H_{min} is the critical diameter of a flat charge; and x is the portion of the inert addition. 80 % of the maximal velocity determined from the known Garni formula is achieved at distance h (14).

Dynamics of high-rate deformation in explosion welding of metals. Assume that the dynamic equations of continuum expressing the laws of conservation of mass, momentum and energy, as well as the additional determining equations specifying the choice of a model deformable media, such as relationship between stresses and strains, equations of state etc., as well as initial and boundary conditions, are valid for all stages of the process under consideration:

$$\frac{\partial \mathbf{U}}{\partial t} + \frac{\partial}{\partial z}\mathbf{F}(\mathbf{U}) + \frac{1}{r}\frac{1}{\partial r} r\mathbf{G}(\mathbf{U}) + \frac{\partial}{\partial r}\mathbf{P}(\mathbf{U}) = 0, \quad (15)$$

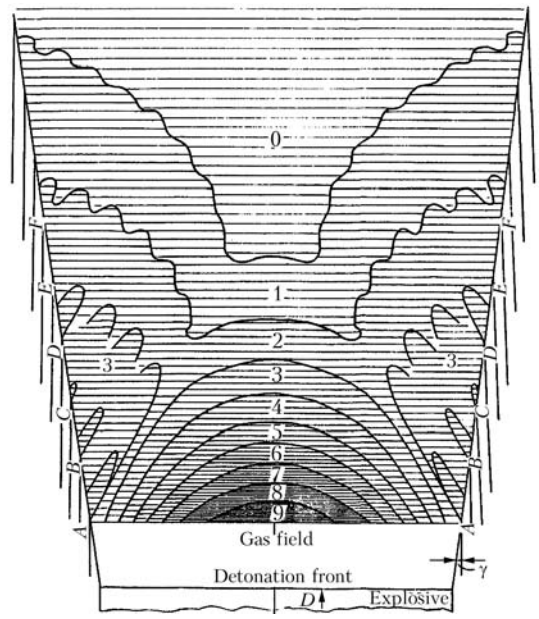

Figure 4. Pressure jumps in detonation products at acceleration of plate packs [8]

$$\mathbf{U} = \begin{bmatrix} \rho \\ \rho u \\ \rho v \\ E \end{bmatrix}, \quad \mathbf{F}(\mathbf{U}) = \begin{bmatrix} \rho u \\ p + \rho u^2 - S_{zz} \\ \rho v u - S_{rz} \\ u(E + p - S_{zz}) - v S_{rz} \end{bmatrix}, \tag{16}$$

$$\mathbf{P}(\mathbf{U}) = \begin{bmatrix} 0 \\ 0 \\ p - S_{\varphi\varphi} \\ 0 \end{bmatrix}, \quad \mathbf{G}(\mathbf{U}) = \begin{bmatrix} \rho v \\ \rho u v - S_{zr} \\ \rho v^2 - S_{rr} + S_{\varphi\varphi} \\ v(E + p - S_{rr}) - u S_{zr} \end{bmatrix},$$

where $p = p(\rho, I)$ and $E = \rho I + \rho(u^2 + v^2)/2$.

For metals, the used equation of state has the following form:

$$p = \sum_{i=0}^{n} k_i (1 - \rho_0/\rho)^i + \gamma\rho(I - I_0), \tag{17}$$

where k_i are the constant experimental parameters; $k_i = 0$ if $(1 - \rho_0/\rho) < 0$.

Stresses and strain rates are related through the Prandtl–Reiss relationships:

$$\frac{\partial S_{rr}}{\partial t} = 2\mu \left(\frac{\partial v}{\partial r} - \frac{1}{3}\left(\frac{\partial u}{\partial z} + \frac{\partial v}{\partial r} + \frac{v}{r} \right) \right) + \left(\frac{\partial v}{\partial z} - \frac{\partial u}{\partial r} \right) S_{zr} - \frac{\mu}{\eta} \varphi S_{rr},$$

$$\frac{\partial S_{\varphi\varphi}}{\partial t} = 2\mu \left(\frac{v}{r} - \frac{1}{3}\left(\frac{\partial u}{\partial z} + \frac{\partial v}{\partial r} + \frac{v}{r} \right) \right) + \frac{\mu}{\eta} \varphi S_{\varphi\varphi},$$

$$\frac{\partial S_{zz}}{\partial t} = 2\mu \left(\frac{\partial u}{\partial z} - \frac{1}{3}\left(\frac{\partial u}{\partial z} + \frac{\partial v}{\partial r} + \frac{v}{r} \right) \right) - \left(\frac{\partial v}{\partial z} - \frac{\partial u}{\partial r} \right) S_{rz} - \frac{\mu}{\eta} \varphi S_{zz}, \tag{18}$$

$$\frac{\partial S_{rz}}{\partial t} = \mu \left(\frac{\partial v}{\partial z} + \frac{\partial u}{\partial r} \right) - \frac{1}{2}\left(\frac{\partial v}{\partial z} - \frac{\partial u}{\partial r} \right) S_{rr} - S_{zz} - \frac{\mu}{\eta} \varphi S_{rz},$$

$$\varphi = \begin{cases} 1 - \dfrac{Y\sqrt{2}}{\sqrt{3(S_{zz}^2 + S_{rr}^2 + S_{\varphi\varphi}^2 + 2S_{zr}^2)}}, & \text{if } \sqrt{\dfrac{2}{3}} Y \le (S_{ij} S_{ij})^{1/2}, \\ 0, & \text{if } \sqrt{\dfrac{2}{3}} Y > (S_{ij} S_{ij})^{1/2}, \end{cases}$$

where t is the time; r and z are the Euler coordinates (cylindrical symmetry); ρ is the density; u and v are the components of velocity vector w (in directions z and r, respectively); I is the specific internal energy; E is the density of the total energy; p is the pressure; S_{ij} is the stress deviator, which was determined by subtracting the isotropic component from the total stress tensor $\sigma_{ij} = (-p\delta_{ij} + S_{ij})$; Y is the dynamic yield stress; μ is the shear modulus; and η is the viscosity factor.

Consider dependence of dynamic yield stress Y of a material and shear modulus upon the intensity of plastic deformation ε^p, pressure, deformation rate, density and temperature, e.g.

$$Y = Y_0(1 + \beta\varepsilon^p)^n \, [1 + bp(\rho_0/\rho)^{1/3} - h(T - 300)],$$

$$Y_0(1 + \beta\varepsilon^p)^n \le Y_{\max}, \tag{19}$$

$$Y = 0, \text{ if } T \ge T_m, \tag{20}$$

$$T_m = T_{m0}(\rho_0/\rho)^{2/3} \exp\,[2\gamma_0(1 - \rho_0/\rho)], \tag{21}$$

$$\varepsilon^p = \frac{\sqrt{2}}{3}\,[(\varepsilon_{rr}^p - \varepsilon_{zz}^p)^2 + (\varepsilon_{rr}^p - \varepsilon_{\varphi\varphi}^p)^2 + (\varepsilon_{zz}^p - \varepsilon_{\varphi\varphi}^p)^2 + 3/2(\varepsilon_{rz}^p)^2]^{1/2}, \tag{22}$$

$$\frac{d\varepsilon_{ik}^p}{dt} = \frac{\varphi}{2\eta} S_{ik}, \tag{23}$$

$$\eta = \eta_0 \exp\,(T_0/T), \tag{24}$$

$$\mu = \mu_0[1 + bp(\rho_0/\rho)^{1/3} - h(T - 300], \tag{25}$$

$$T = \frac{I - I_0}{3R}, \text{ where } I_0 = \sum_{j=0}^{4} \varepsilon_{0j}(1 - \rho_0/\rho)^j. \tag{26}$$

Constant parameters Y, β, b, h, $Y_{\min}$, T_{m0}, T_0 and η_0 in formulae (17) through (26) were determined experimentally for a number of metals, e.g. copper: $\rho_0 = 8.93$, $\gamma_0 = 1.99$, $k_1 = 1.386 \cdot 10^{12}$, $k_2 = 2.749 \cdot 10^{12}$, $k_3 = 5.113 \cdot 10^{12}$, $Y_0 = 1.2 \cdot 10^9$, $\beta = 36$, $n = 0.45$, $b = 3 \cdot 10^{-12}$, $h = 3.8 \cdot 10^{-4}$, $Y_{\max} = 6 \cdot 10^9$, $T_{m0} = 1790$, $\mu_0 = 4.77 \cdot 10^{11}$, $\eta_0 = 0.5$, $T_0 = 4380$, $\varepsilon_{00} = -1.178 \cdot 10^9$, $\varepsilon_{01} = -2.344 \cdot 10^9$, $\varepsilon_{02} = 7.529 \cdot 10^{10}$, $\varepsilon_{03} = 1.526 \cdot 10^{11}$, $\varepsilon_{04} = 2.19 \cdot 10^{11}$, and $R = -\varepsilon_{00}/900$.

To specify the kind of determining relationships in implementation of a numerical experiment, we will additionally use the information about physical properties of the medium and its structure in the form of kinetic relationships for inelastic deformation and fracture mechanisms. In this case, properties of the velocity sensitivity of materials, which affect the process of the dynamic behaviour, are important [8]. If this information is absent, the approaches based on thermodynamic concepts or indirect experimental data are used.

Similar dynamic equations of continuum for a multi-phase multi-component flow with chemical reactions, which express the laws of conservation of mass, momentum and energy, are valid for an explosive at all three stages of the detonation process [13].

The predictor-corrector method was used, in particular, to achieve the second order of accuracy, both in time and space, to solve the finite difference analogues of differential equations of conservation. Artificial viscosity of the tensor type or the Harten TVD dissipation mechanism was additionally introduced to produce non-oscillatory flows. This stabilised the method and maintained its order of accuracy.

To illustrate it, Figures 5–7 show the results of solving the non-stationary problem on initiation of the 8 mm thick ammonite charge by impact with a steel striker 3 mm in diameter, throwing of an aluminium plate 2.5 mm thick, and its collision with a similar plate located at a distance of 2.5 mm from the first one.

In particular, formation and behaviour of non-stationary plastic waves were studied. The flowability condition is met, and a material is in the state of plastic flow in the zones shown in Figure 5, which are limited by maximal level isolines of the second

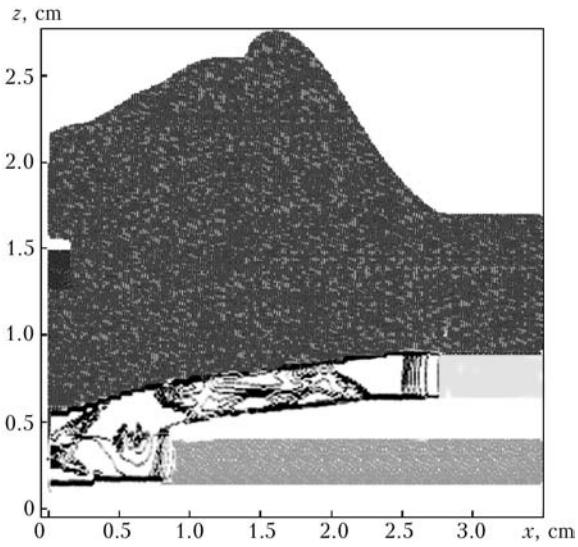

Figure 5. General flow pattern and isolines of the second invariant of stress deviator (7.5 μs)

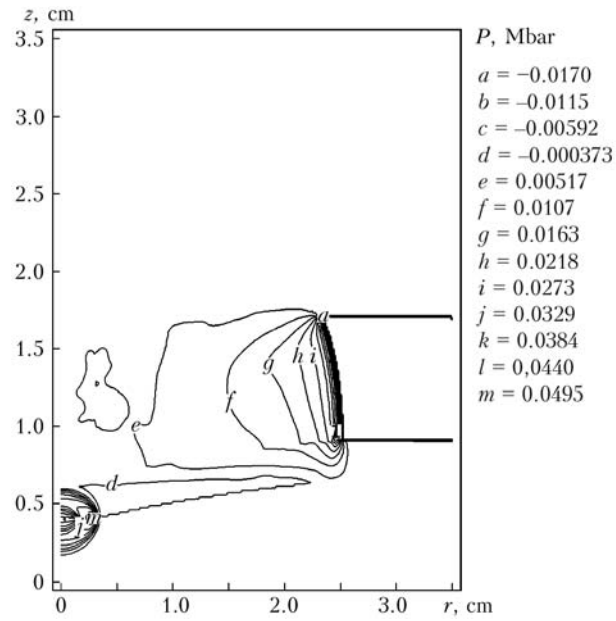

Figure 6. Isobars at acceleration and collision of two aluminium disks 2.5 mm thick (6.5 μs)

invariant of stress deviator. Subsonic motion and surface deformation are formed with time in a region of the initially normal contact of the plates. In case of an asymmetric oblique collision, the jet nucleus, while growing, penetrates with its apex under an excessively high pressure into the incoming metal, forms forward and backward crests, and leaves voids, where surface contaminants and oxides are accumulated. The above flow patterns reflect dynamics of the wave fronts in relatively rigid collision conditions, where the probability exists of distortions of waveforms and vortex zones, caused by a gradient of longitudinal components of velocities of the flyer and target plates. As voids are formed in the vortex wave path, the condition for achieving the total strength coincides with the conditions of stable formation of a moderate laminar deformation wave. Geometric dimensions of deformation waves do not depend upon the contact point velocities or impact velocity, and the degree of plastic deformation at the nucleus is determined exclusively by the collision angle only in the high-velocity flow modes.

Parametric analysis and systemitisation of results allow evaluating the flow stress and specifying the above semi-empirical criteria, which determine the minimal impact (modulus and direction) velocity vector required for inelastic collision, at which plastic waves begin to propagate ahead of the movable contact and lead to pressing out of surface layers in a direction of movement of the collapsing metal plates. The initially normal supersonic to subsonic flow transition conditions are explicitly related in all wave modes (elastic, plastic, surface) (Figure 7) to the required conditions for explosion welding. When metals welded have equal or insignificantly differing strength, expression of the type of (5) does not contradict to experimental data. However, when determining the lower limit of welding for dissimilar metals, if they are substantially different in strength (dynamic yield stress), the question arises: strength of what metal has to be chosen for equation of the type of (5). Numerical calculations made within the frames

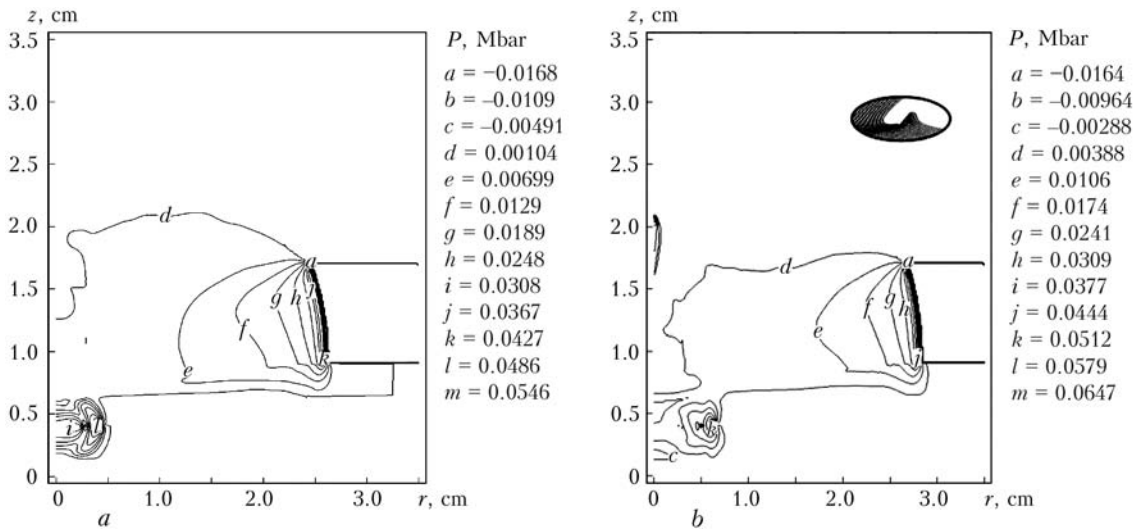

Figure 7. Flow patterns corresponding to 7.0 (*a*) and 7.5 μs (*b*) (swelling of the first hump)

of a more sophisticated model of plastic flow give an idea how the wave formation mechanism related to plastic deformation ahead of the contact point is excited. Step-by-step pressing out and penetration of metals ahead of the contact point at frequency V_c/λ are probable, if resistance to penetration of the jet periodically changes. The calculation confirms that yield stresses substantially change already at the initial stage of impact. The flow of surface layers is adjusted by the deformation rate, and parameters of microjets under moderate conditions are determined by the velocity dependence of the flow stresses of metals. At the same time, the dynamic yield stress is an adequate characteristic of resistance of metal to plastic deformation, as the process is accompanied by very high deformation rates $\dot{\varepsilon} = V_c/\lambda$, and its value is much in excess of the static one. Despite the fact that resistance of metals to plastic deformation at a high deformation rate increases, we failed to substantiate an assumption of levelling of the dynamic yield stresses and their approaching the values of theoretic shear strength of crystal, $\mu b/2\pi a$. Dramatic growth of the deformation temperature turns out to be more important. At the same time, the penetration ability of microjets is almost independent of strength characteristics of a soft metal in pair, and is determined to a greater degree by the yield stress of a hard metal, as is the case of such pairs as titanium–lead, tungsten–copper etc., which are contrast in properties.

Therefore, within the range of low collision velocities and angles, which is close to the elastic zone, where the strains are low and temperature dependence of the yield stress is not yet too pronounced, the flow stress is determined by compression, strain and strain rate. At the same time, under the developed conditions it is primarily determined by a viscous resistance to deformation, which reaches considerable values, and the value of the specific energy of viscous forces is of the same order as the melting heat.

The cumulation parameters determine a portion of the energy dissipated in the impact zone, as well as the phenomena associated with the upper welding limit. Analysis of the numerical experiment shows that the velocity of the jet in its alternate pressing out from the collision zone is close to the contact point velocity determined by the velocity of the surface plastic wave, while portions of the plastic deformation energy per unit width of the zone, released during cycle time $1/V_c$, are proportional to value $\mu_1\lambda_i^2$, and, hence, the specific power is $\sim \lambda\sqrt{\mu^2/\rho}$.

Independence of the critical transition velocity upon the collision angle, as noted above, was experimentally proved. Additional experimental check of the criterion was continued in further experiments conducted at increased technological temperatures to study collision of tungsten and molybdenum plates and copper clad with thin titanium, molybdenum or iron layers, by heating either one flyer plate (tungsten plate) or both plates. In high-rate heating above the brittle temperature of a refractory component up to the recrystallisation temperature, hardness of a material dramatically fell, like the values calculated from the Wittman criterion, whereas the transition boundary and the welding limit changed not that dramatically (1300–1400 m/s for the collision angles ranging from 10 to 15°). This is indicative either of a high value of toughness of metals or of a relatively high shear strength of the lattice. The value of the shear modulus of metals, which falls in this case by no more than 20 %, better correlates with the experimental data. Constancy of the transition velocity noted by Wittman, Cowan and Holtzman is related to the principles of propagation of elastic and plastic surface waves, peculiarities of the behaviour of which at the velocities close to the first mode of the surface wave were experimentally observed by A.I. Yadevich.

Similar processes of redistribution of the impact energy, heating of the particle surfaces by deformation and adhesion (consolidation) occur when a sufficiently intense shock wave propagates in a powdered or porous medium. Numerical analysis of the consolidation experiments showed that the mode of microcumulation in pores at contact of the particles is determined, first of all, by the velocity of the flow behind the shock wave front, which should be comparable, like in explosion welding, with the velocity of shear waves. In this case, density of the dissipated energy over the particle contacts greatly depends upon the orientation of the particles with respect to the front, as well as upon the mass velocity of the flow behind the shock wave. Dissipation power is proportional to $\delta\sqrt{\mu^3/\rho}$, where δ is determined by sizes of the particles, their shape and orientation. The process of pulsed consolidation welding in treatment of high-modulus joints requires very high loading velocities and, accordingly, pressures, which cannot be achieved under conditions of a real experiment. As shown by the calculation, a short time of the effect on the powder particles does not allow heating them homogeneously. Hence, we have a scatter of strength characteristics of a compact. In this case, if microcumulation cannot be achieved at the shock front to satisfy the above welding requirements, we can provide the required deformation temperature and conditions by the method of hot impact pressing. The approach alternative to cold pressing consists in preliminary thermal activation of the process to decrease critical values of the treatment velocity.

Application of pulsed welding and treatment methods. The State Research and Production Association for Powder Metallurgy has been using explosion welding for production of bimetals for subsequent rolling and roll welding since 1968. The leading specialists in the field admit that Belarus produces the widest range different-application bimetals. The efficiency of commercial application of new products and saving of critical and expensive materials and electric power are provided through combining dissimilar materials in composites having the required set of properties, such as corrosion resistance, surface hardness,

Figure 8. Materials and products made by explosion welding and consolidation: *a* — copper–titanium and aluminium–steel adapters characterised by increased heat resistance for electrolytic cells; *b* — panels of light aluminium alloys; *c* — titanium–copper and aluminium–titanium heat exchangers; *d* — movable operating elements of tillage machines; *e* — zirconium bronze and molybdenum billets; *f* — multilayer composite materials; *g* — billets for coaxial piston pumps; *h*, *i* — composite products for microelectronics — Cr, Ti–W, Ni–Cr–Si (*h*), and silicides Ti, W, Mo, Ta (*i*)

wear resistance, impact resistance, toughness, strength, thermal conductivity, thermal expansion coefficients, electric and magnetic characteristics (Figure 8).

High performance of bimetal plates based on structural materials with claddings of titanium, tantalum and stainless steels for vessels applied in nuclear, chemical and vacuum engineering allow using them in the most critical structures operating under the simultaneous effect by high temperature, steam, pressure, chemical reagents etc. Explosion cladding is efficient for manufacture of tube plates for heat exchanging devices, heavy-loaded sliding bearings, axial piston pumps, bipolar electrodes for hydrometallurgy, panels of light alloys, ultrasonic panels, various adapters consisting of more than 300 pairs of dissimilar metals and alloys, reinforced composite materials, and many others. Pack welding of metals by rolling, combined with explosion cladding, widens technological capabilities of the method and ranges of the materials joined, and removes limitations to maximal thickness of layered compositions.

Lately, the Association has suggested and implemented explosion treatment by using special machine tools. The process includes preliminary high-temperature heating and degassing of a material treated, percussion welding and subsequent quenching. Widening of the range of thermodynamic states of the matter made it possible to produce compacts and materials from composites and powders, including from refractory chemical compounds with strong covalent bonds (nitrides, carbides, borides and silicides). Development of these efforts resulted in formation of new research areas for long-term outlook.

1. Abrahamson, G.R. (1961) Residual periodical deformations of surface under action of moving jet. *Proc. of ASMI, Series E, Appl. Mechanics*, 28(**4**), 45–55.
2. Cowan, G.R., Holtzman, A.H. (1963) Flow configurations in colliding plates: Explosive banding. *J. Appl. Phys.*, 34(**4**), 928–939.
3. Deribas, A.A., Kudinov, V.M., Matveenkov, F.I. (1967) Effect of initial parameters on process of wave formation during explosion welding of metals. *Phys. of Combustion and Explosion*, 3(**4**), 561–568.
4. Godunov, S.K. et al. (1971) Wave formation during explosion welding. *J. Appl. Mechanics and Techn. Phys.*, **3**, 63–73.
5. Cowan, G.R., Bergmann, O.R., Holtzman, A.H. (1971) Mechanism of bond zone wave formation in explosion clad metals. *Metallurg. Transact.*, 11(**2**), 3145–3155.
6. Deribas, A.A. (1972) *Physics of explosion strengthening and welding*. Novosibirsk: Nauka.
7. Karpenter, S. (1976) *Explosion welding of metals*. Minsk: Belarus.
8. Belyaev, V.I., Kovalevsky, V.I., Smirnov, G.V. et al. (1976) *High-frequency deformation of metals*. Minsk: Nauka i Tekhnika.
9. Kudinov, V.M., Koroteev, A.Ya. (1978) *Explosion welding in metallurgy*. Moscow: Metallurgiya.
10. Kovalevsky, V.N., Belyaev, V.I., Smirnov, G.V. (1979) Anwendungsmoeglichkeiten des Explosionsschweissens fuer die Herstellung von Verbundmaterialen. *Z. Metallkunde*, **2**.
11. Zakharenko, I.D. (1990) *Explosion welding of metals*. Minsk: Nauka i Tekhnika.
12. Petushkov, V.G., Simonov, V.F., Sedykh, V.S. et al. (1995) *Explosion welding criteria*. Cambridge.
13. Smirnov, G.V. (1990) *Effects of dynamic cumulation*. Minsk: Remiko.

ON THE INFLUENCE OF SHOCK WAVE ON WELDING GAP INCREASE IN PRODUCTION OF LARGE-SIZED SHEET COMPOSITES BY EXPLOSION WELDING

Yu.P. BESSHAPOSHNIKOV[1], **V.E. KOZHEVNIKOV**[1], **V.I. CHERNUKHIN**[1] and **V.V. PAJ**[2]

[1]OJSC «Uralkhimmash», Ekaterinburg, RF

[2]M.A. Lavrentiev Institute of Hydrodynamics, RAS SD, Novosibirsk, RF

Dependence of increase of the length of shock wave formed within the joining zone between tita nium and steel in explosion welding on path length of the detonation wave has been studied. A simplified calc ulation model of the given process is suggested, based on an assumption that the key factor affecting increase in shock wave length is expansion of the gap between the plates located in parallel due to the impact on them of an air plug formed ahead of the contact point.

Keywords: *explosion welding, shock wave, welding gap, shock wave length, collision angle*

Explosion welding of large-sized sheet blanks runs into a problem of stabilizing the main process parameters, namely detonation rate and collision angle. The shock wave formed in the gap between the blanks ahead of the contact point in case of a very long charge can essentially displace the flyer plate. Moving at an acceleration, the plate causes explosive densification by acting on it. As a result, the formed gas plug, on the one hand, increases the welding gap, and on the other, can promote a change in the detonation rate because of the explosive densification. Increase of overall dimensions of welded blanks from metals prone to formation of brittle chemical compounds, namely intermetallics, makes the situation even more complicated.

This means, primarily, an increase in the volume of the intermetallic interlayer as a result of the change of explosion welding conditions, namely increase of

the explosive detonation rate, increase of the angle of collision because of the possible increase of the welding gap, additional heating of the surfaces being welded by the compressed air plug, moving ahead of the contact point.

The above factors can take the parameters of collision mode of the blanks being welded beyond the optimum values (Figure 1). In this connection, stabilization of the main parameters of the process, namely detonation rate and angle of collision, in explosion welding of large-sized blanks, is an important task.

This work presents some results of investigations on the subject of the influence of the air plug moving between the blanks ahead of the contact point, on the increase of the welding gap.

Selected as objects of study were two blanks of tubesheets of 2100 × 2200 mm size from 09G2S steel of thickness δ_2 = 60 mm clad by a layer of VT1-0 titanium of thickness δ_1 = 5 mm. Schematic of explosion welding was «parallel» with the setting welding gap of width h = 4 mm. Firing of explosive, placed on top of the titanium sheet in a layer of thickness H = 50 mm, was performed from the charge corner. After cladding, heat treatment and straightening samples were cut out along the lines normal to the projection of the detonation front (Figure 2). Linear dimensions of the bimetal blanks were measured before that. These dimensions turned out to be greater than the initial ones by 30–40 mm (see Figure 2), which is indicative of formation of high plastic longitudinal deformations during high-velocity loading of the metals being welded.

Microsections were prepared from part of the samples to measure the parameters of waves, formed on the surface of steel + titanium joint during collision of the layers being welded. Results of measurement of the dimensions of these waves along the length are given in Table 1. It is seen from the Table that with increase of distance L from the point of the start of plate collision an increase of average value of wave length from $\lambda \approx 0.8$ mm in the initial welding zone up to $\lambda \approx 1.1$ mm in the conditionally middle welding zone and up to $\lambda \approx 1.4$ mm in its final section takes place. It is known [1, 2] that $\lambda \sim \sin^2(\gamma/2)$, if $\delta_2 >> \delta_1$ (in our case $\delta_2 = 12\delta_1$). Then, assuming that $\lambda \approx 0.8$ mm corresponding to the initial angle of collision, it is easy to find angles of collision corresponding to the middle welding zone and its final section, provided the initial angle of collision is known. In order to evaluate it, an experiment was conducted on plate acceleration using the procedure of [3]. Used here was a titanium plate of 500 × 300 × 5 mm size. Charge of thickness H = 50 mm consisted of the same explosive as in cladding of tubesheet blanks. Explosive density was equal to approximately 0.9 g/cm^3, detonation rate was $D \approx 2500$ m/s. Measurements showed that at acceleration distance of 4 mm angle of rotation β (see Figure 1) of the titanium plate is equal to about 11.8°. Therefore, we believe that the initial collision angle γ = 11.8°. Then it is easy to demonstrate that

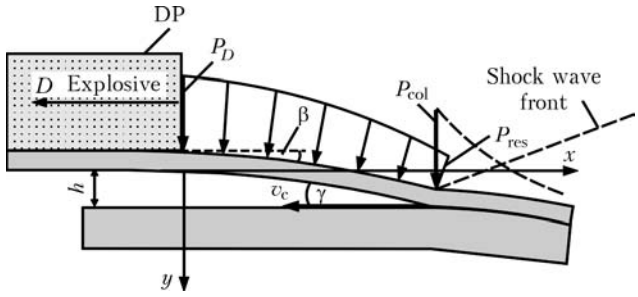

Figure 1. Schematic of explosive welding at parallel location of the plates: D — detonation rate of explosive charge; P_D — pressure at detonation wave front; h — welding gap; β — angle of rotation of flyer plate; P_{col} — pressure of detonation products (DP) before plate collision; P_{res} — DP peak residual pressure; v_c — contact point velocity; γ — collision angle

in the middle zone γ = 13.6°, and in the final section γ = 15.3°. It is interesting to note that if the shock wave length is found from the well-known formula from [2] $\lambda = A\delta_1 \sin^2(\gamma/2)$, in our case the coefficient of proportionality A should be equal to 16.

Calculation of welding gaps, which should correspond to the found angles of collision in the middle and final welding zones, showed that $h \approx 7$ mm at γ = = 13.6° and h = 11 mm at γ = 15.3°. Calculations were conducted using two-dimensional model [4, 5] at polytropic coefficient k = 2.5, as for this value the best agreement of the experimental acceleration curve with the calculated profile of plate acceleration was found.

In addition, the gap can be calculated using the equation of motion, given in the form of the following expression:

$$\Delta h = pt^2/(2m_{pl}), \qquad (1)$$

where p is the pressure in the air plug; t is the time; m_{pl} is the flyer plate mass per a unit of area.

Proceeding from the results of [6] and relatively low detonation rate we believe that the influence of the cloud of finely-dispersed metal particles of the

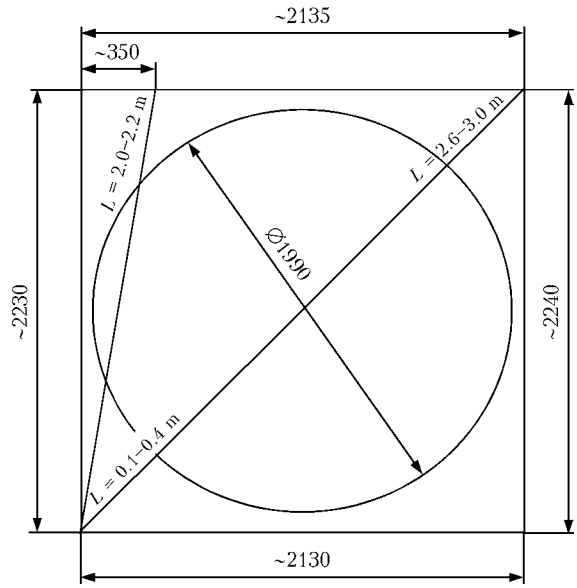

Figure 2. Schematic of marking the bimetal blank from 09G2S steel + VT1-0 titanium for cutting out the tubesheet and samples for investigation

Table 1. Results of measurement of length λ of shock wave (mm)

Welding zone	L, m	1st tubesheet	2nd tubesheet	Total average value
Initial	0.1 0.2 0.4	0.80 0.78 0.80 (middle 0.79)	0.80 0.92 0.90 (middle 0.87)	≈ 0.8
Middle	2.0 2.1 2.2	1.04 1.00 — (middle 1.02)	1.20 1.18 1.20 (middle 1.19)	≈ 1.1
Final	2.6 2.7 2.8 2.9 3.0	1.20 1.56 1.38 1.36 1.38 (middle 1.38)	1.60 1.35 1.45 1.30 1.35 (middle 1.41)	≈ 1.4

Table 2. Results of calculations and measurements of the dependence of welding gap width h on distance b from the point of the start of plate collision

L, m	$t(t - 28)$, μs	$h = h_0 + \Delta$, mm		Relative deviation of calculation from experiment, %
		Calculation to (1)	Experiment + 2D calculation [4, 5]	
0 0.4	0 28 (0)	4 6 (4)	4 4	0 50 (0)
2.1	148 (120)	9 (7)	7	30 (0)
2.8	198 (170)	13 (10)	11	20 (10)

Notes. 1. Values of the respective parameters under the condition of starting the time reading at $L = 0.4$ m are shown in parenthesis. 2. $m_{pl} = 22/5$ kg/m^2; $p = 10$ MPa.

backflow arising at glancing collision of the plates [7] on the air plug parameters is neglectable. Then values of p and t are found from well-known expressions of gas dynamics for the case of solution of the piston problem [8], which in this case have the following form:

$$v_c^2 = (p - p_0)^2 \frac{2/\rho_0}{(k_{air} + 1)p + (k_{air} - 1)p_0}, \quad t = \frac{\rho_0}{\rho} \frac{L}{v_c},$$

where $p_0 \approx 1 \cdot 10^5$ Pa is the initial pressure; $\rho_0 \approx$ ≈ 1.3 kg/m^3 is the air density; $k_{air} = 1.4$ is the polytropic coefficient of air; $\rho = \rho_0 \frac{(k_{air} + 1)p + (k_{air} - 1)p_0}{(k_{air} - 1)p + (k_{air} + 1)p_0}$ is the density of the air plug.

For simplicity let us take distance L for the middle and final zones of welding as its average value — 2.1 and 2.8 m, respectively. Table 2 gives the assessed values of the welding gap, determined by the two above methods at different values of L. It is seen from the Table that agreement of the experimental and caluclated data is markedly improved, if time reading starts from $L = 0.4$ m. Here for the final section the agreement between the calculated and experimental data remains to be satisfactory both allowing for and without allowing for the time shift (28 μs). These results are indicative of the fact that in our case the air plug, capable of noticeably displacing the flyer plate, formed, probably, at a certain distance from the start of the process of plate collision. It may be assumed that in the initial welding zone, the length of which is approximately 0.5 m, the air plug is either absent, or is at the stage of initiation (formation), which requires additional study. In other respects the experimental and calculated results are in good agreement with the conclusions of [9].

1. Cowan, G., Holtzman, A. (1963) Flow configuration in colliding plates. *J. Appl. Phys.*, 34(**4**), 928–939.
2. Deribas, A.A., Kudinov, V.M., Matveenkov, F.I. et al. (1968) About modeling of wave formation process in explosion welding. *Fizika Goreniya i Vzryva*, **1**, 100–107.
3. Kuzmin, G.E., Mali, V.I., Paj, V.V. (1973) About acceleration of flat plates by layers of condensed explosives. *Ibid.*, 9(**4**), 558–562.
4. Kuzmin, G.E. (1978) *Application of numerical methods in problems of explosion compacting and welding*: Syn. of Thesis for Cand. of Techn. Sci. Degree. Novosibirsk.
5. Kuzmin, G.E. (1977) About acceleration of plates in conditions of explosion welding. In: *Mechanics of explosion process. Dynamics of continuum*. Issue 29, 137–142.
6. Ishutkin, S.N., Kirko, V.I., Simonov, V.I. (1980) Investigation of heat effect of shock-compressed gas on the surface of colliding plates. *Fizika Goreniya i Vzryva*, 16(**6**), 69–73.
7. Deribas, A.A., Zakharenko, I.D. (1974) About surface effects at glancing collision of metallic plates. *Ibid.*, 10(**3**), 409–421.
8. Ovsyannikov, L.V. (1981) *Lectures on fundamentals of gas dynamics*. Moscow: Nauka.
9. Kudinov, V.M., Koroteev, A.Ya. (1978) *Explosion welding in metallurgy*. Moscow: Metallurgiya.

DETERMINATION OF THE PARAMETERS OF SHOCK-COMPRESSED GAS IN THE WELDING GAP AHEAD OF THE CONTACT POINT IN EXPLOSION CLADDING

S.Yu. BONDARENKO[1], **D.V. RIKHTER**[2], **O.L. PERVUKHINA**[2] and **L.B. PERVUKHIN**[2]
[1]Altai State Agricultral University, Barnaul, RF
[2]Institute of Structural Macrokinetics and Materials Science, RAS, Chernogolovka, RF

Dynamics of formation of shock-compressed gas region is considered, and dependence of the maximum length of the compressed-gas region on the contact point velocity and plate length has been derived. A hypothesis is offered that thermal ionization of gas to form thin layers of low-temperature plasma takes place at the interface in the welding gap ahead of the contact point in the supersonic flow (5–6 Mach) of the shock-compressed gas over the surfaces being welded.

Keywords: *explosion cladding, gap between the plates, shock-compressed gas, gas parameters, thermal ionization of gas*

In explosion welding of large-sized metal plates the welding quality is affected by gas present in the gap between the plates [1, 2]. After collision of the latter the contact point moves along the plates being welded, forming a region of shock-compressed gas ahead of it, thus having the role of a «piston», the size of which increases with the distance covered [3]. The impact of this flow leads to metal heating and melting of its surface before collision [4], which may have an essential influence on the joint quality [5]. Based on similar experiments, a conclusion is made in [6] that the air shock wave forms high-temperature plasma in the gap. The heat flow coming from the plasma heats the plate surface layer up to the melting temperature, thus ensuring welding together of the plates at subsequent contact.

In [7, 8] a photoelectric method was used for measurement of brightness temperature near the contact point. Experimental data show that temperature at detonation velocity D = 4200 m/s is equal to 7700 K, and at D = 5300 m/s it is 10,500 K.

Analysis of this work, as well as the results of experiments conducted by the method of «traps» [9] to entrap the particles flying out of the welding gap with the shock-compressed gas, showed that the processes occurring in the welding gap ahead of the contact point when producing the joints require additional study.

Calculation procedure. The contact line is of a finite length, so that region of shock-compressed gas forms only within its length (and gap width). As the region of shock-compressed gas here is adjacent to undisturbed air, leakage form the shock-compressed gas region beyond the limits of the «piston» into the ambient space is inevitable. Gradient of pressure formed between the compressed and undisturbed gas to the side of the piston, and aimed along the contact line, accelerates the gas up to a certain velocity, which in this case is the outflow velocity v (Figure 1).

Influence of the region of shock-compressed gas on the surfaces being welded depends, primarily, on its thermal-energy parameters and time t of impact, which is determined by the linear size of this region along the contact point velocity vector.

In keeping with the law of conservation of mass, the region of shock-compressed gas will stop increasing, if the mass of air m_{ent} additionally «entrained» by the shock wave in a unit of time and mass m_{out} of outflowing air are equal

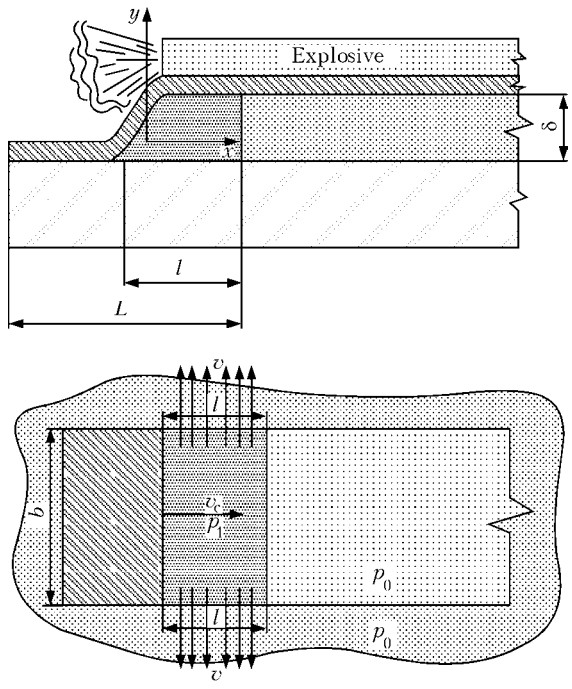

Figure 1. Direction of outflow from the welding gap: L — distance covered by the contact point; δ — gap width; for other designations see the text

$$\frac{dm_{ent}}{dt} = \frac{dm_{out}}{dt} = \text{const}. \quad (1)$$

As a result, we obtain a totality of two problems, namely problem of a moved-in piston (determination of parameters behind the shock wave) and problem of the velocity of gas outflow from the volume, which must be solved simultaneously.

Procedure of calculation of shock-compressed gas parameters. We will use the equation of percussive adiabat given in [10] for calculations:

$$\frac{p_1}{p_0} = \frac{6 - V_1/V_0}{8V_1/V_0 - 1}; \quad \frac{\rho_0}{\rho_1} = \frac{V_1}{V_0} = \frac{p_1/p_0 + 6}{8p_1/p_0 + 1}; \quad \frac{T_1}{T_0} = \frac{p_1 V_1}{p_0 V_0}, \quad (2)$$

and expressing the shock wave amplitude through Mach number, we get

$$\frac{7}{5} M^2 = \frac{p_1/p_0 - 1}{1 - V_1/V_0}, \quad (3)$$

where p_1, p_0 are the absolute pressures in the region of shock-compressed gas and ambient atmosphere; ρ_1, ρ_0 is the gas density before and after rupture; T_1, T_2 is the gas temperature before and after rupture; V_1, V_0 are the volumes of gas before and after compression; M is the Mach number.

Hence, we can obtain any required parameter ratio.

Determinations of outflow velocity, gas flow rate, as well as conditions, essentially affecting the process of its outflow, are the main problems of thermodynamic analysis for the gas flow.

Despite the fact that the region of shock-compressed gas moves relative to atmospheric air at supersonic velocity, and the molecules are entrained into ordered motion behind the shock wave, in the laboratory system of reference they are «stationary» relative to the contact line.

At adiabatic steady-state gas flow, the theoretical gas mass flow per a unit of time m_{out} and theoretical velocity of its outflow v in our case can be determined using expressions given in [5] for critical velocity v_{cr} and temperature T_{cr} of gas flow:

$$m_{out} = f\sqrt{\frac{2\gamma}{\gamma+1} p_1\rho_1 \left(\frac{2}{\gamma+1}\right)^{2/(\gamma-1)}}; \quad v_{cr} = \sqrt{\frac{2\gamma}{\gamma+1} RT_{cr}}, \quad (4)$$

where f is the cross-sectional area; γ is the adiabatic exponent for outflowing gas; R is the gas constant.

As the gas flows, its pressure and temperature usually decrease, and, therefore, also the local velocity of sound. Theoretically, the function of mass and outflow velocity should be an integral function, but in explosion welding at gas outflow beyond the limits of the plate region and gas mass loss, no pressure drop occurs, and mass loss is compensated by reduction of the region of shock-compressed gas, i.e. by parameter f, and pressure restoration.

Determination of geometrical characteristics of the shock-compressed gas region. To determine the geometrical characteristics of the shock-compressed gas region, we will use the above dependencies to jointly solve two problems and follow the dynamics of growth of the shock-compressed gas region. In the classical theory of explosion welding the velocity of the shock wave front motion is taken to be approximately 1.2–1.4 times higher than the contact point velocity. At the initial moment of contact point motion, this is exactly the case. But at the moment of the shock wave separation from the contact line and at value l of the shock-compressed gas zone length (see Figure 1) different from zero, velocity decreases with l increase in connection with an increasing gas flow, until it becomes equal to contact point velocity v_c, i.e. this shock wave is the head wave at flowing around the body.

Derived dependence $l = f(L)$ becomes

$$l = \frac{L\rho_0 b}{\rho_1 b + 2\frac{L}{v_c}\sqrt{\frac{2\gamma}{\gamma+1} p_1\rho_1 \left(\frac{2}{\gamma+1}\right)^{2/(\gamma-1)}}}, \quad (5)$$

where b is the length of contact line (sheet width) (see Figure 1).

Calculations show (Figure 2) that the dimensions of the shock-compressed gas region are stabilized and depend essentially on v_c. Thus, a piston of shock-compressed gas moves in the welding gap at the velocity equal to v_c, i.e. high-velocity flowing of shock-compressed gas around the surfaces being welded takes place (see Figure 1).

Performed calculations of shock-compressed wave parameters ahead of the contact point do not allow for gas temperature increase at high-velocity flowing around the surface of the plates being welded. Calculations allowing for the braking temperature show that in explosion welding modes, applied in commercial production of the bimetal (D = 2500 m/s) increase of gas temperature in the boundary layer without allowing for heat conductivity will be equal to

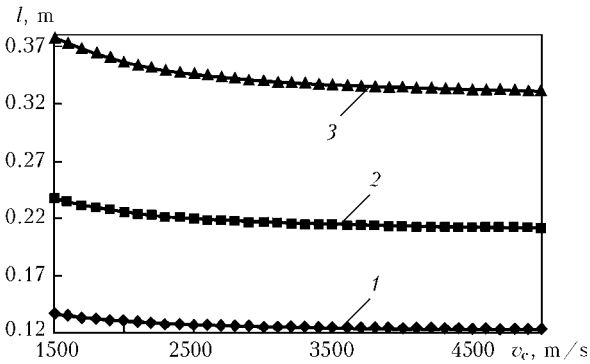

Figure 2. Dependence of extent l of the zone of shock-compressed gas on contact point velocity v_c and plate width b: *1* — b = 0.5; *2* — 1.0; *3* — 2.0 m

3400 K; at increase of detonation velocity up to 3500 m/s it will be equal to 6400 K.

Thus, summation of calculated temperature in the region of shock-compressed gas with the temperature in the boundary layer points shows that the temperature in the point of flowing of the shock-compressed gas over the surfaces being welded is equal to about 6000–12,000 K, i.e. reaches the temperature of gas transition into the plasma state («cold» plasma) [11].

CONCLUSIONS

1. Determination of the parameters of shock-compressed gas between the plates being welded in parallel explosion welding ahead of the contact point is the problem of supersonic flowing around a body, which can be conditionally divided into two problems, namely that of a moved-in piston with determination of gas parameters behind the shock wave, and problem of the velocity of gas outflow from the welding gap. A simultaneous solution of these problems is proposed and it is shown that the size of the region of shock-compressed gas is limited and at the same gas it depends only on plate width and contact point velocity. Gas parameters in this region, namely p_1, temperature T_1 and density ρ_1, were determined.

2. Conducted assessments of temperature in the shock-compressed gas allowing for its high-velocity flowing around the surface being welded allowed putting forward the following hypothesis: thermal ionization of gas with formation of thin layers of low-temperature («cold») plasma takes place in the welding gap ahead of the contact point at supersonic (5–6 Mach) flowing of shock-compressed gas around the surfaces being welded.

1. Richter, U. (1973) Application of explosive-welded bimetals to constructing apparatuses for chemical industry. In: *Proc. of 2nd Int. Conf. on Explosives* (Marianske Lazne, CSSR, 1973), 253–261.
2. Kudinov, V.M., Koroteev, A.Ya. (1978) *Explosion welding in metallurgy*. Moscow: Metallurgiya.
3. Deribas, A.A., Zakharenko, I.D. (1975) On surface effects in glancing collisions of metal plates. *Fizika Goreniya i Vzryva*, 11(**1**), 151–153.
4. Berdychenko, A.A., Zlobin, B.S., Pervukhin, L.B. et al. (2003) About possible inflammation of particles propelled into the gap in explosion welding of titanium. *Ibid*., 39(**2**), 128–136.
5. Ishutkin, S.N., Kirko, V.I., Simonov, V.A. (1980) Investigation of heat effect of shock-compressed gas on colliding plate surface. *Ibid*., 16(**6**), 69–73.
6. Ashaev, V.K., Doronin, G.S., Ermolovich, E.I. et al. (2006) Application of explosion welding and heat treatment methods for manufacturing of multilayer armored compositions having higher bullet-proof and survivability. In: *Transact. on Armament, Automation, Control*. Kovrov.
7. Alekseev, Yu.L., Smirnova, G.M. (1994) Joint formation in explosion welding. *Fizika i Khimiya Obrab. Metallov*, **4**/**5**, 126–130.
8. Alekseev, Yu.L., Smirnova, G.M. (1994) About conditions of explosion welded joint formation. *Ibid*., **2**, 112–116.
9. Pervukhina, O.L., Berdychenko, A.A., Pervukhin, L.B. et al. (2006) Influence of atmosphere composition on formation of titanium-to-steel joint in explosion welding. In: *Transact. on Higher Education Institutions on Explosion Welding and Properties of Welded Joints*. Volgograd: VolgGTU, 59–64.
10. Zeldovich, Ya.B., Rajzer, Yu.P. (1966) *Physics of shock waves and high-temperature hydrodynamic phenomena*. Moscow: Nauka.
11. Frank-Kamenetsky, D.A. (1975) *Plasma is the fourth state of matter*. Moscow: Atomizdat.

INDUSTRIAL APPLICATIONS OF EXPLOSION CLAD (REVIEW)

J.G. BANKER
Dynamic Materials Corporation, Boulder, CO, USA

The explosion welding technology was developed in several facilities around the world, primarily in the 1960s. Since then the application of the technology to make explosion welded clad plates has evolved into a significant worldwide industry. The explosion cladding technology is a proven, robust, cost effective and highly versatile process for manufacturing clad plates. It is suitable for manufacture of clad of virtually any combination of commonly used industrial metals. Today explosion welded clad plates are used in a broad range of industrial applications. The technology has a clear value niche in today's industrial world.

Keywords: *clad metal, explosion cladding, explosion welding, welding transition joints, pressure vessels, heat exchangers, autoclaves*

For nearly a century, there have been infrequent reports of metal pieces being «welded» together during explosive detonation events. In 1944 AIMME published a short reference to one of these events. During the 1950s several institutions worldwide increased R&D activities in the realm of explosion metalworking, primarily for forming, hardening, piercing and compaction. In 1959, DuPont filed the first internationally recognized patent on explosion welding (ExW). Three years later they began commercial explosion cladding primarily to provide tri-layer slabs for manufacture of US coinage. During the 1960s DuPont codified their production process, broadened their industrial applications and licensed their Detaclad® technology to explosive manufacturers in Europe and Asia. In parallel with this effort, a number of institutions independently developed variants of the technology, the most extensive and best known being operations in the Soviet Union. During the subsequent years there has been extensive research addressing the technology. Today there are over 40 industrial explosion clad manufacturing companies worldwide [1–7].

During those development years, explosion welded solutions were developed for a broad range of welding situations. These included micro-sized spot welds for the electronics industry, pipe-to-pipe butt welds for the gas transmission industry, tube-to-tubesheet welds for the power industry, all sorts of spot welds and overlapping butt welds and even bi-metal razor blades. Although ExW proved to be a highly versatile technology, most of the applications proved not to be commercially viable. The primary exceptions were clad plate manufacture and a variant process to make transition joints for welding of dissimilar metals.

In today's ExW industry around 80 % of the world's ExW production is clad plates, primarily used in the process industries for corrosion or wear-resistant equipment (Figure 1). Around 10 % is bi-metal transition joints, used as junctions for making commercial fusion welds between «non-weldable» metal components, predominantly aluminum-to-steel (Figure 2). The balance includes a broad range of bi-metal plate products ranging from armor to sputtering targets to electronic packaging materials.

ExW is a highly versatile technology, and it can be used to join virtually any combination of common industrial metal. It is suitable for joining both metal combinations of similar composition and metal combinations of highly dissimilar composition. The latter was the primary impetus behind the commercial development of the technology. Today production of reliable welds between aluminum and steel and be-

Figure 1. Explosion clad plates to be used for construction of a nickel laterite pressure acid leaching autoclave (plate size of 2200 × × 8000 mm × (10 mm titanium + 117 mm steel))

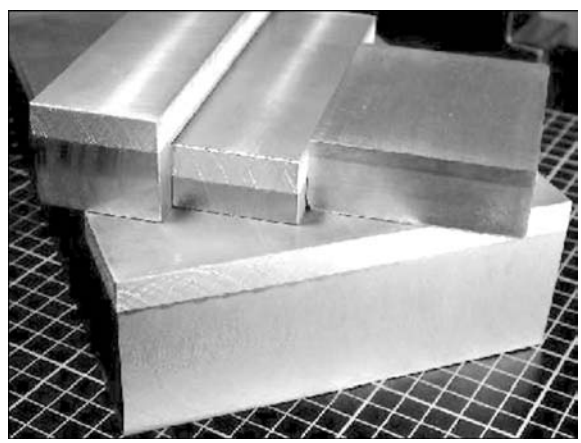

Figure 2. Bimetal transition joints for welding of dissimilar metals

tween titanium and steel are very significant applications of ExW. The success with these metal systems results from the absence of any significant bulk heating of the metals. The time-temperature conditions needed for diffusion and formation of brittle intermetallic compounds do not exist during the ExW.

ExW is ideally suited for making large area planar welds between metal plates or sheets. The lateral size of clad plates (length and width) is primarily limited by the size of metal sheets or plates that are commercially available, not by technical limits of the process. The commercial metal size available varies considerably between the various metal types. For most common commercial flyer metals, widths at 3 mm and less, are limited to 1200 mm, thicker gages are commonly produced in widths of 2500–3500 mm dependent upon alloy type. For many metal types, two or more sheets can be edge butt seam welded prior to cladding (using common fusion welding processes) to increase plate size options. Although larger plates are technically possible, the maximum widths produced by high-end manufacturers today are in the 5000 mm range, lengths are in the 12–13 m range. The process thickness range is also very broad. The thickness of the flyer plate, often called the cladder, can range from 0.1 mm to about 50 mm. The thickness of the base plate can range from 0.1 mm to over 1 m. When cladding metals are less than 3 mm thick and base metals less than 10 mm thick, the maximum production sizes are typically reduced. This is primarily driven by metal handling issues not process technical limitations.

The dominant application of ExW today is manufacture of large, flat clad plates. Table presents a list of typical metal types which are commonly supplied. Explosion clad plates can be readily formed into cylinders and heads and fabricated into process equipment such as reactors, columns and heat exchanger components.

Comparison of explosion clad with other cladding technologies. There are three common industrial clad plate manufacturing technologies: hot rollbonding, weld overlay, and explosion cladding [8]. In many ways ExW is the superior and most versatile of these processes.

Hot rollbonding is performed by a small group of heavy plate rolling mills. In this process, the clad metal and base metal are bonded together during the hot rolling operation. Being a high temperature process, hot rollbond is essentially limited to joining metallurgically similar materials, such as stainless steel and nickel alloys to steel. Rollbond's niche is production of large quantities of light to medium thickness clad plates; it is frequently lower cost than explosion clad when total metal thickness is under 25 mm, but very much dependent upon the alloys and other factors. Rollbond products are generally suitable for most vessel applications but have lower bond shear strength and may have inferior corrosion resistance when compared with the other two technologies. The latter can be a particular concern with alloys which are dependent upon solution annealing followed by rapid cooling. This includes higher-alloyed austenitic stainlesses, duplexes, and some nickel alloys.

In weld overlay cladding, the clad metal layer is deposited on the base metal using arc welding processes. Weld overlay can be a cost-effective technology for complicated shapes, for field service jobs, and for production of heavy-wall pressure vessel reactors. During overlay welding, the cladding metal and base metal are melted together at their interface; the resulting dilution of the cladding metal chemistry may compromise corrosion performance and limit use in certain applications. Weld metal shrinkage during cooling can cause distortion when the base layer is thin, consequently overlay is rarely the technically preferred solution for construction of new equipment when thicknesses are under 75 mm. As with rollbond, weld overlay is limited to metallurgically similar metals, primarily stainless steels and nickel alloys joined to steel.

Explosion cladding is the most versatile clad plate manufacturing technology. Being a robust cold welding technology, explosion-welded clad products exhibit high bond strength combined with unaltered corrosion resistance (when compared with that of the pre-clad components). The explosion cladding process is suitable for joining virtually any combination of common engineering metals. ExW is used to clad a very broad range of metals to steel including aluminum, titanium, zirconium, nickel alloys, and stainless steels. The alternative clad manufacturing technologies are typically limited to the latter two. When the cladding alloy and base are not metallurgically compatible, for example, titanium, zirconium, aluminum, or tantalum clad to steel, ExW is the only commercially significant technology for clad plate manufacture.

Explosion cladding is essentially limited to production of flat plates or concentric cylinders. The clad plates can be further formed and fabricated as needed.

Typical metal types supplied joined by ExW

Cladding metal	Base metal
Aluminum and its alloys	Carbon steel plate and forgings
Coppers/brasses/bronzes/Cu–Ni	Alloy steel plate and forgings
Nickel and nickel alloys	Stainless steel plate and forgings
Austenitic stainless steels	Aluminum
Ferritic/martensitic stainless steels	Copper
Duplex stainless steels	
Titanium	
Zirconium	
Silver	

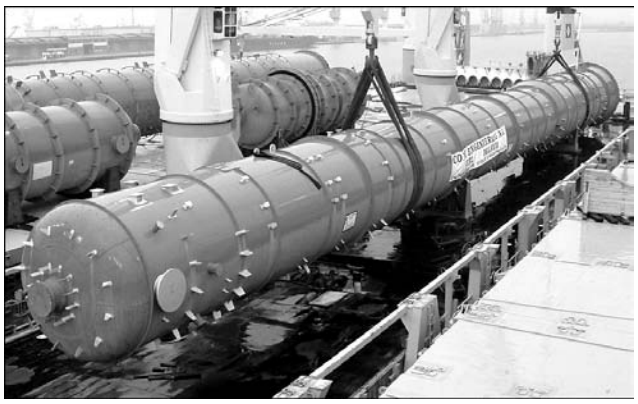

Figure 3. Titanium clad column for PTA manufacture (diameter 5000 mm, weight 450 t)

When fabricated properly, the two metals will not come apart.

Clad plate applications. Explosion clad is used extensively in the manufacture of pressure vessels and heat exchangers for high pressure and/or high temperature corrosion-resistant processes. Applications are dominantly in the chemical, petrochemical, refinery, hydrometallurgy, and upstream oil-and-gas industries. Some of the more interesting applications are addressed below. For greater detail on these applications, equipment fabrication, and clad performance issues, there are many good references [9–16].

Purified terephthalic acid (PTA) production equipment. PTA is a feedstock for manufacture of polyester and a broad range of related products including PET. Consistent high purity of the PTA crystals is critical for color consistency of these consumer products. The primary process for PTA manufacture involves the liquid phase oxidation of an aromatic hydrocarbon, most commonly para-zylene at around 250 °C. The process is not particularly corrosive, however, to achieve the necessary purity the allowable corrosion rates for the main process reactors is exceptionally low. Titanium provides excellent corrosion resistance in the process environment. The established material of choice is titanium-steel explosion clad. Figure 3 shows a large titanium clad column [10].

Hydrotreater reactors. Modern refineries use catalyzed hydrogen enhanced processes for upgrading of heavy residual hydrocarbon stocks to more readily marketable products. These reactors typically operate around 500 °C at very high pressures, consequently the structural metal is typically selected from the Cr–Mo steel family. Figure 4 shows a typical hydrotreater reactor. As with PTA, the process conditions are not highly corrosive. However, hydrogen embrittlement is a major concern. Stainless steel cladding is commonly used, primarily driven by the need for a hydrogen barrier. However, hydrogen disbonding has been observed to occur with overlay cladding if weld deposition procedures are not chosen correctly. ASTM G-146 is the established test method for determining resistance to disbonding under hydrotreater service conditions. Multiple testing programs have demonstrated that DMC's Detaclad® explosion clad plates do not disbond under G-146 test conditions [11, 12].

Figure 5. Titanium clad autoclave for pressure acid leaching of nickel and cobalt from laterite ores (diameter 5100 mm, weight 1100 t)

Nickel pressure acid leaching PAL autoclaves. PAL is one of the preferred processes for extracting nickel lateritic ores. The process involves high temperatures and pressures (250 °C and 5 MPa) combined with sulfuric acid concentrations in the 5–10 % range. Titanium is the only common engineering metal that provides adequate corrosion resistance in this environment. To achieve the necessary throughput, the vessels are typically quite large, around 5 m ID × 30 m long. Titanium clad is the material of choice for these autoclaves (Figure 5) [13].

Power plant condenser tubesheets. Conventional and nuclear electric power generation plants require very large, low pressure condensers for final conden-

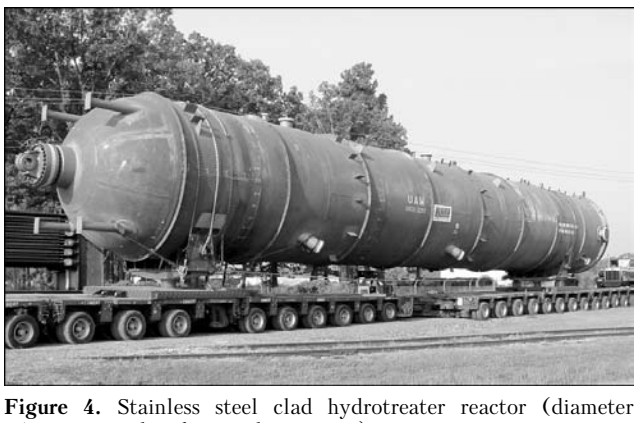

Figure 4. Stainless steel clad hydrotreater reactor (diameter 4500 mm, wight of more than 1000 t)

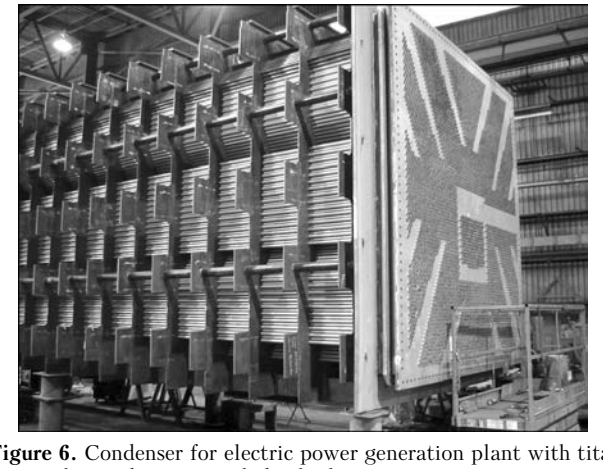

Figure 6. Condenser for electric power generation plant with titanium tubes and titanium clad tubesheets

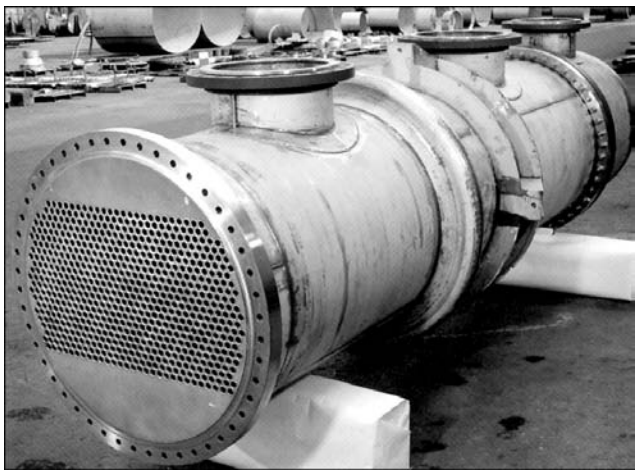

Figure 7. Shell and tube heat exchanger with zirconium tubes, stainless steel shell and zirconium–steel clad tubesheets used in manufacture of nitric acid

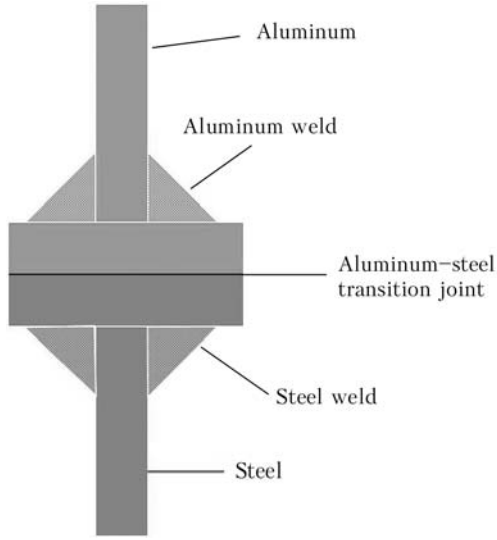

Figure 8. Using aluminum-steel transition joints cut from explosion clad plate to facilitate welding of aluminum to steel in conventional fusion welding shops

sation of the steam circuit. The condensers are typically a tubular heat exchanger design with stainless steel or titanium tubes to handle the modestly corrosive cooling water. Matching metallurgy between the tubes and tubesheet is important on the cooling water side of the unit. Explosion clad tubesheets, with a cladding metal of titanium or any one of a broad family of stainless steels, are used extensively worldwide. Figure 6 shows a typical condenser tubeplate.

Nitric acid cooler condensers. Shell-and-tube heat exchangers are used extensively for process media heating or cooling throughout the process industries, such as in chemical plants and refineries. Either the process media or the cooling media or both can be highly corrosive. Typically the more corrosive media is on the tube-side (running through the tubes) and the less corrosive media is on the shell side (running across the outside of the tubes). Tube materials can range from carbon steel for minimally corrosive media to titanium, zirconium or tantalum for highly corrosive conditions. As noted earlier, the alloy selected for the tubesheet face normally matches the alloy selected for the tubes. As pressures increase tubesheets get very thick quickly, consequently explosion clad provides a significant cost advantage in many installations. Figure 7 shows a nitric acid cooler condenser. The tubes are zirconium to handle the hot condensing nitric acid running through them. The shell is stainless steel to handle poor quality cooling water. The tubesheet is zirconium–stainless steel explosion clad [14].

Welding transition joints. Welding transition joints, produced from ExW clad plates, provide a means for making fully-welded dissimilar metal joints in normal fabrication environments. ExW works well for welding dissimilar metals, such as aluminum and steel, but the high energy released during the ExW event makes it unsuitable for use in most normal equipment fabrication environments. Figure 8 presents the transition joint concept. Large clad plates of the required metals combination are cut into bars, rounds, or custom shapes. These are supplied to welding fabrication shops where they are welded together with other components using conventional fusion welding procedures. ExW transition joints are used extensively for joining aluminum to steel (including the stainless steels). Other common metals combinations are aluminum-to-copper, aluminum-to-titanium, and titanium to steel.

Transition joints are primarily used as a replacement for mechanical connections in environments where mechanical joints have major technical weaknesses. Primary applications include:

- ship construction for making high strength, crevice-free joints between aluminum bulkheads and steel decks. Corrosion maintenance costs are dramatically reduced when bolted or riveted joints are replaced with welded transition joints [17];
- truck and rail car installations for making maintenance-free joints between light weight aluminum bodies and durable steel undercarriages;
- aluminum smelting plants for making resistance-free electrical connections between aluminum buss and steel anodes and cathodes [18];
- leak free pipe couplings between aluminum and stainless steel, primarily for the cryogenic industries.

CONCLUSION

Explosion cladding is a highly versatile and robust technology for making large clad plates and bi-metallic welding transition joints. Explosion clad products offer features unequalled by the alternative cladding processes: hot rollbond and weld overlay. Explosion clad is predominantly used for manufacture of corrosion- or wear-resistant equipment for the process industries.

1. Blazynski, T.Z. (1983) *Explosive welding, forming, and compaction*. Essex: Appl. Sci. Publ.
2. Holtzman, A.H., Cowan, G.R. (1965) Bonding of metals with explosives. *Welding Res. Council Bull.*, **104**.
3. Cowan, G.R., Douglass, J.J., Holtzman, A.H. *Explosive bonding*. Pat. 3,137,937 US. Publ. 1964.
4. Pocalyko, A. (1981) *Explosively clad metals*: Enc. of Chemical Technology. Vol. 15, 275–296.

5. Ryabov, V.R., Dobrushin, L.D., Moon, J.G. (2003) Welding of bimetals. In: *Welding and Applied Processes Series*. Ed. by B.E. Paton. Kiev: PWI.
6. Banker, J.G., Reineke, E.G. (1993) *Explosion welding*: ASM Handbook. Vol. 6, 303–305.
7. Patterson, A. (1993) Fundamentals of explosion welding. *Ibid*., 160–164.
8. Smith, L.M., Celant. M. (1998) *Practical handbook of cladding technology*. Edmonton: CASTI Publ.
9. Banker, J.G. (1996) Try explosion clad steel for corrosion protection. *Chemical Eng. Progress*, July, 40–44
10. Laermans, J., Banker, J. (2003) Large titanium clad pressure vessels, design, manufacture and fabrication issues. In: *Proc. of Corrosion Solutions Conf*. (Sept., 2003, Wah Chang).
11. Banker, J.G., Cayard, M.S. (1994) Evaluation of stainless steel explosion clad for high temperature, high pressure hydrogen service. In: *Proc. of Hydrogen in Metals Conf*. (Oct. 1994, Vienna, Austria).
12. Young, G. (2005) Explosion clad works for reactors. *Hydrocarbon Eng.*, March, 109–110.
13. Banker, J.G., Winsky, J.P. (1999) Titanium/steel explosion bonded clad for autoclaves and vessels. In: *Proc. of ALTA Autoclave Design & Operation Symp*. (May 1999, Melbourne, Australia).
14. Banker, J.G. (1996) Commercial applications of zirconium explosion clad. *J. Testing and Evaluation*, 91–95.
15. Frey, D., Banker, J. (2003) Recent successes in tantalum clad pressure vessel manufacture. In: *Proc. of Corrosion Solutions Conf*. (Sept. 2003, Wah Chang).
16. Young, G.A., Banker, J.G. (2003) Explosion weld clad for magnesium melting crucibles. In: *Proc. of TMS Conf*. (Febr. 2003, San Diego, CA).
17. McKinney, C.R., Banker, J.G. (1971) Explosion bonded metals formarine structural applications. *Marine Techn., Soc. of Naval Architects and Marine Engineers*, July, 285–292.
18. Banker, J.G., Nobili, A. (2002) Aluminum-steel electric transition joints, effects of temperature and time upon mechanical properties. In: *Light metals*. Ed. by W. Schneider. TMS, 439–445.

WIDENING OF TECHNOLOGICAL CAPABILITIES OF EXPLOSION TREATMENT FOR REDUCING RESIDUAL STRESSES IN WELDED JOINTS ON UP TO 5000 m^3 DECOMPOSERS

L.M. LOBANOV[1], L.D. DOBRUSHIN[1], A.G. BRYZGALIN[1], S.Yu. ILLARIONOV[1], P.S. SHLENSKY[1], L.A. VOLGIN[2], V.G. LASHKEVICH[2] and **E.V. GRABAR[2]**

[1]E.O. Paton Electric Welding Institute, NASU, Kiev, Ukraine

[2]Engineering Centre «Explosion Treatment of Materials» of the E.O. Paton Electric Welding Institute, Kiev, Ukraine

Efficiency of reducing residual stresses by stepwise explosion treatment of long multi-pass welds, as well as welded joints on decomposers with 40 mm wall thickness was studied.

Keywords: *explosion treatment, low-carbon steel, decomposers, welded joints, residual stresses, stress corrosion cracking*

Explosion treatment (ET) is now the only method capable of providing stress corrosion crack (SSC) resistance of welded joints on decomposers, which are commercially applied at alumina and aluminium plants. 26 decomposers of the Uralsky Aluminium Plant, 12 decomposers of the Dneprovsky Aluminium Plant, 36 decomposers of the Pavlodarsky Aluminium Plant, 24 decomposers of the Birach Aluminium Plant (Yugoslavia), 63 decomposers of the Nikolaevsky Alumina Plant, as well as other tank equipment at these plants, were subjected to ET during a period from 1971 to 2007. Totally, more than 400,000 running metres of the welds on 300 large-size tanks were treated. Long-time service of the treated tanks with no serious damages detected up to now proved the high efficiency of ET used to ensure high performance of the equipment operating in aggressive alkaline environments.

ET is implemented by using captive explosive charges, which are placed on the internal surface of a tank along the welds. The shape and weight of an explosive per unit length depend upon the thickness of a material treated and type of a welded joint. Owing to the inside location of the charges, the tank walls serve for protection from the hazardous effect of explosion. The maximal weight of the explosive charge used at a time, which determines power of the shock wave formed in explosion, is calculated, as a rule, on the basis of ensuring integrity of glazing of buildings located near a facility treated. Facilities subjected to the treatment are shown in Figure 1. From 20 to 180 running metres of the welds can be treated per blasting, depending upon the conditions of explosion operations and thickness of the metal treated.

Improvement of design of the decomposers and increase of their working volume to 5000 m^3 led to extension of total length of the welds made in assembly and increase in wall thickness of the lower flanges to 40 mm. In this connection, it is of current importance to evaluate the efficiency of ET of thick-plate joints for operational conditions of the decomposers and stepwise (in several blasts) treatment of the long welds.

First of all, it should be noted that in the 1970s–1980s the $\sigma_{max} \le 0.25\sigma_y$ condition [1], where σ_{max} are the maximal residual stresses and σ_y is the yields stress of the steel used to manufacture the decomposer wall, was used as a criterion of resistance to SSC for decomposers with a wall thickness of no more than 20 mm. Investigations conducted by the E.O. Paton Electric Welding Institute [2] showed that resistance of

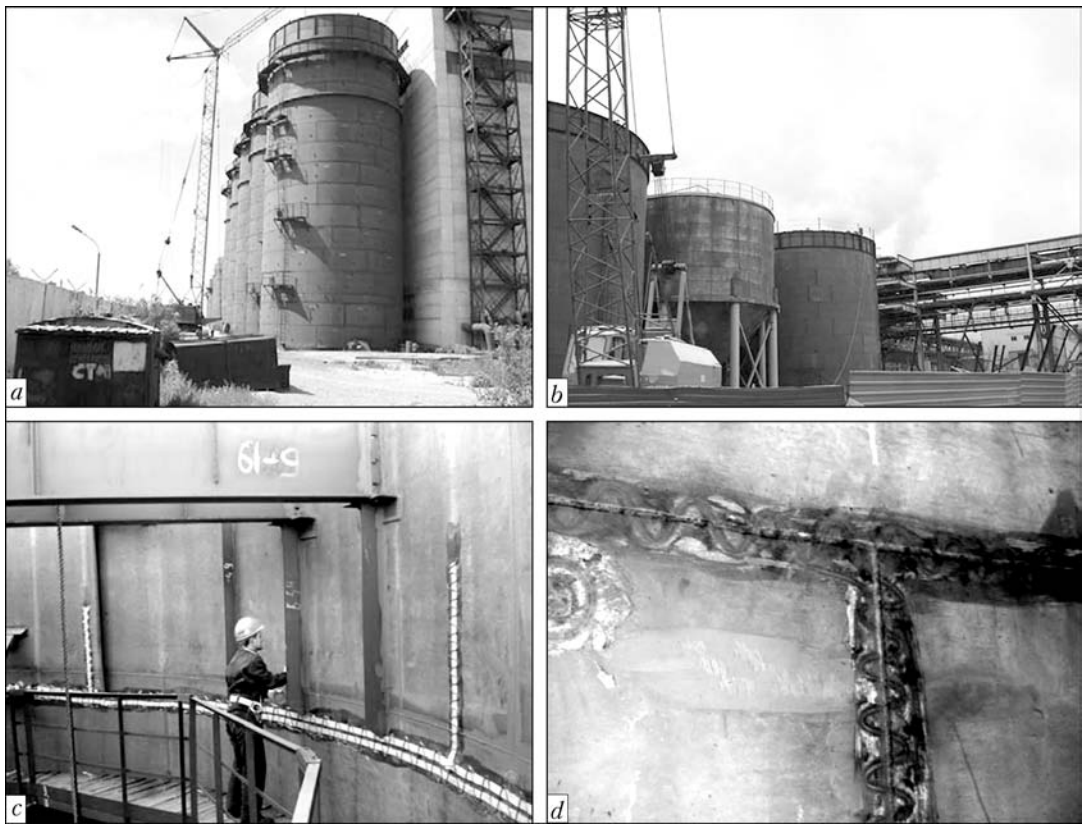

Figure 1. Appearance of structures subjected to ET: *a* — range of decomposers being constructed; *b* — technological tanks; *c* — mounting of charges in progress; *d* — welded joints after ET

welded joints on steel St3 to SSC in alkaline environments increased with increase in thickness of a joint, and that the following values could be used as a criterion of resistance of modern decomposers to SSC:

$\sigma_{max} \le 0.25\sigma_y$ at decomposer wall thickness less than 14 mm; $\sigma_{max} \le 0.35\sigma_y$ at 14–24 mm, and $\sigma_{max} \le 0.5\sigma_y$ at more than 24 mm.

Investigations of residual stresses in welded samples made from plate steel St3 (σ_y = 33 MPa) were carried out by the cutting method, and strains were measured by using the mechanical strain meter with a scale-division value of 2 μm. A sample 40 mm thick, measuring 600×450 mm, was made by semi-automatic CO_2 arc welding (X-groove, 17 passes) using the technology developed particularly for construction of decomposers at the Nikolayevsky Alumina Plant (NAP). Explosion treatment was performed by Engineering Centre «Explosion Treatment of Materials» of the E.O. Paton Electric Welding Institute using the technology developed by the E.O.Paton Electric Welding Institute. One side of a sample was treated according to the technological process developed for ET of welded joints on the NAP decomposers. Diagrams of longitudinal and transverse residual stresses are shown in Figure 2.

As noted above, ET of the decomposer being constructed was performed on the internal side, i.e. on the side of contact of the decomposer with an aggressive environment. Longitudinal and transverse stresses on the ET side did not exceed the required level of $0.5\sigma_y$.

Distribution of residual stresses through thickness after ET was non-uniform. This explains some lack of balance in the diagrams of stresses on the sample surfaces. However, there was a marked decrease in maximal tensile residual stresses on the untreated side as well, their values in the as-welded condition being at a level of yield stress. Based on the positive results of investigations conducted earlier by the E.O. Paton

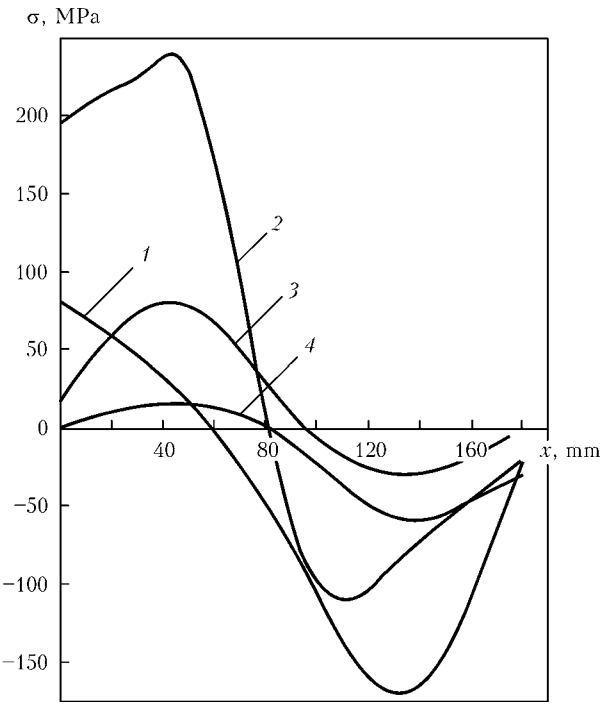

Figure 2. Diagrams of longitudinal residual stresses in 40 mm thick plate on the ET side (*1*) and on the untreated side (*2*), as well as transverse residual stresses on the untreated (*3*) and ET (*4*) side

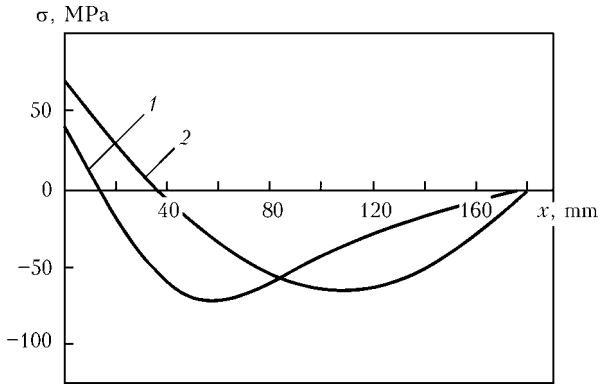

Figure 3. Longitudinal residual stresses in 10 mm thick plate on the ET side in the first (*1*) and second (*2*) treated halves of the plate length

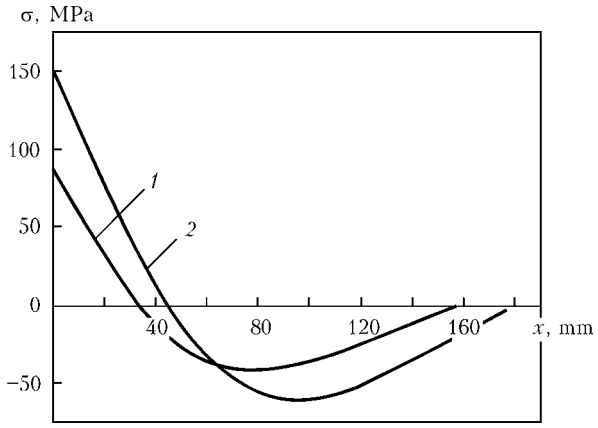

Figure 4. Thickness-average longitudinal residual stresses in plate, half of the length of which was explosion treated, in treated (*1*) and untreated (*2*) part

Electric Welding Institute on samples 30 and 35 mm thick, it can be concluded that ET of thick-plate welded joints on decomposers on the side of contact with an aggressive environment provides reduction of residual stresses to a required level.

Welded samples of steel St3 (σ_y = 370 MPa), measuring 1500 × 500 mm and having a wall thickness of 10 mm, were made to investigate the efficiency of stepwise ET. Semi-automatic welding was performed by the technology developed for NAP — X-groove and three passes (the first pass — root one, and second and third passes — filling ones on two sides of the plate). In assembly of the decomposers, the pass deposition sequence provides for inducing the minimal transverse stresses on the inside. Accordingly, ET was performed on the sides of the second pass. One sample was treated to half of its length with one blast, and the second sample was treated stepwise to its entire length by two separate blasts.

Figure 3 shows diagrams of longitudinal residual stresses for a treated sample on the ET side. The efficiency of ET of half of the sample, which was the first to be treated, turned out to be a bit higher. However, the maximal stresses in both halves (45 and 70 MPa) did not exceed the permissible ones (90 MPa).

The results of measurements of residual stresses in a sample explosion treated only to half of its length are shown in Figure 4. The maximal longitudinal stresses in the treated part of the sample were not in excess of the permissible ones. Substantial decrease in residual stresses occurred in the untreated part, this being indicative of redistribution of residual stresses along the length of the weld in ET of part of the weld.

The investigations conducted allow a conclusion that stepwise ET of long welds provides an efficient reduction of residual stresses, and can be applied to address problems associated with ensuring SSC resistance of welded joints.

CONCLUSIONS

1. ET on the internal side of welded joints on decomposers made from steel St3 with a wall thickness of 40 mm reduces residual stresses to a level required to ensure SSC resistance in alkaline environment.

2. Practical application of the ET technology on decomposers being constructed can consist of the stepwise treatment of long welded joints.

1. Steklov, O.I. (1976) *Strength of welded structures in aggressive media*. Moscow: Mashinostroenie.
2. Petushkov, V.G. (2005) *Application of explosion in welding engineering*. Kiev: Naukova Dumka.

EXPLOSIVE CLADDING FOR ITER COMPONENTS

E. CARTON and **M. STUIVINGA**
TNO Defense, Safety and Security, Rijswijk, The Netherlands

The International thermo-nuclear experimental reactor (ITER) is a huge experimental facility for the fusion energy research field to be built in the coming years in France. The extreme conditions (high temperatures, large heat loads, thermal fatigue, and nuclear radiation) require very special materials and dissimilar bonding of metals to be used. TNO develops the explosive cladding technology (as an alternative bonding mechanism) in order to demonstrate the potential of this bonding route for ITER components.

Keywords: *explosive cladding, fusion energy, components, ITER*

ITER stands for International thermo-nuclear experimental reactor, which is a huge international project with the aim of demonstrating the feasibility to use fusion-power (the same nuclear reactions as are active on the Sun). The reactor is to be built in France in the next 10–12 years by a joint effort of the USA, Europe, Japan, Russia, Korea and India [1]. The Tokamak-type reactor (Figure 1) is of an enormous size compared to earlier built fusion reactors and consists of an extremely large donut-shaped vacuum vessel (maximal radius 6.2 m, minimal radius 2 m). The vacuum vessel, which also forms the main containment for the nuclear radiation, is made out of two parallel layers of 60 mm thick stainless steel (316 L (IG)) walls and water in between.

Inside the vacuum vessel, a plasma will be generated in which a current runs of 15 MA. Due to the extremely high temperature inside the plasma (tens of millions of degrees Celsius), thermo-nuclear reactions are initiated that generate a fusion power of 500 MW. The fusion reactions will not take place continuously but in bursts of about 400 s. This means that the heat load and therefore temperature inside the reactor will fluctuate. This is the more so as it is expected that the plasma in some cases may relocate inside the reactor (e.g. a vertical displacement error) during which a direct contact between the plasma and the first wall material may occur (with excessive thermal loads).

The stainless steel is not capable to withstand even the normal (yet huge) thermal loads (between 0.5 and 20 MW/m^2 depending on the position in the vessel) without melting and contaminating the plasma. Therefore, the inner wall of the vacuum vessel (surface area of about 850 m^2) will be covered by water cooled copper blocks that have a clad layer of beryllium and/or tungsten. Although HIP (diffusion bonding) and brazing are the baseline bonding methods for these brittle, refractory metals to the copper substrates, they do have their limitations such as lowering the maximal allowable temperature of the interface, and prolonged high temperature exposure of the copper substrate (reducing its strength) [2].

TNO has worked on alternative methods for dissimilar metal bonding using explosive cladding. As this bonding technique allows the formation of a direct bond between two (or more) dissimilar metals, it is an extremely short process (microseconds) and does normally not involve a high temperature exposure of the metal parts, it may be an alternative way to obtain bimetallic components for ITER.

Experimental. Apart from the PFW components, clad (bi)metals may be used in several other locations within ITER as well.

TNO works at two of those: the upper port launcher, and triangular support of the outer diverter.

For dimensional stability the upper port launcher (a device to control the position of the plasma) needs to be water cooled. Two copper plates 2 and 6 mm thick were used, the 6 mm thick plate was machined such that several cooling channels existed in it. By using machining instead of drilling, a lot of channel cross-sections and forms may be advantagely used. The machined channels need to be temporarily filled up (using a metal with a low melting point) so that the cladding process of the thinner plate will not be interrupted by the channel holes. After the copper-to-copper cladding two holes are drilled into the channels and by heating the clad metal, its filler flows out

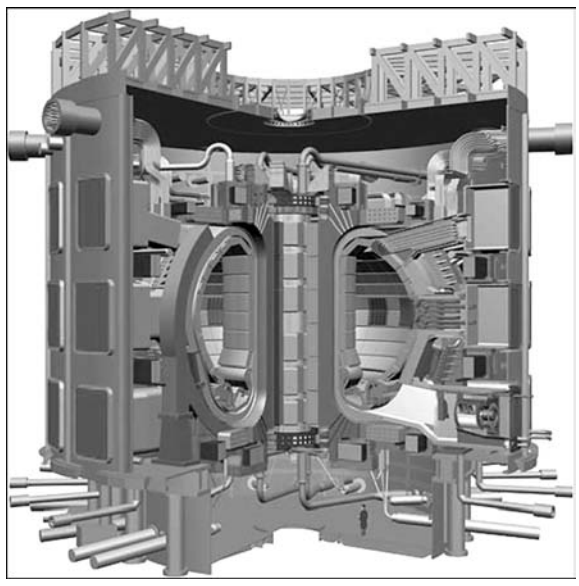

Figure 1. Cross-sectional view of ITER (notice the person below the fission reactor) [1]

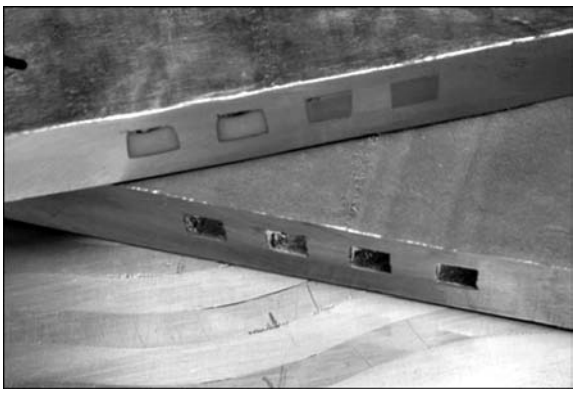

Figure 2. Pre-machined copper plates in several stages to complete the fabrication of a copper plate with specially designed water cooling channels

leaving the originally machined (apart form some minor deformation) channels in the copper plate (Figure 2).

The triangular support just like the vacuum vessel consists of a water filled stainless (316L (IG)) steel box, with a wall thickness of 60 mm. As the electrical conductivity of stainless steel is rather low, it is expected that too much (electro-magnetic) energy may be dissipated in it. It therefore needs to be clad with a pure copper liner of about 1.5 mm. As the triangular support, supports the outer diverter inside the vacuum vessel, it is curved with a radius of about 4 m. On top of that, several obstacles in the form of stub-keys are protruding the steel surface to be clad. These stub-keys (each with a diameter of 200 mm and 90 mm height) present a huge problem in an otherwise easy to clad metal combination (Figure 3). It is clear that the normal cladding configuration will not present a good cladding result, particularly behind the stub-keys due to detonation wave interactions that will take place here. Using experiments as well as computer simulations of the detonation process around the obstacles an solution for the cladding of the triangular-support will be found.

Tungsten-copper cladding. The main part of the PFW of ITER will be beryllium clad (about 700 m^2), and the remainder is tungsten clad (100 m^2) or carbon-reinforced carbon (about 50 m^2). As beryllium is not only brittle at room temperature, but also very toxic (especially BeO dust) we have started our experiments using tungsten, which is also quite brittle at room temperature. Figure 4 shows the variation of ductile-to-brittle transition temperature (DBTT) with the thickness of the tungsten plate. Although

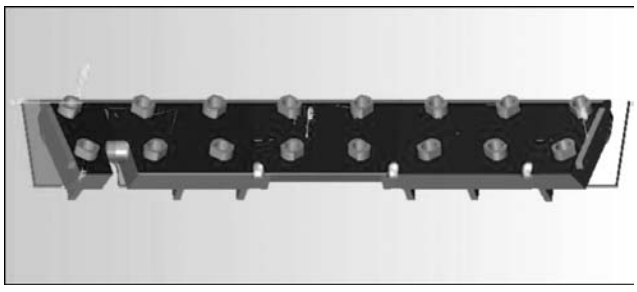

Figure 3. 3D view of a segment of the triangular support ring with protruding stub-keys 200 mm in diameter

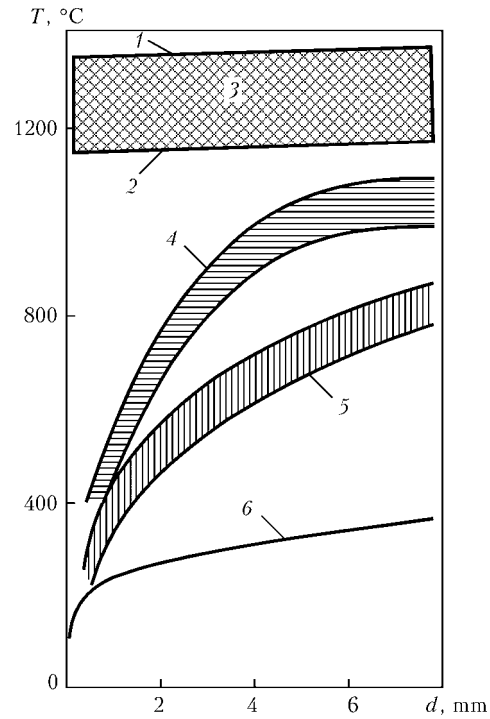

Figure 4. DBTT of tungsten for different plate thicknesses [3]: *1* — complete recrystallization after 1 h; *2* — beginning of recrystallization; *3* — recrystallization interval; *4* — punching; *5* — bending; *6* — transition temperature

these values will not be accurate for the high dynamical conditions during explosive cladding (very high strain rates), they present some guideline on how the DBTT relates to the level of prior deformation. A very interesting observation is the large drop in DBTT for very thin tungsten plates (foils). For these foils (<0.5 mm) the DBTT is below 200 °C. Indeed such thin tungsten foils can be cut at room temperature without introducing large cracks in the material, although the foils are very susceptible for in plane crack formation due to the layered stacking of very elongated tungsten-grains during rolling. Experiments were started by cladding copper plates with tungsten foils. The foil cladding configuration (Figure 5) using a 1 mm thick stainless steel driver plate had been used by TNO before [4]. In this work use was made of a cap sensitive commercially available ammonium nitride based explosive called Sytamit 1 (WasagChemie, Germany) which detonates at about 3 km/s at the layer thickness of 15 mm used here.

The tungsten foil was applied to the driver plate using a tape with an adhesive layer on both sides. A gap of 2 mm was used in order to allow the driver plate to be accelerated. In some experiments multiple foils were clad on top of each other in one cladding

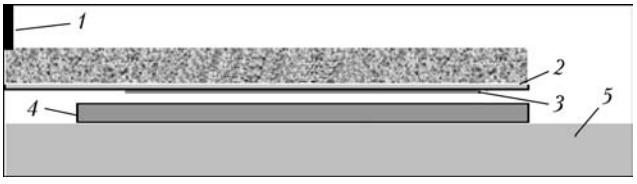

Figure 5. Experimental set-up for foil cladding at room temperature: *1* — detonator; *2* — flyer driver plate; *3* — tungsten foil; *4* — plate; *5* — target

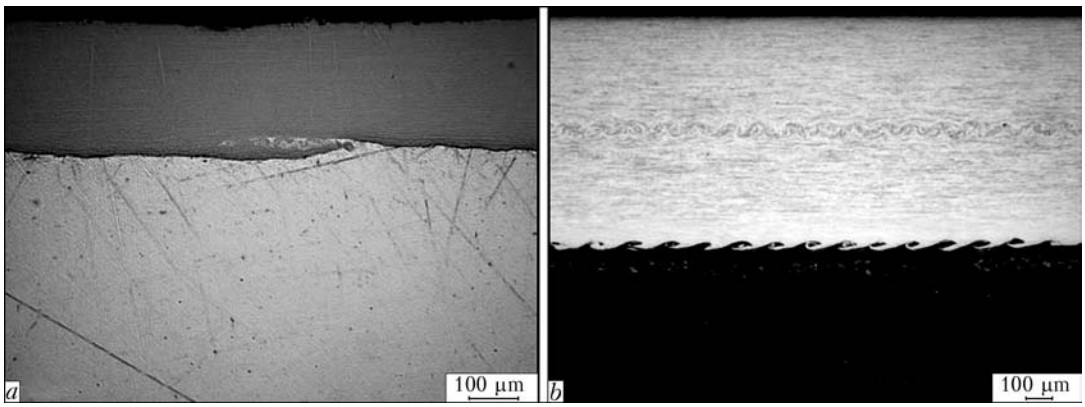

Figure 6. Cross-section of a singe (*a*) and a double (*b*) tungsten foil clad on copper

operation. In this case a standoff distance of 0.5–1.0 mm was maintained between each foil. The cladding experiments were performed inside a detonation chamber at room temperature.

Figure 6 shows cross-sections of two tungsten foil cladding experiments. Figure 6, *a* shows the straight interface of a single tungsten foil (d = 300 μm) on copper (d = 2 mm). Here it can be assumed that jetting of only the softer and ductile copper allowed the bonding to be occured (tungsten acted only elastically and therefore a straight interface occurred). However, Figure 6, *b* (due to etching of the tungsten) shows wavy interfaces both between the tungsten foils (500 μm each) and at the bimetal interface. At both interfaces the tungsten heavily deformed in the localized wave forming deformation process [5]. The occurrence of plastic strain, especially in such a large amount, in tungsten at room temperature is a very interesting observation. Probably the huge compressive stress as a result of the metal collisions allows a deformation mechanism becoming active during which the metal heats up and the deforming layer of metal is above its DBTT. At larger magnification of the tungsten–tungsten interface even some recrystallized melt pockets could be observed (the melting point of tungsten is above 3500 °C).

Hot cladding experiments. As the room temperature cladding experiments were only successful for tungsten foils (< 0.5 mm), also hot explosive cladding experiments have been performed. By preheating the tungsten above its DBTT value the ductility (as well as drop in hardness) may be sufficient for its cladding (see Figure 4). As the explosive should not be heated significantly (to prevent melting and thermal degradation or even spontaneous detonation), in the hot cladding experiments the tungsten plates (2 mm thick) were used as base plate only. This also avoids the much less ductile thick walled tungsten to undergo the forces and bending that occur during the acceleration by the detonation process. Best results were obtained by preheating the tungsten plates separately next to the copper flyer plate and its explosive top layer (Figure 7). The tungsten plate lay on top of a stainless steel plate that was connected to a metal wire which rum outside of the detonation chamber. The temperature of the preheated tungsten plate was measured with a thermocouple on top of the plate at the preheating location. When the plate had reached its temperature (350–500 °C) the metal wire was pulled from outside the detonation chamber, during which the tungsten plate relocated to below the copper flyer plate (detonator and explosives remain at room temperature). Then the detonator was activated and the cladding process took place inside the detonation chamber.

Figure 8 shows a cross-section of a hot (480 °C) clad tungsten 2 mm thick to copper 2 mm thick cladding. Again a wavy interface is obtained demonstrating the ductility of this metal under large compressive (hydrodynamic) stresses. The hot clad bimetal plates were free of cracks probably since the tungsten was above its DBTT during the cladding operation. However, in some cases remaining thermal stress inside the system created in plane cracks inside the (now brittle again) tungsten plate sometimes day after the cladding operation. These stresses occur due to the large mismatch in thermal expansion coefficients between tungsten and copper.

Directly after the cladding process, the copper (at room temperature) is heated fast by the (still hot) tungsten plate. The value of the equivalent temperature that the bimetal system obtains is determined by the thickness ratio of the plates and the preheating

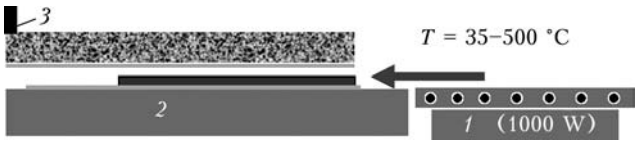

Figure 7. Experimental set-up for hot explosive cladding: *1* — heater; *2* — target; *3* — detonator

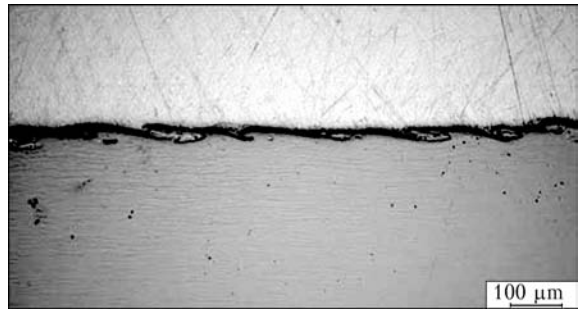

Figure 8. Cross-section of a copper clad on a preheated tungsten plate (T = 480 °C)

temperature. During subsequent cooling to room temperature the copper contracts more then the tungsten, which leads to large thermal stress at the metal interface (up to 800 MPa as was calculated using thermomechanical computer simulations). However, the 2 mm plates (tungsten preheated to 480 °C) have been remained free of cracks. The material will be further analyzed and tested by the Nuclear Research Group (Petten, The Netherlands).

ITER creates a huge international technological challenge that is to materialize the coming decennium. Although some base-line design and bonding methods for ITER have been selected, there is always room for improvement (both technically and economically). TNO has worked on the further development of the explosive cladding technology in order to fabricate demonstrators and test samples for components that can be used on several locations in ITER. Especially the cladding of tungsten foils at room temperature and hot cladding of tungsten plates 2 mm thick is a remarkable result demonstrating the ductility of this metal under compressive stresses.

Acknowledgement. *The authors would like to acknowledge Friso Schmalz and Jaap van der Laan of the Nuclear Research Group in Petten, the Netherlands for useful discussions and advice.*

1. *ITER web-site on http://*www.ITER.org
2. Merola, M. et. al. (2002) *J. Nuclear Materials*, **307–311**, 1524–1532.
3. *Plansee W-folder 2006*. Austria.
4. Cart, E.P. (2003) *AIP shock compression of condensed matter*, 1110–1113.
5. Carton, E.P. (2004) *Mater. Sci. Forum*, **465–466**, 219–224.

PHOTOGRAMMETRY APPLICATIONS FOR EXPLOSIVE FORMING

H.D. GROENEVELD
Exploform BV, Lelystad, The Netherlands

Explosive formed products are more and more commonly applied. The state-of-the art is rapidly extended towards new product groups. Material characterization and process control becomes more important for efficiently designing new explosive forming processes. A method was developed for determining the forming limits of metals in explosive forming. A test shape was designed with features that represents different strain paths in the forming limit diagram. A regular dotted pattern is electrochemically etched on the sheet surface. Test plates are formed and analyzed using photogrammetry. The resulting forming limit curve is used as an input for forming simulation software that works with a hydrostatic code. This approach provides a straightforward method for predicting the forming characteristics that come with a certain workpiece and it strongly enhances the design of new products that are to be formed by explosive forming. This approach is also applied for heat-treated and for welded metals. The forming limit diagrams of both the simulation and the photogrammetric analysis of a real explosive formed shape are compared for validation.

Keywords: *explosive, forming, photogrammetry*

The process of explosive forming is more and more commonly applied in the last years. The process was also applied commonly in the 1960–1970s but applications have vanished in the 1980s.

The current revival can be explained by the current market conditions. Short delivery times are now more important and special shapes are required in special metals in lower quantities. Also more work is subcontracted to specialized manufacturers and specialists can be found more easily through the Internet.

3D CAD/CAM now enables more effective performance of projects for which explosive forming is particularly suited. Another reason for the revival of the technology of explosive forming is the application of modern analysis methods. Numerical simulations provide a better understanding of the effect of the many and complex process parameters. The results of forming tests are also more predictable since numerical simulations are applied.

Explosive forming. The process of explosive forming knows many variants. The general method is that a metal sheet is placed on a die. The die cavity is vacuumed and the assembly is lowered in a water basin. The explosive charge is positioned above the sheet in a certain configuration. The explosion forces the sheet in the die at high speed.* Figure 1 gives an overview of the process.

The process parameters can be adapted for any workpiece shape, material and thickness. Variants to the general method are e.g. the forming of tubes or cones instead of sheets.

Current achievements range in thickness up to 60 mm stainless steel (for the experimental nuclear fusion reactor ITER) and in size to 10 × 2 m (for the nuclear RES pool in Cadarache, France). Materials with a yield strength such as nickel, titanium and cobalt alloys are explosive formed for e.g. gas turbines.

Larger and more complicated shapes can be formed from welded assemblies. Welding methods that are

*Minors, D.J., Zhang, B. (2002) Applications and capabilities of explosive forming. *J. Mater. Proc. Technol.*, **125/126**, 1–25.

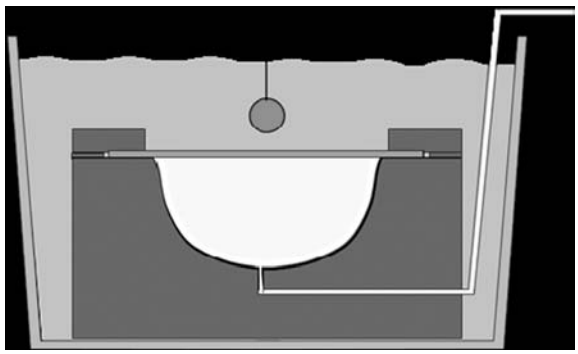

Figure 1. Overview of explosive forming

succesfully applied for explosive forming are MIG, TIG, laser, friction stir, electron beam and explosive welding.

Deformation analysis. The explosive forming process is normally simulated with the Hydroform module from Autoform. The hydroforming process differs from the explosive forming process but can be applied efficiently. Ansys/Autodyn simulations provide are applied for particular cases when the complex explosion process parameters must be taken into account. Forming limit diagrams (FLD) are available for materials that are commonly in the automotive industry. The availability of FLD for aerospace materials is, however, poor.

Precipitation hardened aluminium alloys have highly increased formability in explosive forming. These circumstances caused the authors to develop a method for determining FLDs for the explosive forming process.

Numerical simulations. Hydroforming simulations (Autoform) are applied for the design of explosive forming processes in general. The hydroforming process is much like the explosive forming process. The authors believe that this is the most straightforward and efficient approach process. However, care must be taken because the explosive forces are not hydrostatic. Nevertheless, experience shows that the predicted strains match the results well enough for general practice. Figures 2 and 3 show an example of a shape that was successfully designed on the edge of the forming limits using Autoform hydroforming simulations.

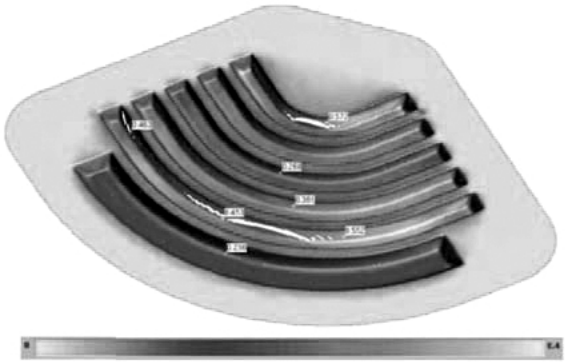

Figure 2. Result of scouting Autoform hydroforming simulation showing cracks

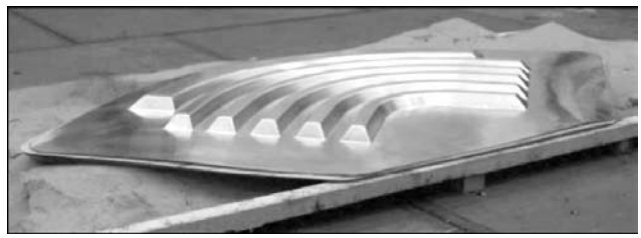

Figure 3. Workpiece 2.5 m in size as realized with a shape designed on the forming limit edge

Photogrammetry. Photogrammetry is a method for determining the deformation of metal sheets as occurs in a real forming process. A blank sheet that is to be formed, is provided with an equally spaced pattern of dots. The authors used an electrochemical method because this method is efficient and the dots will remain visible when a workpiece is heat treated. The pattern of the dots changes during forming. This provides information about the deformation of the sheet. The dots on the workpiece surface are recognized by software (Phast) from digital pictures that are made from several angles (Figure 4). A beacon with calibrated circular barcodes is placed close to the workpiece. The software recognises the barcodes and determines the exact positions and angles of the camera for the different pictures that are taken. The software recognizes the dots on each of the pictures which gives the necessary information for deriving the 3D locations of every dot. The software calculates the strains, thinning etc. from the relative 3D locations of the centers of the dots.

Method for determining the forming limit curve (FLC) for explosive forming. The forming speed that appears in explosive forming ranges from about 10 to 100 s^{-1}. It is known that certain metals show increased ductility at these high strain rates. This caused the authors to develop a method for determining the FLC

Figure 4. Making digital pictures for photogrammetry analysis

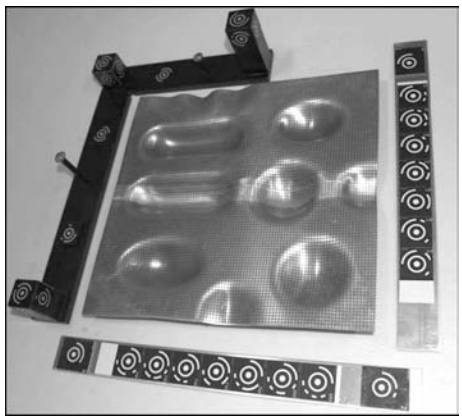

Figure 5. Testpiece with multiple shapes representing multiple strain paths

for explosive forming applications. A blank sheet of 250 × 250 mm is provided with a dotted pattern. It is formed in a die that has no bottom, so that the sheet can form until it breaks. The die has multiple different shapes. Figure 5 shows a formed test plate.

The different shapes represent different strain paths (Figure 6). The explosive charge can be applied in such a way, that the three shapes over the middle line of the plate are just on the edge of cracking. The formed test plate is analyzed by photogrammetry. The result of a test plate of an aluminium alloy is shown in the FLD in Figure 7. The FLC (*1*) is drawn below

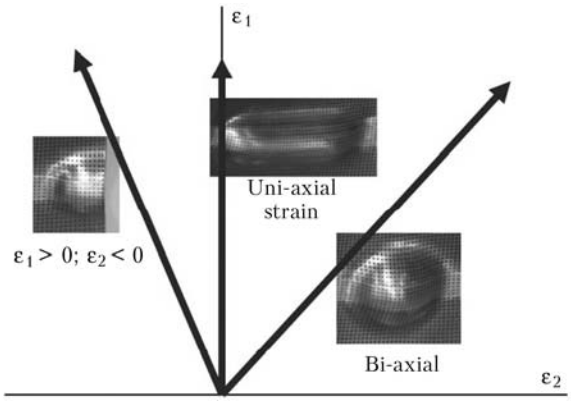

Figure 6. FLD with strain paths on three of the shapes

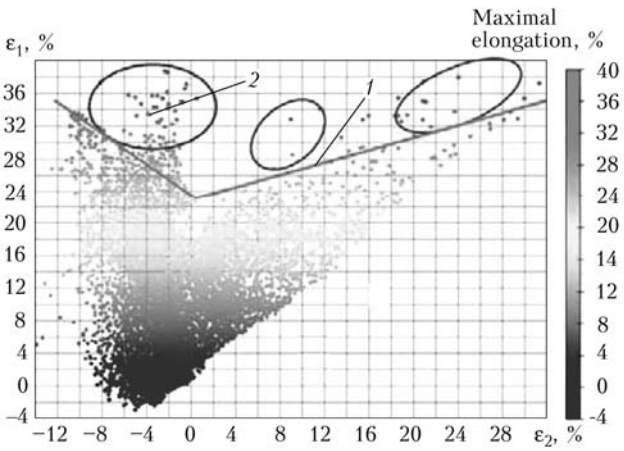

Figure 7. FLD: FLC (*1*) is drawn below the points that are close to cracks (*2*)

Figure 8. Art sculpture in wax

the points that relate to locations close to cracks or with excessive orange peel (*2*).

The method can also be applied for determining the ductility of welded assemblies. The testpiece in Figure 5 was friction stir welded by Airbus (Bremen, Germany) over the middle of the plate. The material was also aluminium 2219, and the FLC is only about 5 % below the FLC of the base material.

Shape measurement by photogrammetry. Photogrammetry can also be used for measuring 3D shapes from surface texture. This is illustrated by the realization of an art sculpture in metal facade panels for a building in Eindhoven, The Netherlands.

Figure 8 shows the art sculpture as the artist made it out of wax. This shape was to be realized in more than 100 metal plates. An artist can make any desired shape in wax, but realizing this same shape from sheet metal is another issue. The shape is very complicated and the possibilities for realizing this shape need to be verified by simulation. A CAD file of the shape is required for making a metal-forming simulation. This file is obtained by the following procedure. First, the sculpture surface is painted white and sputtered with black ink (Figure 9). A beacon is placed on the sculpture and the surface is photographed from different positions (Figure 10). The photogrammetry software splits the surface in squared with a pre-difined shape.

Figure 9. Sputtering the surface with black ink

Figure 10. Making photos of the sculpture surface

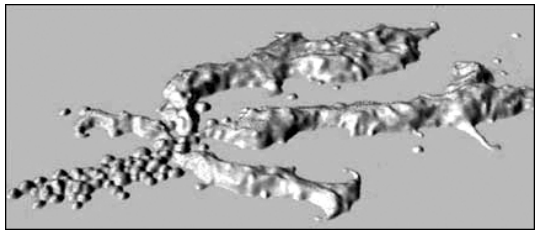

Figure 11. Point cloud on the generated CAD surface

Each square has a unique black-white pattern that is recognised from each of the pictures. The photogrammetry software generates the $X–Y–Z$ coordinates of each of the squares. The resulting point cloud (Figure 11) is used for generating a 3D surface in CAD.

Now we have the CAD model of the shape. Before making a forming simulation, the material data also are needed. A standard material can be used from the material library of the simulation software, but there are two issues that makes this problematic. Primarly, the forming speeds in explosive forming are much higher than in the tests of the materials in the library. Further, the formability varies for each production batch and we need to go up to the very edge of the possibilities of the metal for the sculpture. This was taken care of by buying a material batch from a manufacturer that is known to supply very well formable metal. The FLC is determined following the procedure above-mentioned. Now the explosive forming process can be simulated. The result is plotted in Figure 12.

The first simulation showed that there are high risks of cracking and buckling in some areas. This was solved by modifying the shape in such a way in CAD, that the artist still remained satisfied about the appearance. The success final result can be seen by comparing Figure 13 to 12. The shape was machined from a massive metal block by CAD/CAM and the metal

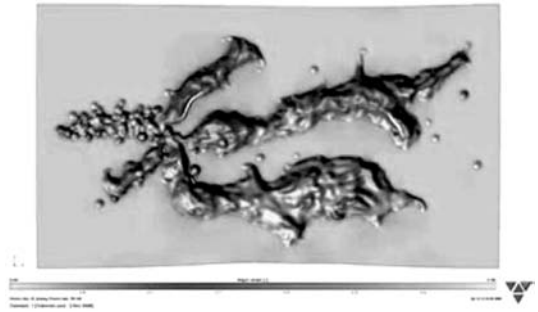

Figure 12. Result of the first simulation

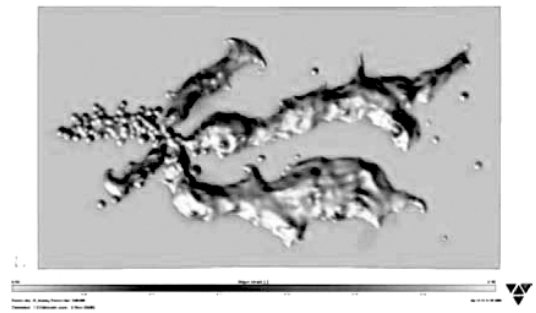

Figure 13. Result of the simulation of modified shape

Figure 14. Mock-up of prototype at the construction site

plates were formed in this matrix. Figure 14 shows the mock-up at the construction site. At this moment, all panels are formed and being installed on the facade.

Deformation feedback. The artist insisted on getting an idea of the shape of the sculpture before machining the large, expensive matrix. Figure 15 shows how the artist designed a small, equivalent sculpture that was scanned by photogrammetry and adjusted in CAM according the same procedures above-mentioned. The surface of the blank metal plate for the test shape was etched with an equally spaced dotted pattern. This enables a comparison of the simulated deformation to the deformation as appeared in real. Figure 16 shows the photogrammetry analysis. Note that not all dots are detected. This is because of the reflections of light on the metal surface. This can be solved by enhancing the pictures digitally but takes much efforts. Figures 17 and 18 show the results of the deformations as predicted by simulation on the surface of the small test shape. Figures 19 and 20 show the results of the deformations as determined by the photogrammetry analysis on the real test shape.

When comparing Figures 17 to 19 and 18 to 20, the conclusion can be made that the results of the

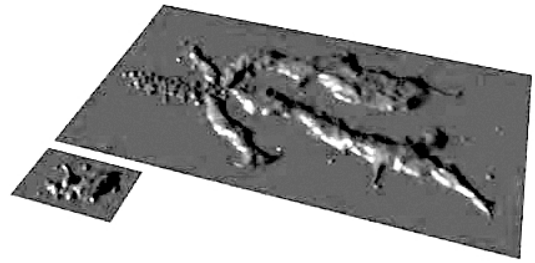

Figure 15. Full size sculpture with a small equivalent test shape

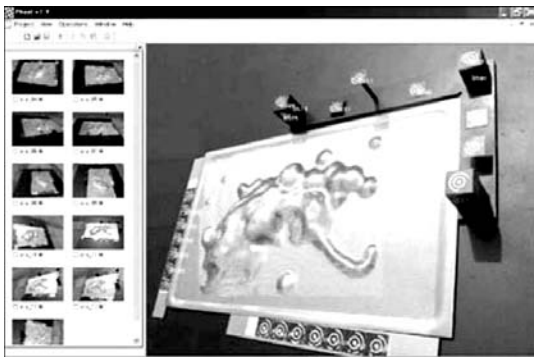

Figure 16. Photogrammetry analysis for comparison of the simulated and real deformation

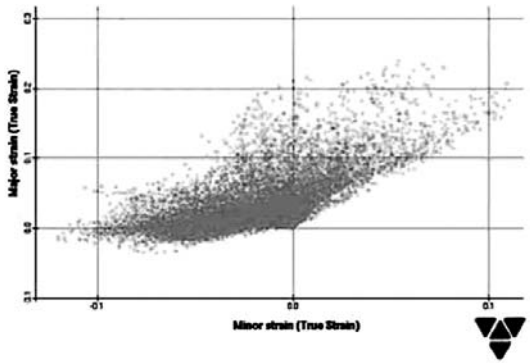

Figure 17. FLD of the simulated deformation

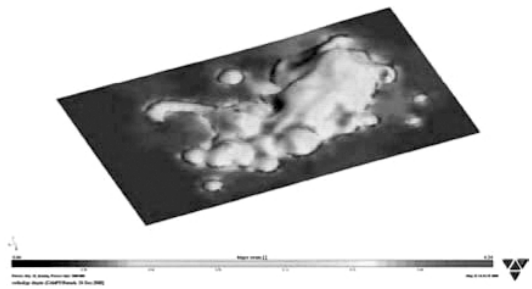

Figure 18. 3D plot of the simulated deformations on the small test shape surface

simulation matches very well with the results of the photogrammetry analysis on the real formed test shape.

Shape control for additional treatments. Another application with photogrammetry is shape determination using circular barcodes.

As described, a beacon (see Figure 16) is used with circular barcodes on it that are calibrated. This kind of barcodes can be printed on stickers and put on any surface that is to be measured. Figure 21 shows an example of a photogrammetry shape measurement using barcode stickers. The method with barcodes provides some benefits compared to method by which the surface texture is used for generating a 3D point cloud. The method is more straightforward to perform because the software detects barcodes much more easy than a surface texture. Each barcode has a unique number which makes it possible to relate each point

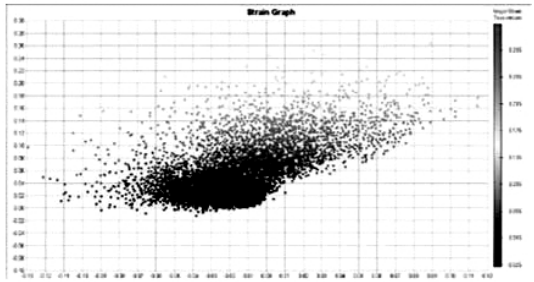

Figure 19. FLD of the deformations measured on the real test shape

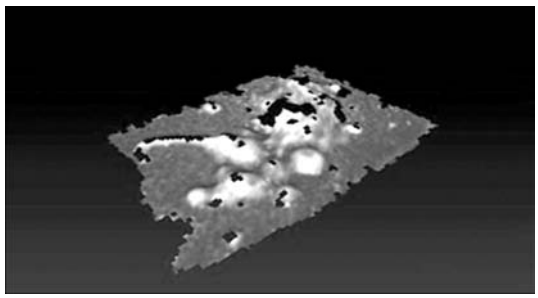

Figure 20. 3D plot of the deformations measured on the real test shape

Figure 21. Shape determination of a 60 mm thick explosive formed stainless steel panel with photogrammetry using circular barcodes

in the 3D point cloud to a point on the workpiece surface. This makes it possible to compare the shape of a workpiece before and after e.g. trimming the edges or after a welding operation. Barcodes are also etched on the workpiece surface so that the deformation of the shape can be determined due to heat treatments. Stickers cannot be applied because these would burn off.

CONCLUSION

A test method was developed for determining FLC for explosive forming using photogrammetry analysis. Photogrammetry is used for determining the deformation on a real workpiece and comparing the results to software simulations. It is also used for determining shapes using the «texture method» for a complicated 3D shape and the «barcode method» for a less complicated shape. The barcode method allows the determination of the shape changes due to e.g. edge trimming, welding and heat treatments.

NEW TECHNOLOGY FOR PRODUCTION OF JOINTS ON HIGH-STRENGTH ALUMINIUM ALLOYS BY EXPLOSION WELDING

S.Yu. ILLARIONOV, L.D. DOBRUSHIN and **Yu.I. FADEENKO**
E.O. Paton Electric Welding Institute, NASU, Kiev, Ukraine

A new technology is offered for explosion welding of series 7xxx high-strength aluminium alloys. The technology is based on natural ageing, which is a property of heat-hardening aluminium alloys, i.e. the process of spontaneous strengthening of an alloy after quenching, which makes it possible to perform explosion welding during the incubation period.

Keywords: *explosion welding, explosion cladding, high-strength aluminium alloys, heat-hardening aluminium alloys, natural ageing*

Owing to their high strength (up to 600 MPa), series 7xxx high-strength aluminium alloys are widely applied in aircraft engineering, and in aircraft frame components in particular.

Series 7xxx alloys are heat-hardening. Their required mechanical properties over wide ranges are achieved by heat treatment. These alloys have an Al–Zn–Mg or Al–Zn–Mg–Cu alloying system.

Importance of the problem of providing reliable welded joints on high-strength heat-hardening aluminium alloys grows because of transition from riveted to welded structures of civil aircraft frames. The above alloys are considered hard-to-weld or even unweldable by traditional welding methods, which are accompanied by intensive heating of a material. This can be explained by the fact that their mechanical properties are determined to a great degree by a heat treatment cycle, the parameters of which should be precisely kept to, otherwise a loss in strength, liquation cracking etc. may take place in the heat-affected zone. Sound joints on some alloys of series 7xxx can be provided by laser, electron beam or friction stir welding.

By request of «Airbus UK Ltd.», the E.O. Paton Electric Welding Institute conducted investigations on explosion welding of series 7xxx alloys to evaluate their weldability. The main difficulty in explosion welding of these alloys is their low ductility. Elongation of an alloy may be only 3–16 %, depending on the alloy grade and type of its strengthening heat treatment. Traditionally, a soft interlayer of commercially pure aluminium is used for welding such materials. In some cases it is unacceptable, because the integral tear strength of a joint will be determined only by the strength of commercially pure aluminium, allowing for the effect of contact strengthening of the soft interlayer. Therefore, the problem of joining aluminium alloys is still topical.

The purpose of this study is to evaluate the efficiency of using the new explosion welding technology for production of joints on different alloys of series 7xxx, which are applied in transition pieces between the aircraft units.

Modified analogue of alloy 7050, 150 mm thick, was used as a clad alloy. Cladding materials were alloys 7017 T651, 10 mm thick, and 7018 T7651, 10 and 15 mm thick. Typical chemical compositions and mechanical properties of these alloys are given in Tables 1 and 2.

The parallel scheme of explosion welding, where the cladding plate is located in parallel to the clad one before welding, was used for cladding the samples. The parallel scheme is simpler in fit-up than the angular one, and it is characterised by equality of detonation velocity D of an explosive and contact point velocity v_c of the mating surfaces. A mixture of certain proportions of ammonite # 6ZhV and ammonium nitrate was used as an explosive.

As noted in studies [1, 2], this class of aluminium alloys (the above studies considered the analogue of the investigated materials — alloy V95) is characterised by the narrowest range of weldability among all other aluminium alloys when joined by explosion

Table 1. Chemical compositions (wt. %) of alloys investigated

Alloy	Si	Fe	Mg	Cu	Zn
7017 T651	0.12	0.22	2.27	0.12	4.78
7018 T7651	0.16	0.30	1.0	0.12	4.8
Analogue of 7050	Up to 0.06	Up to 0.08	1.2–1.8	1.3–2.0	7.0–8.0

Table 2. Mechanical properties of alloys investigated

Alloy	σ_t, MPa	$\sigma_{0.2}$, MPa	δ, %
7017 T651	468	425	13.0
7018 T7651	350	291	16.4
Analogue of 7050	510	476	7.0

Figure 1. Appearance of a sample after explosion cladding

welding. Because of their low ductility, they have a high degree of localisation of plastic deformation of the joining zone metal in explosion welding, this leading to substantial heating of metal near the weld. The unloading wave arriving to the weld can fracture the forming joint. Study [2] suggested widening the weldability range by shifting position of its lower limit to lowering the level of energy input to the welded joint, which was achieved by using preliminary homogenising annealing of the alloys. As proposed in [2], the joints after explosion welding should be subjected to strengthening heat treatment.

It was impossible to use such annealing in the present study, as heating of the base plate was inadmissible. It should be noted that the process of heat treatment of the clad metal is proprietary, and the authors could not change anything in properties of the material. It also applied to the entire joint as a whole.

Considering the above limitations on production of welded joints on the series 7xxx alloys, while optimising the explosion welding conditions the authors attempted to increase as much as possible the time of impact on the cladding plate by the detonation products. In practice, it was achieved by decreasing the welding gap (0.6–0.7 of thickness of the flyer plate) and increasing the explosive layer thickness [3]. To decrease the energy input to the joining zone, the explosive detonation velocity was chosen to be relatively low: D = 1800–1900 m/s.

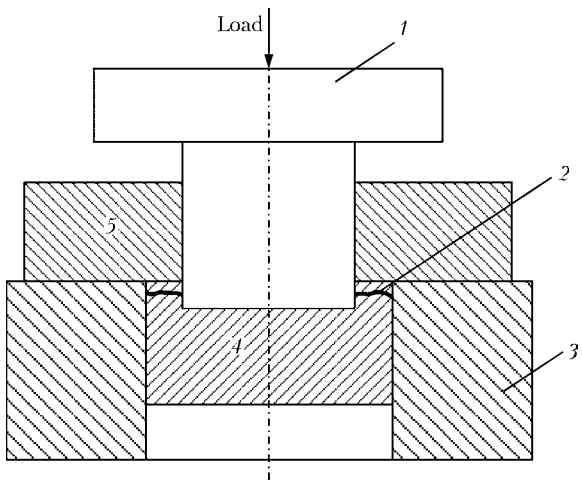

Figure 2. Schematic of tests to static tear strength of the cladding layer: *1* — punch; *2* — boundary of the joint; *3* — support; *4* — cladding alloy; *5* — base alloy

In the course of investigations, the authors suggested a new technology for explosion welding of high-strength aluminium alloys, based on the known property of heat-hardening aluminium alloys — natural ageing, i.e. the process of spontaneous strengthening of an alloy.

The principle of using the ageing effect is as follows. The cladding plate, which is delivered in the strengthened state, is subjected to quenching, this leading to dissolution of the strengthening phases, decrease in strength properties and increase in ductile properties. Then the natural ageing processes take place (at room temperature). Explosion welding should be performed immediately after quenching, as long as the cladding material remains sufficiently ductile, while after welding the value of strength of the cladding plate and, hence, of the joint continues growing. The positive factor is the presence of the so-called incubation period, where ductility does not yet decrease after quenching. This period for the series 7xxx alloys lasts 24 hours, and for alloy D16, for example, it is only 2–3 h. This effect is used in forming as well.

The process of natural ageing for the series 7xxx alloys may last several months, or even years, according to some information. However, the main increase in strength is achieved during a month. It should be noted that natural ageing does not provide maximal strength of an alloy. The optimal combination of the desired properties (maximal strength or strength combined with ductility) is achieved by natural ageing.

The new technology was practically implemented as follows: the cladding plates of alloys 7017 and 7018 were subjected to heating in furnace to 465 °C for 1 h, and then to water cooling. Explosion welding was carried out not later than 3 h after that. It can be seen in Figure 1 that there is no brittle fracture of the cladding plate along edges of the welded sample, i.e. the cladding alloy is sufficiently ductile.

The joints made with and without the new technology were investigated: metallographic examinations were carried out by the method of optical microscopy of the sections cut out along the direction of propagation of the explosion welding process, and tests to static tear strength of the cladding layer were conducted (Figure 2).

Hardness of the cladding layer under a load of 600 N was periodically checked to monitor the process of its natural ageing.

As seen from Figure 3, when no heat treatment was performed, the joining zone contains defects, and the level of strength is low (a specimen fractured as early as when it was made by using a machine tool). Results of mechanical tests to tear of the cladding layer of alloy 7017 are given in Table 3.

Control of hardness of the cladding layer showed that it was *HRB* 87–89 in 20 days after quenching,

Figure 3. Typical microstructure (×100) of the joint on alloy 7017 without heat treatment of the cladding plate (*a*) and that on analogue of alloy 7050 by using the new explosion welding technology (*b*)

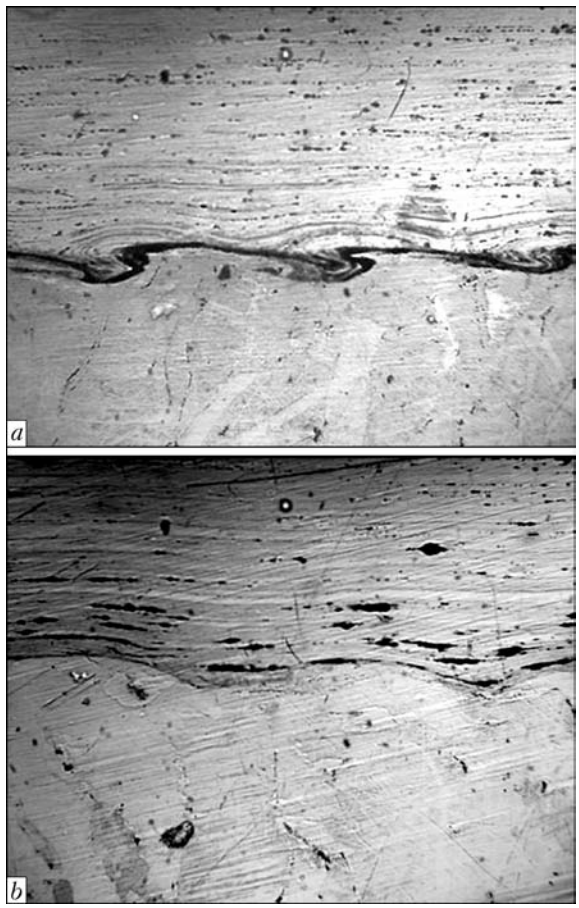

Figure 4. Typical microstructure (×100) of the joint on alloy 7018 without heat treatment of the cladding plate (*a*) and that on analogue of alloy 7050 by using the new explosion welding technology (*b*)

and *HRB* 90–92 — after 32 days, whereas in the initial state of a maximal strength it was *HRB* 105–106.

As shown by measurements of hardness and tear strength of the joint, the attempts to achieve initial mechanical properties of alloy 7017 by natural ageing failed. Nevertheless, the effect of using the new technology in this case remained high.

As seen from Figure 4, without heat treatment the joining zone is characterised by the presence of turbulences and wave crests, which is indicative of a substantial localisation of plastic deformation of the joining zone metal, leading to high heating of metal near the weld and structural heterogeneity. In this case this does not affect the static strength of the joint. However, allowing for its low ductility, this must have a negative influence on the fatigue and cyclic strength. Results of mechanical tests to tear of the cladding layer are given in Table 4.

Control of hardness of the coating of alloy 7018 showed that it was *HRB* 80–82 in 20 days after quenching, and *HRB* 87–89 — after 32 days, whereas in the initial state of a maximal strength it was *HRB* 101–102.

A number of the series 7xxx alloys can be used in design of modern aircraft. As the intensive efforts are now in progress for replacement of riveted joints by the welded ones, this leads to the need for welded transition pieces to be used between the units made from dissimilar alloys of series 7xxx, explosion welding being a promising method for this application.

Table 3. Results of mechanical tests to tear strength of the cladding layer of alloy 7017

State of cladding layer metal	σ_t^j, MPa	σ_t^j: σ_t^{in}, %
Quenching + natural ageing, days		
6	272	58
32	420	89

Note. Here and in Table 4, σ_t^j and σ_t^{in} are tensile strengths of the joint and initial metal, respectively.

Table 4. Results of mechanical tests to tear strength of the cladding layer of alloy 7018

State of cladding layer metal	σ_t^j, MPa	σ_t^j: σ_t^{in}, %
Quenching + natural ageing, days		
6	290	82
32	340	97
70	350	100
Without heat treatment	350	100

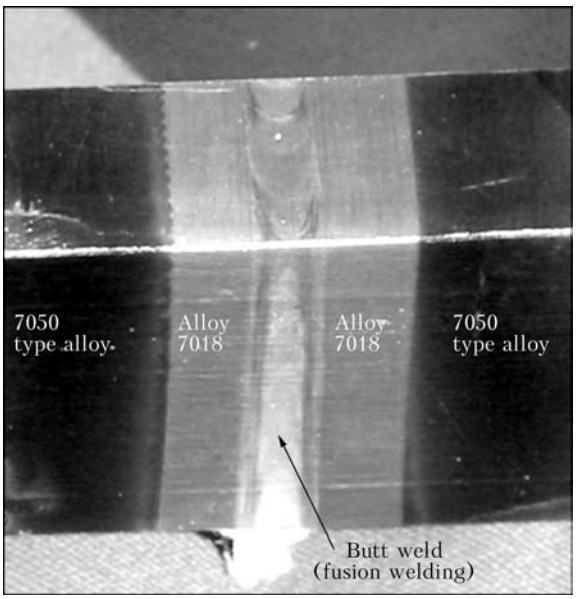

Figure 5. Macrostructure of a combined butt joint on hard-to-weld high-strength aluminium alloy

As noted above, the series 7xxx alloys are considered hard-to-weld. Reliable joints of a large thickness can be produced on some alloys of this series by fusion welding, whereas on other alloys of this series this method involves problems. A rational way out of this situation can be the use of such a technological scheme where edges of the joint of a hard-to-weld aluminium alloy are clad by explosion welding with an alloy of the same system, but having a good weldability, e.g. in electron beam or laser welding. An example of such a combined joint is shown in Figure 5.

Therefore, application of the new technology for production of joints on heat-hardening high-strength aluminium alloys by explosion welding makes it possible to considerably widen the range of their weldability. Sometimes this is the only method for providing a reliable joint.

Application of the new technology allows avoiding postweld heat treatment (after explosion welding), which is used to increase strength of the joints. This is especially important for the cases where heat treatment is inadmissible for the cladding layer of a series 7xxx alloy, as it can change its initial strength properties. The new explosion welding technology can be effectively employed in combination with traditional fusion welding methods.

1. Lysak, V.I., Kuzmin, S.V. (2005) *Explosion welding*. Moscow: Mashinostroenie.
2. Voevodin, L.B. (1987) *Development of explosion welding technology for manufacturing of composites on the base of aluminium alloys*: Syn. of Thesis for Cand. of Techn. Sci. Degree. Volgograd.
3. Kudinov, V.M., Koroteev, A.Ya. (1978) *Explosion welding in metallurgy*. Moscow: Metallurgiya.

APPLICATION OF EMULSION EXPLOSIVES FOR EXPLOSION WELDING

V.V. SILVESTROV, A.V. PLASTININ and **S.I. RAFEJCHIK**
M.A. Lavrentiev Institute of Hydrodynamics, RAS SD, Novosibirsk, RF

Characteristics of low-velocity emulsion explosives with a detonation velocity of 2–3 km/s are presented. Their application is considered for explosion cladding of metal plates with foils (from aluminium to molybdenum) 100–300 μm thick without a damping layer between the plates and a flyer foil, as well as for welding of a steel tube 11 mm in diameter to a steel bushing by the parallel welding scheme.

Keywords: *emulsion explosives, explosion welding, thin foils, tube plates*

Emulsion explosives are of interest to address the problems associated with explosion treatment of materials (welding, forming, pressing, etc.) [1]. Emulsion explosives contain no strong individual explosives, the only potentially explosive component in their composition being ammonium nitrate. These explosives are characterised by lower costs, compared with trinitrotoluol, hexogen or other high explosives, by extremely low sensitivity to mechanical and thermal impacts, along with good susceptibility to detonation, by low gas hazard and high water resistance [2]. Emulsion explosives can be manufactured on site of explosion operations, this making transportation of their non-explosive components much simpler.

The possibility of detonation of emulsion explosives in layers up to 0.5 mm thick (critical diameter $d_{cr} < 6$ mm) was reported in study [3]. As shown later, commercial emulsion explosives that contain aluminium inclusions have critical thickness $\Delta_{cr} = 3.3$ mm and detonation velocity $D_{cr} \approx 3$ km/s [4]. Emulsion explosives developed in study [5] detonated in a layer with thickness of up to $\Delta_{cr} \approx 2$ mm ($D_{cr} \approx 2.7$ km/s), but their detonation velocity rapidly increased with thickness of the explosive layer: even at $\Delta > 5$ mm it exceeded 4 km/s.

As a result of utilisation of an ultra-dispersed emulsion with oxidiser droplets not more than 1–2 μm in size, and addition of a big amount of low-density sensitising inclusions (physical sensitiser — glass microbaloons), the ultimate velocity of detonation of the emulsion explosives decreases to 2–3 km/s, their high detonation ability being maintained [6]. At a sensitiser content of more than 20 wt.% above the emulsion weight, detonation velocity D is almost independent of a transverse size of the emulsion explosive charge, thickness of a flat charge being $\Delta \geq 10$ mm.

The purpose of the present study was to consider the capabilities of low-velocity emulsion explosives by an example of two classical tasks of explosion welding: cladding of metals with thin metal foils up to 0.1 mm thick, and joining of small-diameter thin-walled metal tubes to tubular bushings under explosion welding conditions.

Parameters of emulsion explosives. Emulsion explosives made under laboratory conditions were used for the studies. Emulsions had the following composition (wt.%): 68 ammonium nitrate, 11 sodium nitrate, 15 water, 2 hard wax, 2 sorbitan monooleate emulsifier, and 2 industrial oil (as part of the emulsifier). Oxygen balance of the emulsion was close to zero, and density was $\rho_e = 1.41$ g/cm^3. The oxidiser droplets were not more than 1–2 μm in size. To produce the emulsion explosives, hollow glass microbaloons of the MS-V type (Open Joints Stock Company «Term», Moscow Region) were added to the emulsion on top of its weight in an amount of $\mu = m_{mb}/m_{me}$ (wt.%) (m_{mb} — weight of the microbaloons, and m_{em} — weight of the emulsion). The mean size of the microbaloons was about 60 μm, and their apparent density was $\rho_{mb} = 0.14$–0.15 g/cm^3. At a big amount of inclusions, the emulsion explosives are formed manually, but they have satisfactory plasticity.

Density ρ_0 of the emulsion explosives decreases from 1.08 to 0.52 g/cm^3, as the content of microbaloon is increased from 5 to 50 %. Dependence of density ρ_0 of a composition upon parameter μ is determined by ratio $\rho_0 = \rho_e(1 + \mu)/(1 + \mu\rho_e/\rho^*_{mb})$, where $\rho^*_{mb} = 0.23 \pm 0.01$ g/cm^3 is the real density of the microbaloons. One part of the emulsion explosive volume, v_{mb}, is filled with an inert material, i.e. hollow microbaloons, while the other, $v_{em} = 1 - v_{mb} = 1/(1 + \mu\rho_e/\rho^*_{mb})$, is filled with an emulsion matrix, which, in fact, is an explosive material. At $\mu = 50$–60 %, the volume part of the emulsion decreases to 30–25 %, and the detonation velocity slows down to 2 km/s or lower.

Within a density range of 0.5–1.1 g/cm^3, the velocity of detonation of a 20 mm diameter cylindrical charge decreases linearly with the density: $D = 4.68\rho_0 - 0.46$. At $\mu > 20$ %, the detonation velocity is below 3 km/s, and density of such compositions is 0.75–0.51 g/cm^3. Dependence of the detonation velocity upon the weight content of inclusions is described by power dependence $D = D_e(1 + \mu\rho_e/\rho^*_{mb})^{-\alpha}$ at $\alpha = 0.76$ and $D_e = 5.74$ km/s.

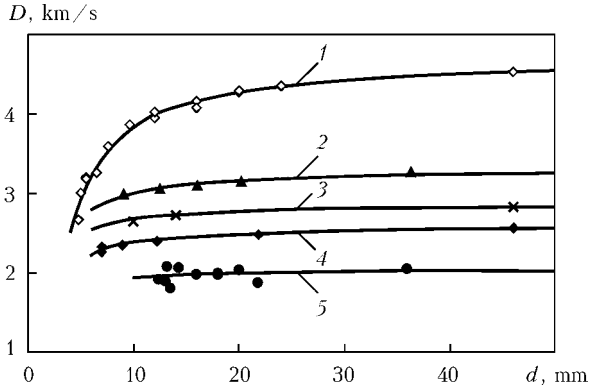

Figure 1. Dependence of detonation velocity on transverse size of charge for emulsion explosives: *1* — μ = 8; *2* — 20; *3* — 25; *4* — 35; *5* — 50 %

Figure 1 shows the results of measuring the detonation velocity (within the «welding range» velocities) for the emulsion explosives at different μ depending upon the transverse size, diameter of the cylindrical charge or thickness of the flat layer. The charges were enclosed in thin-walled tubes or flat boxes made from plastic. The detonation velocity of an emulsion explosive depends but slightly upon the transverse size of a charge at a concentration of hollow microbaloons MS-V increased to 20–25 % or more. However, the critical detonation parameters, such as diameter d_{cr} of a cylindrical charge and thickness Δ_{cr} of a flat charge, increase with growth of the content of inclusions (Table 1). Ultimate detonation velocity D_{max} and difference $\Delta D = D_{max} - D_{cr}$ were estimated from $D(d)$ using the Eyring equation [7].

At μ = 25–50 %, the detonation velocity of the emulsion explosives was below 3 km/s, permissible thickness of the flat layer being 3–12 mm. This velocity range is applicable for explosion welding of the majority of metals by using the parallel scheme. At μ = 8 %, the minimum permissible thickness of the emulsion explosives is 2 mm for a flat charge, and the detonation velocity is less than 3 km/s at $\Delta \leq 3$ mm.

Detonation pressure for the low-density emulsion explosives at $D \leq 3$ km/s is low: the estimation made by using formula $P_D \sim \rho_0 D^2/(n+1)$ and explosion products polytropic exponent $n \approx 2.4$ yields 0.6–2.0 GPa, this being sufficient for explosion acceleration of thin metal plates and shells to the velocities above 100 m/s, which are required in some applications. Consider the results illustrating utilisation of the low-velocity emulsion explosives for cladding metals with foils without a buffer layer, i.e. damper, and for welding of small-diameter thin-walled tubes to tube plates by the parallel explosion welding scheme.

Table 1. Parameters of emulsion explosives

μ, %	ρ_0, g/cm^3	d_{cr}, mm	Δ_{cr}, mm	D_{cr}, km/s	D_{max}, km/s	ΔD, km/s
8	1.0	5	1.8–2.0	2.7	4.7	2.0
20	0.75	6–7*	3*	2.6*	3.3	0.7
35	0.62	7–8	3.5	2.3	2.6	0.3
50	0.51	11–12	11–12	1.9	2.1	0.2

*Estimated from the dependence of detonation parameters on parameter μ.

Cladding of metals with thin foils. In a number of applications it is necessary to deposit thin functional coatings, e.g. heat-resistant, chemical-resistant, anticorrosive etc., on the metal surface. If such problems are addressed by using the explosion welding method, it is necessary to apply either the buffer layer (damper between the foil and explosive to decrease the rotation angle and velocity of a flyer foil) or the angular scheme of explosion welding to reduce contact point velocity V_c. This is associated with a big minimum permissible thickness of the explosive layer (based on ammonites) or a high detonation velocity of individual explosives. For the emulsion explosives under consideration, there is hardly any need to use the buffer layer.

Below we give some results of welding of foils with thickness $\delta = 0.1$–0.3 mm to a steel (or copper) target by the parallel welding scheme using the low-velocity emulsion explosives. Sizes of the steel or copper target were as follows: thickness 40–10 mm, length 300 mm, and width 60 mm. Material of the metal foils was aluminium, titanium, stainless steel, bronze, copper and molybdenum with a density of 2.8–9.0 g/cm^3 (Table 2).

An explosive was placed between the flyer foil and 0.5 mm thick layer of PET (polyethylene terephthalate) plastic covering the box with the emulsion explosive. Weight ratio $r = \tilde{m}_{ex}/\tilde{m}_{met}$ was changed by almost an order of magnitude: from 0.67 to 6.3. Here $\tilde{m}_{ex}$ is the weight of the emulsion explosive per unit surface area, and $\tilde{m}_{met}$ is the weight of metal per unit surface area. An air gap approximately equal to thickness of the flyer foil was set between the foil and target.

Because of a relatively high detonation velocity equal to 2.7–3.0 km/s at 10 % with the flat scheme, the resulting welds were developed and wavy. To clad steel with a titanium foil 100 μm thick, a fluoroplastic film 160 μm thick was placed between the emulsion explosive and foil. In all the cases no visible damage to integrity or separation of the foil was fixed in explosion welding over the entire surface of the clad plate. Figure 2 shows microstructures of metal in cross sections of some joints revealed by scanning electron microscopy. No special measurements of strength of the joints were made. However, while attempting to detach the foil from the target, the fracture occurred not in the weld but in the bulk of the foil. At $\delta \leq$ $\leq$ 300 μm, the weight of the emulsion explosive per unit surface area was 0.2–0.4 g/cm^2.

Flying properties of the emulsion explosives have not been studied as yet. So, let us evaluate parameters of collision of the flyer plate with the target from geometric characteristics of the formed waves. In cladding steel with a copper foil 200 μm thick the wave amplitude was $a \approx 25$–30 μm, wave length was $\lambda \approx$ $\approx$ 145 μm, and contact point velocity was $V_c = D \cong$

Table 2. Parameters of experiments on explosion welding using emulsion explosives

Pair to be welded	ρ_f, g/cm^3	δ, mm	μ, %	Δ_{EE}, mm	r	Result
Flat scheme						
Aluminium/copper	2.8	0.2	10	2.5	4.2	Wavy weld
Aluminium/copper	2.8	0.2	35	5.5	6.2	Same
Titanium/stainless steel	4.5	0.1	10	3.0	6.3	»
Stainless steel/copper	7.8	0.2	10	2.4	1.5	»
Bronze/steel	8.4	0.3	10	3.4	1.3	»
Copper/steel	8.9	0.2	10	2.7	1.4	»
Molybdenum/steel	9.0	0.2	10	2.8	1.2	»
Copper/steel	8.9	1.0	50	12.0	0.67	»
Cylindrical scheme						
Stainless steel/steel	7.8	750	50	∅10–42	0.21	Pressing out
			35		0.27	Same
			20		0.32	Wavy weld

$\cong$ 2.7–3.0 km/s. And in cladding steel with a copper plate 1 mm thick the above parameters were as follows: $a \cong 25$–30 μm, $\lambda \approx 170$ μm, and $V_c = D \cong 2$ km/s. Now let us estimate the angle of collision of the flyer plate with the target from formula $\lambda/\delta = 26 \sin^2 \frac{\gamma}{2}$, which relates a relative wave length to collision angle γ at the asymmetric collision [8]. In the first case $\gamma \cong$ $\cong 19°$ at $r \approx 1.4$, and in the second case it is much lower — $\gamma \cong 9°$ at $r \approx 0.67$. Given that the rotation angle is small, the flyer plate velocity is $v_p \approx$ $\approx 2D \sin(\gamma/2) \approx 990$ m/s for a 200 μm foil and $v_p \approx$ ≈ 314 m/s for a 1 mm copper plate. In both cases, for the copper/steel pair the collision parameters fit the «welding window» in plane (V_c, γ) near the upper and lower limits of the explosion welding range [8, 9].

Therefore, the low-velocity emulsion explosives can be applied for explosion cladding of metal with thin foils/plates of different metals. Such studies are of a particular interest in the cases where it is necessary to minimise the amount of the explosives used [10, 11].

Welding of tube to tube plate model. The cylindrical geometry was implemented by welding of a metal tube to carbon steel bushing by the parallel scheme of explosion welding of tubes to tube plates, as suggested in [12]. Internal diameter of a stainless steel tube was 11 mm, and wall thickness was 0.75 mm. The artificial gap between the tube and bushing was equal to wall thickness of the tube. The cylindrical emulsion explosive charge was put into the tube to length $l = 15$–20 mm. The charge was initiated by using standard detonating cord DShV with a di-

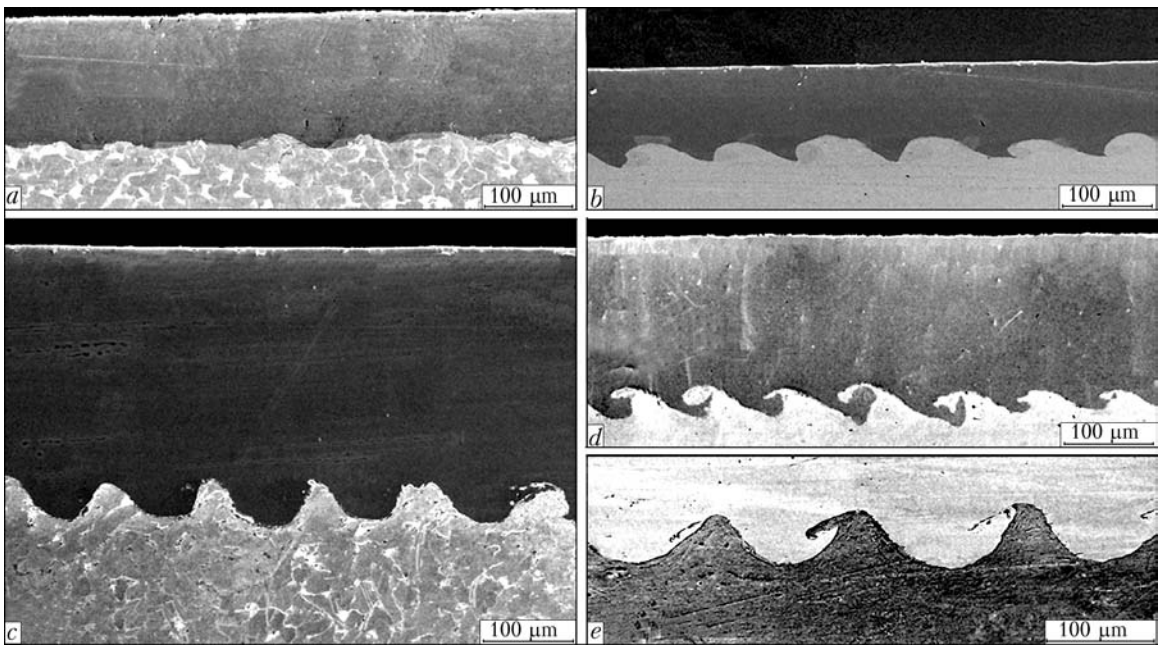

Figure 2. Microstructures of metal resulting from cladding with metal foils by using emulsion explosives: *a* — 200 μm aluminium/copper; *b* — 100 μm titanium/stainless steel; *c* — 300 μm bronze/steel; *d* — 0.2 mm molybdenum/steel; *e* — 1 mm copper/steel

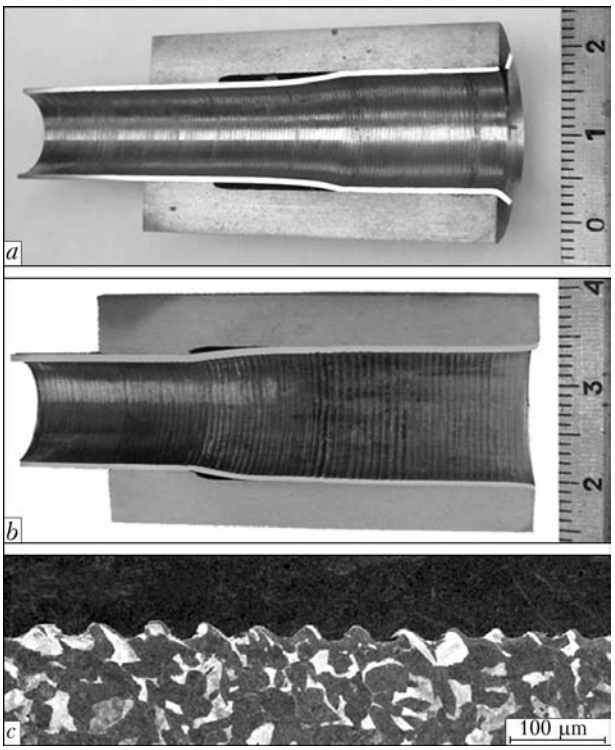

Figure 3. Explosion joining of tube to steel bushing: *a* — pressing out; *b* — welding, section of bushing after explosion; *c* — microstructure of explosion joining zone metal

ameter of 5 mm, which was inserted into the emulsion explosive to a depth of about 10 mm. In the first two experiments the emulsion explosive was used at μ = = 35 % (r = 0.21) and 25 % (r = 0.27). The experiments resulted in quality pressing out of the tube, but explosion welding did not take place (Figure 3, *a*).

The explosion welding mode did take place by using a stronger composition at μ = 20 % (emulsion explosive density 0.75 g/cm^3, detonation velocity 3 km/s, and loading coefficient r = 0.32) (Figure 3, *b*). Wave formation took place in the initial region about 3 mm long. Further on, a wavy weld was formed along length l ($\lambda \approx$ 50–100 μm, $a/\lambda \cong$ 0.2–0.3), resulting in a strong tight joint between the tube and bushing (Figure 3, *c*). The wave formation stopped at the end of the emulsion explosive charge. Weight of the emulsion explosive in one charge was no more than 1.5 g (it depends upon the required weld length).

This example proves applicability of the low-velocity emulsion explosives for the technology of explosion welding of small-diameter thin-walled tubes to tube plates [11]. In this case there is no need to use extra heat penetration of the tube end to ensure tightness of the tube/bushing joint.

CONCLUSION

Ingenious compositions were developed for the emulsion explosives with a detonation velocity of 2–3 km/s. The compositions are characterised by a low dependence of the detonation velocity upon the diameter of a cylindrical explosive charge or thickness of a flat one. These explosives feature the use of an ultra-dispersed emulsion and high content of hollow glass microbaloons.

Detonation characteristics of the low-velocity emulsion explosives allow applying them in the cases where it is expedient to use explosion, but necessary to minimise the explosion load on the materials treated. Examples are given of application of the low-velocity emulsion explosives for explosion cladding of metals with foils up to 0.1 mm thick (without a buffer layer to damp the shock wave), and for explosion welding of 10 mm diameter tubes to a tube plate in the wave formation mode.

Consistency of the emulsion explosives can vary from a soft paste-like state at $\mu \leq$ 20 % to a state that looks like a slightly dried glazing compound at a high content of microbaloons. Charges of the required profile can be formed only manually so far, this limiting application of these explosives to explosion treatment of small-scale parts.

This study was carried out with the support rendered under program # 12.10 of the Presidium of the Russian Academy of Sciences, grant # 09-08-00164-a of the Russian Foundation for Fundamental Research, and partial support under grant # NSh-1886.2008.1 of the President of the Russian Federation.

1. Matsuzawa, T., Murakado, T., Aimoto, H. et al. *Method for explosive cladding*. Pat. 4844321 US. Publ. 04.07.1989.
2. Wang Xuguang (1994) *Emulsion explosives*. Beijing: Metallurgical Industry Press.
3. Yoshida, M., Iida, M. et al. (1985) Detonation behavior of emulsion explosives containing glass microballons. In: *Proc. of 8th Int. Symp. on Detonation*, 171–177.
4. Petel, O.E., Mack, D., Higgins, A.J. et al. (2007) Minimum propagation diameter and thickness of high explosives. *J. Loss Prevention in the Proc. Industries,* 20(**4**), 578–583.
5. Silvestrov, V.V., Plastinin, A.V., Karakhanov, S.M. et al. (2008) Critical diameter and thickness of emulsion explosive. *Fizika Goreniya i Vzryva*, 44(**3**), 121–127.
6. Silvestrov, V.V., Plastinin, A.V. (2009) Study of low-velocity emulsion explosives. *Ibid*., 45(**5**) (to be publ.).
7. Eyring, H., Powell, R.E., Duffey, G.H. et al. (1949) The stability of detonation. *Chem. Rev.*, 45(**1**), 69–81.
8. Deribas, A.A. (1980) *Physics of explosion strengthening and welding*. Novosibirsk: Nauka.
9. Simonov, V.A. (1995) *Fields of explosion welding. Main parameters and criteria*. Pepr. RAS SD. M.A. Lavrentiev Institute of Hydrodynamics. Novosibirsk.
10. Masushi, A., Kubota, S. et al. (2000) Impact welding for urgent steel pipe repairs by emulsion explosives. In: *Proc. of 22nd Int. Symp. on Shock Waves*. Vol. 1. London, 565–570.
11. Meuken, D., Carton, E.P. (2004) Explosive welding and cladding. In: *Proc. of Conf. of the American Phys. Soc. on Shock Compression of Condensed Matter* (July 20–25, 2003, Portland, USA,). New York, 1110–113.
12. Crossland, B., Bahrani, A.S., Williams, J.D. et al. (1967) Explosive welding of tubes to tube plates. *Welding and Metal Fabric.*, 35(**3**), 88–94.

PRODUCTION OF ALUMINUM–STEEL BIMETAL WITH PROFILED INTERFACE

A.Z. BOGUNOV[1] and **A.A. KUZOVNIKOV**[2]
[1]CJSC «Pulse Technologies», Siberian Federal University, Krasnoyarsk, RF
[2]Institute of Engineering Physics and Radio Electronics, Siberian Federal University, Krasnoyarsk, RF

Peculiarities of microstructure and strength properties of aluminum–steel bimetal with profiled interface are considered, and potential application fields for such a bimetal are identified.

Keywords: *explosion welding, profiled interface, strength of bimetals, microstructure, steel-aluminum adapters, explosion riveting*

In the cases when a welded joint may fracture in a brittle way, its strength characteristics in many aspects are determined by the processes of crack initiation and propagation. In particular, cracking is aggravated if the contact interface is not flat, and a crack changes its direction in propagation. Accordingly, not only the quality of welding of metals, but also geometry characteristics of the contact interface influences the joint strength. It was proposed to fill the cavities with a metal welded [1], since the rough surface my have a detrimental effect on the quality of explosion welding. If ridges are made in the one of mating surfaces and inserted in slots in the other one, the explosion welding process is accompanied by simultaneous explosion riveting [2].

The purpose of the present study is to investigate microstructure and strength properties of bimetals with profiled interface, made by explosion welding with simultaneous riveting, and study influence of the interface geometry characteristics on the joint strength. The final task of the investigations is to develop steel-aluminum adapters with the advanced level of characteristics for upgrading the anode unit of aluminum electrolytic cells [3].

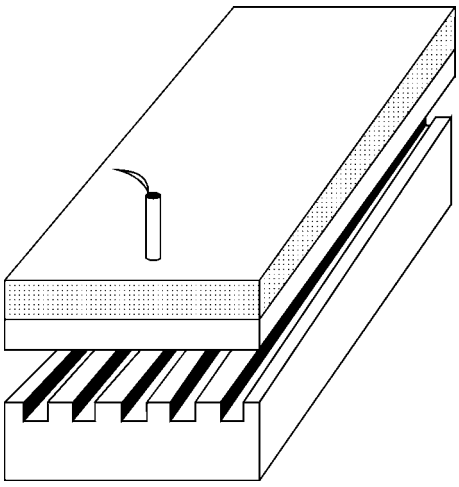

Figure 1. Scheme of producing bimetals with profiled interface

A scheme for producing bimetals with profiled interface is shown in Figure 1 [4]. Here the lay-out does not differ from that typically used in explosion welding, except that the target surface has parallel slots of a rectangular section milled out in it, with the orientation differing by no more than 30° from the direction of detonation propagation. At collision of a flyer plate with the ridges, they compress in the longitudinal direction and expand in the transverse one. Simultaneously, the plate material is punched through the converging throat and fills up the slots. As a result, the weld interface in bimetal has a «dovetail» section, alternating on the side of flyer plate and target (Figure 2). It should be noted that this scheme was chosen out of many variants of producing permanent joints [5] because of its easiest technological implementation.

Aluminum A5M, 10 and 20 mm thick, was used as a flyer plate, and a target was made from 30–50 mm thick steel St3. Width and height of the ridges were varied in a range of 3 to 10 mm, and width of a slot ranged from 4 to 20 mm. Explosive was a mixture of ammonite No. 6ZhV with NaCl in an equal weight ratio. Generally, welding was carried out in modes with a wavy interface. The detonation velocity of 1.8–2.2 km/s was measured by the Dotrisch method under the test ground conditions.

Typical microsection of the joint for a $5 \times 5 \times 5$ mm sample with slots is shown in Figure 2. As the initial surface geometry consists of three different regions, the welded joint is also characterized by heterogeneity. Aluminum directly contacts steel at the ridge and in the middle part of the slot bottom. Cracks 10 to 25 μm wide occupy a major part of slot cheeks and bottom. The cracks are filled with a brittle material that spalls out in grinding (Figure 3). Besides, porous regions of the solidified melt, 10 up to 300 μm wide (Figure 3,

Figure 2. General view of microsection of joint

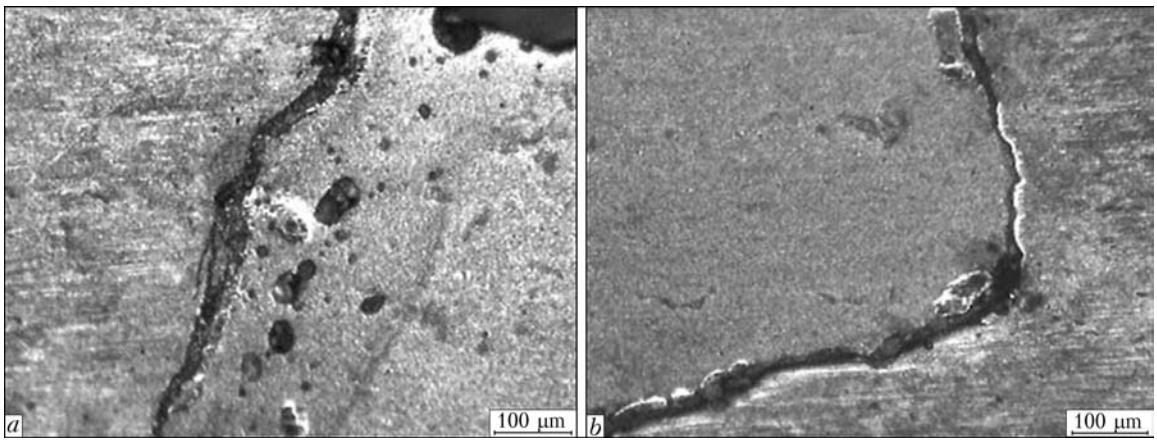

Figure 3. Microsection (annealing at 500 °C for 90 min) of cheek (*a*) and corner in slot on the opposite side (*b*)

a), isolated from aluminum with a clear interface can be seen on the slot cheeks and bottom corners. If detonation is directed not strictly along the slots, the melt is seen only on the one of slot cheeks (Figure 3, *b*). The heat affected zone up to 50 μm wide, with a structure refined by an order of magnitude, is revealed in adjacent steel. Spalls with displacement of the spalling material to the slot are observed at corners of the steel ridges.

Dependence of microhardness of different joint regions at a 500 °C temperature on time of annealing to 3 h was studied (Table 1). Microhardness in the melt zone changes non-monotonically, which reflects the process of transition of the quenched structure into the equilibrium state. Though the microhardness here significantly exceeds that of aluminum, it is lower than the values characteristic of intermetallic compounds of the Al–Fe system.

To carry out X-ray fluorescent analysis, the bimetal was milled out from the aluminum and steel surfaces to expose the steel ridges and aluminum in the slots. Then the sample was fractured in the slots along the cracks. The resulting bars with a total area of about 2 cm^2 on the side of aluminum and steel, respectively, were put together, and the surface of such a pack was examined by X-ray fluorescent analysis. Metastable intermetallic compound Fe_4Al_{13}, which is close in composition to $FeAl_3$ but formed in quenching, was revealed at the interface on the aluminum side. Clear reflexes of baierite $Al(OH)_3$ are fixed in a low angle area, which is uncharacteristic of metals. As this compound is observed also on the steel side, it can be related to the fracture zone, which is similar for both samples. Low temperature stability of baierite does not allow it to be in contact with molten aluminum. Therefore, it seems that the compound appeared in the process of samples preparation.

Cup-type samples [6] and their simplified modification were used for determination of tensile strength σ_t, where the coaxial slots were cut with two different-diameter bimetal crowns in the steel-aluminum plate from the steel surface through interface of the joint, penetrating into aluminum, and similarly on the aluminum side. The crowns with 21, 32, 43 and 46 mm diameters were used to make the slots. Size of the fractured ring was several times larger than that of the dovetail. П-shaped samples [6] cut normal to the surface geometry, with a multiple length to its period, were used in the case where size of the surface geometry was larger than 6 mm. Cross-section area of the samples in a fracture location was 250 to 680 mm^2. Thickness of the fractured region was approximately 3 mm, and in all the cases it was several times smaller than its length. Strength measurements were carried out mainly for the 200 × 200 mm bimetal plates in their central part. Obviously, the values of σ_t obtained by the above methods are of a comparative character. At the same time, procedures for determination of σ_t, which are specified by GOST, are inapplicable here.

Samples with a different surface geometry were made under the conditions of close values of the detonation velocity and rotation angle of the flyer plate.

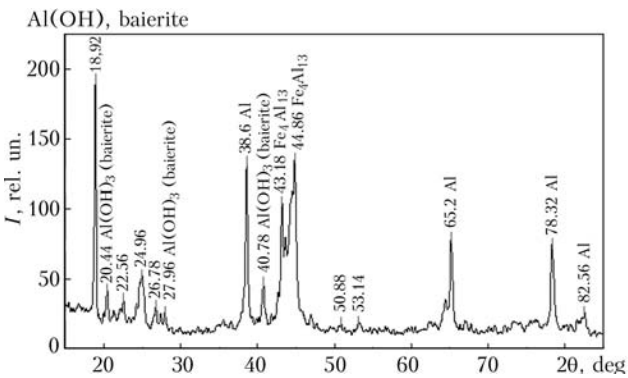

Figure 4. X-ray fluorescent analysis spectrum of zone of the Fe–Al joint on the aluminum side

Table 1. Values of microhardness of samples with the «dovetail» joint depending on the time of annealing

Place of measurement	Annealing time, min				
	Without annealing	20	35	90	180
Aluminum	0.6	0.4	0.3	0.3	0.3
Steel (ridge)	2.5	2.3	2.5	2.2	1.9
Side surface	2.1	2.5	1.3	3.3	3.5
Slot bottom	2.2	2.3	2.0	3.0	3.1
Interlayer at ridge	–	–	–	4.2	5.1

Table 2. Influence of geometry characteristics of interface on joint strength

Sample marking	Aluminum thickness, mm	Width, mm		Slot depth, mm	Tensile strength, MPa
		Ridge	Slot		
04	10	4	4	4	62
051	10	3	5	5	66
052	10	5	5	10	78
05	10	5	5	5	97
05	20	5	5	5	106
08	20	8	8	4	56
012	20	12	12	4	41

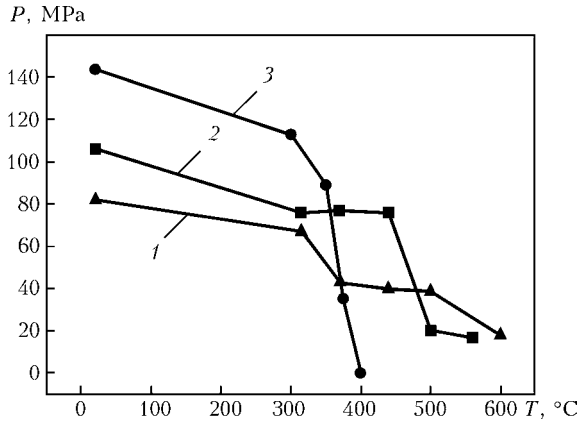

Figure 5. Comparison of strength after annealing for steel–aluminum bimetal of the dovetail type [7]: *1* — Al 10 mm thick; *2* — Al 20 mm thick and with flat interface; *3* — Al 12 mm thick

The data on σ_t are given in Table 2. Analysis of the character of fracture of the samples shows that fracture takes place in aluminum outside the weld interface at strength values above 80 MPa, at lower strength values aluminum starts getting out of the slots, and at strength of 50–60 MPa the fracture occurs along the interface.

Comparison of the results on tensile strength of the dovetail bimetal (surface geometry $5 \times 5 \times 5$ mm) with known data on the aluminum–steel bimetal with a flat interface after a heat treatment [7] is shown in Figure 5. It can be seen that the dependencies look approximately identically: a plateau where the strength value gradually decreases changes into a region where the rapid fall takes place. For the «dovetail» samples, the fall occurs in temperature range of 400–490 °C whereas for the bimetal with a flat interface it occurs in a temperature range of 350–380 °C. At the same time, strength of the joint does not tend to zero but comes out to a level of 1.5 MPa for the dovetail bimetal even under the conditions of formation of continuous intermetallic interlayer at high temperatures. This level is made up from strength of aluminum jammed in the slots and strength of the interlayer.

As shown by analysis of structure of the joint in a slot, providing of quality welding in this case involves problems. As can be seen from Table 2, strength of the joint with profiled interface at a level of aluminum is achieved due to the combination of two conditions: selection of the optimal geometry and ensuring quality welding over ridge apexes. Then, depending on the ratio of the slot to ridge sizes, as well as size of the fractured region, strength should level at some distance from the interface. At the same time, the range of the strength values starts from the values provided by aluminum jammed in the slots. Accordingly, σ_t can be raised with increase in such aluminum portion [8]. For example, slots normal to the existing ones and of the same size were milled on the surface of sample 05 in such a way that the steel ridges became 5×5 mm squares, $\sigma_t = 36$ MPa.

In manufacture of bimetal with profiled interface, the integrity of the joint is preserved even in those modes where the plates with a flat interface simply fly away one from another, for example in sample 05 at $D = 3.2$ km/s (ammonite No. 6ZhV without salt), $\gamma = 8°$; $\sigma_t = 19$ MPa; $\gamma = 0°$ (flat collision); $\sigma_t = 12$ MPa. In this connection, application of the profiled interface can be useful for problematic regions in terms of the quality of welding, for example, along the perimeter of the clad plate. As can be seen from Table 2, the profiled surface provides a strong joint with 20 mm thick aluminum, welding of which to the steel billet with a flat surface is complicated. In this case, it is likely that the dovetail interface promoted keeping the mating surfaces in contact up to the end of joint formation processes.

As a result of annealing at high temperatures (Figure 5), the welded contact loses its ductile properties, and it starts fracturing by the brittle mechanism. The profiled surface makes crack propagation difficult, which shows up in some increase in strength on the temperature dependence. At the same time, a change in the character of fracture from ductile to brittle one shows up most significantly in fall of the fracture energy [9]. In this connection, the dovetail-type joint has a considerable advantage, as strength is determined by fracture of aluminum in the slots, and the fracture energy makes up a proportional fraction of the corresponding aluminum characteristic.

Therefore, the joint with profiled interface produced by this technology can be useful in regions that are problematic in terms of the welding quality, for example, along the clad plate perimeter, in welding of thick plates, in particular, of aluminum, as well as in the cases of high possibility of degradation of the welding quality under service conditions. Around 80,000 steel-aluminum adapters with a profiled interface are operating successfully in anode assemblies of electrolytic cells at five aluminum plants of the Russian Federation since 2000.

1. Bushtedt, Yu.P., Dobrushin, L.D. et al. *Method of explosion welding of metal sheets*. USSR author's cert. 875741. Int. Cl. B23K 20/08. Publ. 24.05.76.
2. Kovalevsky, V.N., Zhukovsky, I.I., Shabeka, L.S. et al. *Explosion welding method*. USSR author's cert. 1102146. Int. Cl. B23K 20/08. Publ. 04.04.83.
3. Bogunov, A.Z., Kuzovnikov, A.A., Malyshev, V.V. et al. *Current conductor for electrolyzers of aluminium*. Pat. 2165482 RF. Publ. 29.08.1999.

4. Bogunov, A.Z., Kuzovnikov, A.A., Malyshev, V.V. et al. *Higher strength bimetal and method of its manufacturing*. Pat. 2315697 RF. Publ. 15.02.2005.
5. Matsui, S. et al. *Composite structures*. Pat. 5,244,746 US. Int. Cl. B23B 003/30, B60M 001/30. Publ. 14.09.1993.
6. Deribas, A.A. (1972) *Physics of explosion strengthening and welding*. Novosibirsk: Nauka.
7. Banker, J., Nobili, A. (2002) Aluminum-steel electric transition joints, effects of temperature and time upon mechanical properties. *Light Metals*, 439–445.
8. Bogunov, A.Z., Kuzovnikov, A.A., Malyshev, V.V. et al. *Heat-resistant bimetal insert*. Pat. 2318670 RF. Publ. 19.01.2006.
9. Ryabov, V.R., Pervukhin, L.B., Volferts, T.A. et al. (1995) Influence of explosion welding conditions on strength and plastic properties of steel-aluminium joints. *Avtomatich. Svarka*, **12**, 32–38.

POSSIBILITY OF PRESERVATION OF SHAPE AND SIZE OF CYLINDRICAL TUBULAR BILLETS OF MOULDS IN EXPLOSION CLADDING

Yu.P. MESHCHERYAKOV, V.M. OGOLIKHIN and **I.V. YAKOVLEV**
Engineering and Design Branch of the M.A. Lavrentiev Institute of Hydrodynamics, RAS SD, Novosibirsk, RF

The paper deals with the possibility of preservation of specified shape and size of tubular billets of moulds in explosion cladding of pipes with mounting of fillers inside the latter, namely shot, shot with water, gun grease and saltpeter melts. It is shown that utilization of metal shot as a filler is promising for preservation of shape and dimensions without large additional costs.

Keywords: *mould, cylindrical tubular billets, cladding of tubular billets, explosion welding, internal cavity, filler material, metal shot, mounting and removal of filler, pulse, stress, shape and size of billets*

Mould, in which a metal ingot is melted and solidified, is a key working unit of a number of vacuum arc and electroslag remelting furnaces. In a melting mode, the walls of the mould are affected by heat flows that reach high values. Thus, cylindrical moulds are manufactured from thick-wall copper pipes, which are cooled from the outside by water [1, 2], to provide intensive heat removal from the melting zone. Thermal stresses forming in a material of the pipe in melting and cooling of ingots cause deformation of the latter, which complicates drawing out of the cooling ingot and requires periodical boring of inside surface of the mould. Obviously, it is necessary to increase the pipe rigidity without reduction of heat removal characteristics of walls of the mould to eliminate these deformations. Utilization of special steel frames mounted on copper pipes for these purposes does not always give positive results. In this connection, it was suggested in [3] that the mould should be made from bimetal (Figure 1) by cladding the external surface of the copper pipe with a steel pipe, thus providing a sound copper to steel joint by explosion welding (Figure 1, pos. *7*), and channels should be milled in a steel layer down to copper along the generating cylindrical surface to ensure a direct contact of cooling water with copper. Steel bridges remaining between the channels serve as stiffeners, to which an external steel shell (Figure 1, pos. *6*) closing the channels is welded by means of the fusion plug welds.

It is well-known that external and internal explosion cladding of pipes is characterized by a number of peculiarities [4, 5], which relate to violation of the collision geometry and preservation of shape and size of the welded billets. In particular, selection of a material filling the internal cavity of the clad pipe is necessary for external cladding. This material, maintaining shape and internal diameter of the pipe, should easily, with low laboriousness, fill up the cavity before explosion and be removed after it.

Any low-compressibility medium can be used as filler. Some technological peculiarities of utilization of fillers based on low-melting-point metals, salts, metal shot and water for welding of bimetal parts and assemblies of thermal-electric equipment are considered in study [6].

For practical purposes, the most suitable fillers are metal shot media, which meet the specified requirements and are characterized by low cost of a solution. The shot media fill well the internal cavity of the billet and can be easily removed after explosion. The metal shot media feature a low compressibility and ability to greatly extend the shock wave pulse, thus providing a manifold reduction of stresses due to explosion loads and preventing development of extensive plastic strains inside the shot medium. Therefore, low compressibility of the metal shot media together with lower levels of mean stresses, in comparison with homogeneous fillers, ensures good preservation of the shape and constancy of the internal diameter of the billet. Abilities of the shot media to extend the pulse and damp the explosion loads received theoretical confirmation in study [7]. It was established that utilization of the metal shot media, in comparison with the homogeneous ones, provides a manifold increase in time of the pulse, and approximately a five-fold reduction of stresses (Figure 2) [7].

Besides, a range of experiments by using the scheme shown in Figure 3 was carried out to check

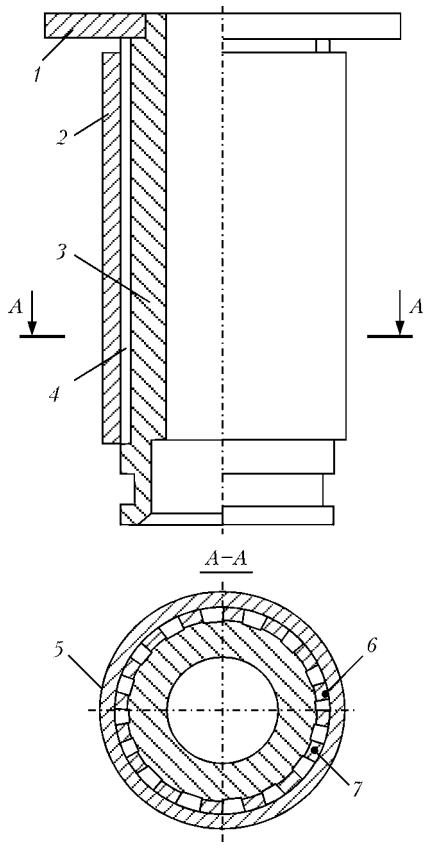

Figure 1. Scheme of bimetal cylinder mould: *1* — steel ring; *2* — steel shell; *3* — copper pipe; *4* — channels for cooling liquid circulation; *5* — stiffeners; *6* — path of fusion welding; *7* — path of explosion welding

the possibility of employing saltpeter melts, shot, shot with water and gun grease as a filler for the cavities formed between the internal surface of a copper pipe and external surface of the central rod in cladding the external surface of the copper pipe with a steel pipe.

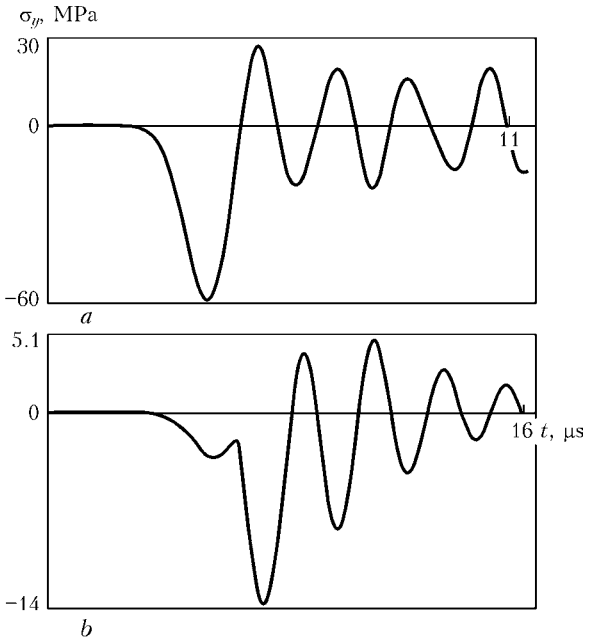

Figure 2. Stresses σ_y on internal surface of center of the container bottom in acceleration of the 6 mm thick flyer plate at a velocity of 2 m/s into the container through a continuous metal layer 16 mm thick (*a*), and into the container filled with metal shot medium 16 mm thick (*b*)

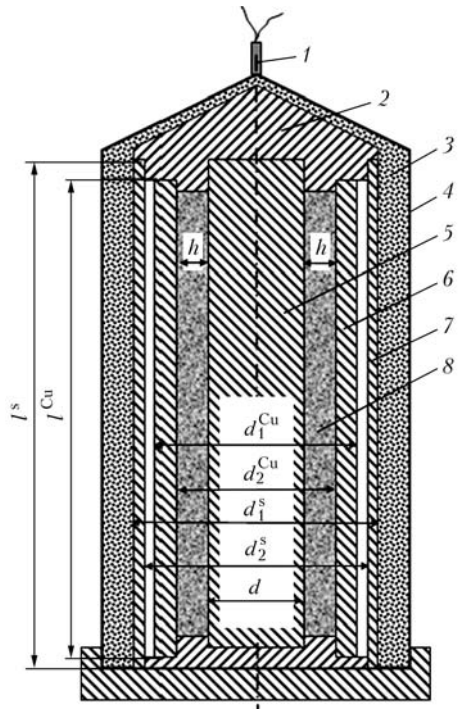

Figure 3. Scheme of explosion welding of tubular billets: *1* — detonator; *2* — cover; *3* — explosive charge; *4* — container; *5* — central rod; *6* — copper pipe; *7* — flyer steel pipe; *8* — filler; d — rod diameter; d_1^{Cu} and d_2^{Cu} — internal and external diameters of copper pipe, respectively; d_1^s and d_2^s — internal and external diameters of steel pipe, respectively; l^s and l^{Cu} — lengths of steel and copper pipes, respectively; h — gap between the rod and copper pipe, containing filler

Initial sizes of the pipes, rod and gaps with a filler, characteristics of the explosive charge, and averaged values of the external and internal diameters of welded bimetal billets are given in the Table.

If a relative decrease of the copper pipe internal diameter is $\varepsilon = (d_2^{Cu} - d_1^{Cu})/d_2^{Cu}$, then results of this series of experiments show that filling the gap between the central rod and the internal surface of the copper

Figure 4. Appearance of bimetal cylindrical mould

Results of investigation of the efficiency of different fillers

Experiment number	Initial sizes of pipes, mm						d, mm	h, mm
	Copper			Steel				
	d_1^{Cu}	d_2^{Cu}	l^{Cu}	d_1^s	d_2^s	l^s		
1	145	98	760	180	166	960	20	39
2	145	98	760	180	166	960	88	5
3	308	200	1200	348	328	1520	75	64.5
4	308	200	1200	348	328	1520	190	5
5	494	430	1850	535	515	2160	200	115
6	494	430	1850	535	515	2160	200	115
7	442	355	1800	492	472	1800	346	2.5

Table (cont.)

Experiment number	Filler	Explosive type	Charge height δ_0, mm	Detonation velocity D_l, m/s	Diameter of bimetal billet, mm		ε
					External d_1^1	Internal d_2^1	
1	Shot	A/S 1:3	55	2200	155	94	0.040
2	Saltpeter melt	A/S 1:3	55	2200	160	96	0.020
3	Shot with water	A/S 1:2	60	3300	330	195	0.025
4	Saltpeter melt	A/S 1:3	60	2920	328	196	0.020
5	Shot	AT-3	60	2900	510	415	0.034
6	Shot	AT-3	60	3000	510	410	0.046
7	Gun grease	A/S 1:3	50	2200	457	346	0.025

Note. A/S — mixture of ammonite 6ZhV with ammonium nitrate in different proportions (manufactured manually on site); AT-3 — mixture of ammonite 6ZhV with ammonium nitrate in 1:4 proportion (prefabrication).

pipe with saltpeter melts provides a minimum value of the relative decrease of the copper pipe internal diameter (see the Table). However, in welding of large-diameter and long cylindrical billets, the operation of filling the gap with a saltpeter melt significantly complicates the technology, since it requires preliminary heating of the copper shell and central rod to temperatures of 250 to 300 °C and subsequent washing out of the saltpeter with hot water after welding. Satisfactory results were obtained with filling the gap with a steel shot and water. However, for that it was necessary to mount special gaskets in the lower part of the assembly to seal the gap between pipes welded.

In experiment No. 7, the gap between the central rod and internal surface of the copper pipe was filled with gun grease (GOST 19537–83). A relative decrease of the copper pipe internal diameter in a bimetal billet after explosion welding was insignificant (see the Table). However, after explosion the rod was strongly jammed by the copper pipe, and it could be removed only by pressing out with preheating.

A mould was manufactured from the bimetal billet (Figure 4). It was tested under industrial conditions by using the EShP-0.25 furnace for zirconium production. Performance of approximately 100 melting operations showed the absence of any noticeable changes of shape and size of the mould. Since the average service life of copper moulds is 50 melting operations with three restorations, it can be considered that the service life of the bimetal mould is increased not less than 6–7 times [3].

The technology developed for manufacture of water-cooled bimetal moulds can be used for explosion welding of tubular billets up to 500 mm in diameter and up to 2000 mm long. It is expedient to manufacture the large-size moulds from pipes produced from double-layer plates, since the existing equipment allows rolling of pipes more than 600 mm in diameter at a wall thickness of 30–40 mm.

The experiments carried out showed that the use of metal shot as a filler is promising for preservation of shape and size of the cylindrical tubular billets of the moulds in explosion cladding without additional heavy expenditures.

1. (1980) *Electrothermal equipment*: Refer. Book. Ed. by A.P. Altgauzen. Moscow: Energiya.
2. Medovar, B.I. (1976) *Electroslag furnaces*. Kiev: Naukova Dumka.
3. (1985) *Development and application of new technological explosion welding processes of dissimilar metals in manufacturing of electrothermal equipment*: Report of researches 02850058758. Novosibirsk: SO AN SSSR.
4. Gokhshtejn, B.E., Sedykh, V.S. (1965) Explosion welding of cylindrical joints and adapting pipes from dissimilar metals. In: *High-efficiency methods of welding in chemical and oil machine-building*. Issue 3. Explosion welding. Moscow: TsINTIKhIMNEFTEMASh.
5. Gaek, Yu.V., Melikhov, V.P. (1977) Focusing of cumulative jets in explosion welding of rotation bodies. In: *Application of explosion energy in welding technique*. Kiev: PWI.
6. Ogolikhin, V.M., Yakovlev, I.V. (2009) *Explosion welding in electrometallurgy*. Novosibirsk: SO RAN.
7. Meshcheryakov, Yu.P. (2008) Numerical investigation of damping properties of rod structures in pulse loading. *Izvestiya VolgGTU*, 41(**3**), Issue 3, 101–104.

INTEGRATED TECHNOLOGIES OF PRODUCING MULTIPURPOSE LAYERED COMPOSITE MATERIALS

Yu.P. TRYKOV, L.M. GUREVICH and **V.G. SHMORGUN**
Volgograd State Technical University, Volgograd, RF

The paper describes the experience of many years of development of integrated technologies of manufacturing a new class of structural materials (layered composites) with a unique combination of high-temperature and thermophysical properties, including explosion welding to produce bimetal and multilayer materials in combination with allied technologies (different types of heat treatment and plastic working).

Keywords: *integrated technologies, explosion welding, hot initial rolling, heat treatment, layered composites*

The paper presents materials science problems addressed over the recent years by the Chair of Materials Science and Composite Materials of Volgograd State Technical University to develop a new class of structural materials — layered composites (LC) with a unique combination of high-temperature and thermophysical properties. The progress made is based on the accumulated science and technology experience in explosion welding (EW) application for producing bimetal and multilayered joints and materials from difficult-to-weld metals and alloys (Ti–Fe, Cu–Al, Ti–Al, Mg–Al, etc.) in combination with related technologies (different kinds of heat treatment (HT) and plastic working). During development of energy and metal-physics concepts of the kinetics of joint formation in EW and structural changes during subsequent technological processing [1–3], which became the scientific basis of development of LC structure and manufacturing technology, the following problems were solved.

1. Promising systems and combinations of dissimilar metals, forming very hard intermetallic compounds at thermomechanical impact in different aggregate state have been determined.

2. Earlier proposed integrated technological processes were improved and new ones were proposed [4] to produce in the versatile equipment of mechanical engineering and metallurgical plants large-sized blanks of multilayered intermetallic composites with the specified high-temperature, thermophysical, wear-resistance and special properties, including EW, hot and cold rolling (R), and special kinds of HT in the solid state, above the melting temperatures of low-melting composite layers or eutectics forming in the contact zone.

3. Calculation-experimental methods of determination of optimum technological parameters of the applied operations (EW, R, HT) were developed [5–12], which provide scientific substantiation for specifying the required quantity and thickness of the layers of the initial dissimilar metals at the design stage, ensuring the required quality of explosion-welded multilayered blanks, performing the next technological processing to produce sheet composites with the calculated volume content of the intermetallic layers. Generalization of research results was the basis to define the principal postulates of LC structure and property formation at different stages of integrated technologies:

- in elastoplastic deformation of explosion-welded LC in the low deformation region, local softening zones form by the dislocation mechanism [2];
- LC energy conditions influence the processes of formation of the structural, phase and chemical inhomogeneity at solid-state reactive diffusion: increase of plastic deformation energy on the joint boundary W_2 leads to shortening of the latent period and increase of the velocity of diffusion zone thickness growth [4];
- derived equations [4] of the kinetics of growth of the diffusion layers in solid-phase state allowing for energy W_2 for promising systems and combinations of dissimilar metals and alloys allow specifying during LC development the optimum parameters of heating, ensuring realization of the required ratio of the base and intermetallic layers, and determining the modes of recrystallization annealing, preventing formation of «hazardous» diffusion boundaries;
- formation of the structure and phase composition of intermetallic layers at temperatures above the melting point of the lowest-melting LC layer occurs in three main stages, conditionally named «initial», «growth» and «saturation» (Figure 1). Stage-like nature of the processes of titanium interaction with the aluminium melt in titanium-aluminuim composites is attributable to the presence of oxide layers with ruptures on the joint boundary, formed during rolling because of the different ductility of the oxide and the metal and subsequent HT due to the difference in the coefficients of linear expansion of oxides and metal [13];
- metallographic and X-ray structural analyses showed that LC diffusion zones have a multilayered structure, depending mainly on the temperature-time conditions of heating [2–4]; generalized data were derived on the influence of EW and HT modes on formation and redistribution of fine structure elements (stresses of the second kind, crystalline lattice parameters) in LC near-weld zone [4]. A principal pos-

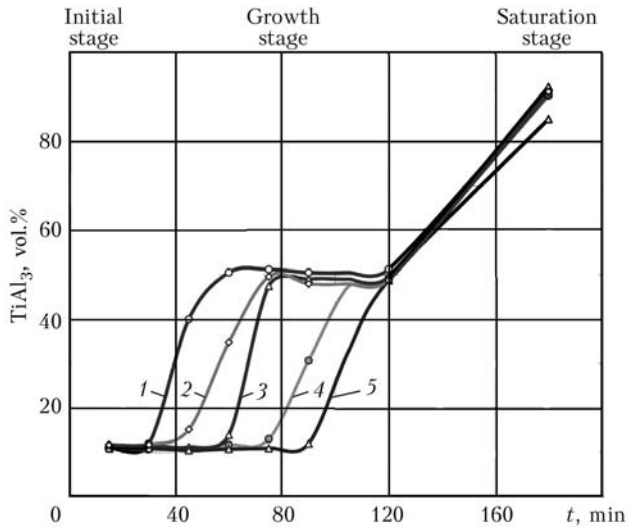

Figure 1. Dependence of the change of volume content of intermetallics in VT1-0 + AD1 composite (AD1 thickness is 0.4 mm) at 750 °C at different distance from the boundary with titanium: *1* — 0–100; *2* — 100–200; *3* — 200–300; *4* — 300–400; *5* — 400–500 μm

sibility of obtaining three variants of intermetallic layer structure was demonstrated: continuous interlayers, formed at HT below the melting temperature of the composite initial layers and the developing structural components (Figure 2, *a*); layers consisting of eutectic and crystals of intermetallics, formed at contact melting (Figure 2, *b*); layers of dispersed intermetallics with solid solution interlayers formed at temperatures above that of melting of the composite low-melting layers (Figure 2, *c*).

4. Short-term strength at LC high-temperature tensile testing (copper–aluminium, titanium–steel and titanium–aluminium systems) was studied [13–15]. Analysis of the derived results showed that temperature dependence of LC mechanical properties is determined by the volume fraction of the intermetallic component and allowed dividing LC into two groups. The first group includes composites, the strength of which gradually decreases with increase of testing temperature. Volume fraction of their intermetallic constituent V_{int} is low, its increase is accompanied by lowering of strength and relative elongation. The second group includes composites with a high volume fraction of intermetallics, the strength of which increases with temperature, reaches the maximum value and then decreases. Developed models, describing LC strength, showed that use of LC of copper–aluminuim system (Figures 3 and 4) at temperature below 200 °C is not rational, as their strength is below that of copper. To ensure high values of σ_t in the temperature range of 200–600 °C the volume fraction of the intermetallics should be not less than 30 %. It is not rational to use titanium-steel LC (Figures 5 and 6) at temperatures below 400 °C, as in this case the intermetallic volume fraction is equal to 50 %.

5. Investigations of thermophysical characteristics of layered intermetallic composites (LIC) enabled determination of coefficients of thermal conductivity of three main types of intermetallic layers formed in promising combinations of dissimilar metals and alloys, and development of methods to predict the ther-

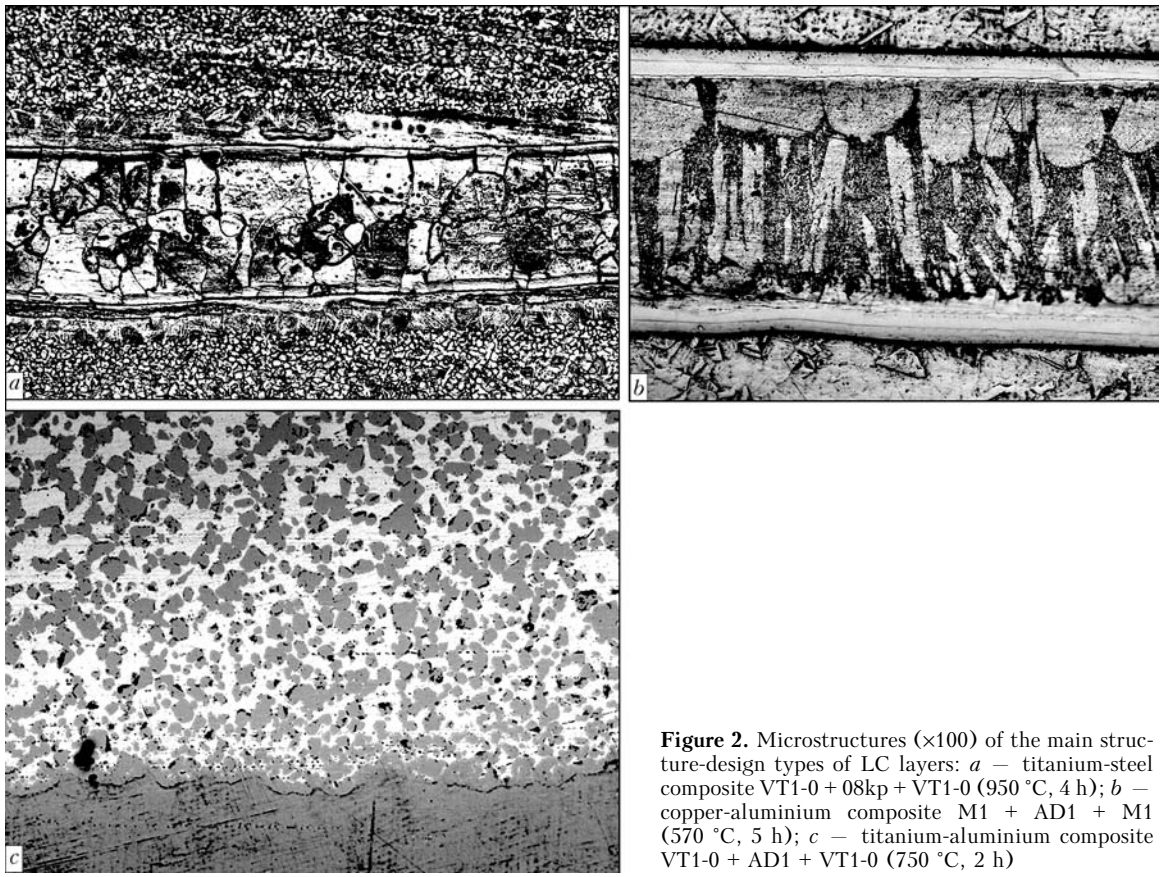

Figure 2. Microstructures (×100) of the main structure-design types of LC layers: *a* — titanium-steel composite VT1-0 + 08kp + VT1-0 (950 °C, 4 h); *b* — copper-aluminium composite M1 + AD1 + M1 (570 °C, 5 h); *c* — titanium-aluminium composite VT1-0 + AD1 + VT1-0 (750 °C, 2 h)

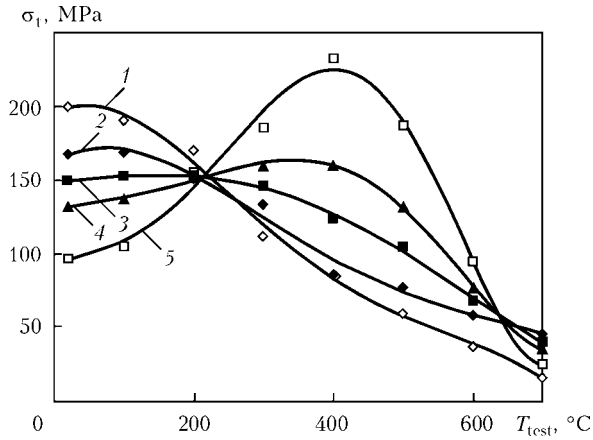

Figure 3. Experimental (*1*) and calculated (*2–5*) dependencies of tensile strength on testing temperature at tension of copper (*1*) and copper-aluminium LC with V_{int} = 10 (*2*), 20 (*3*), 30 (*4*), 50 (*5*) %

mal conductivity of LC with different structural-design characteristics.

Operational and design features of power and cryogenic equipment necessitated development of technologies to produce four kinds of structural and functional LC, characterized by the required high-temperature, thermophysical, corrosion and other special properties, the maximum overall dimensions of which are determined by technical capabilities of thermic and rolling equipment of the modern metallurgical and mechanical engineering enterprises:

• multilayered sheets with alternating base and intermetallic layers of more than 0.03 mm thickness of each layer made by an integrated technology, which includes simultaneous or successive EW of up to 30 and more sheets from dissimilar metals and alloys with parameters guaranteeing realization of equivalent strength of welded joints and absence of hazardous kinds of microinhomogeneities; rolling of explosion-welded multilayer blanks into sheets of down to 0.5–1.0 mm thickness with preservation of the initial proportion of layer thicknesses;

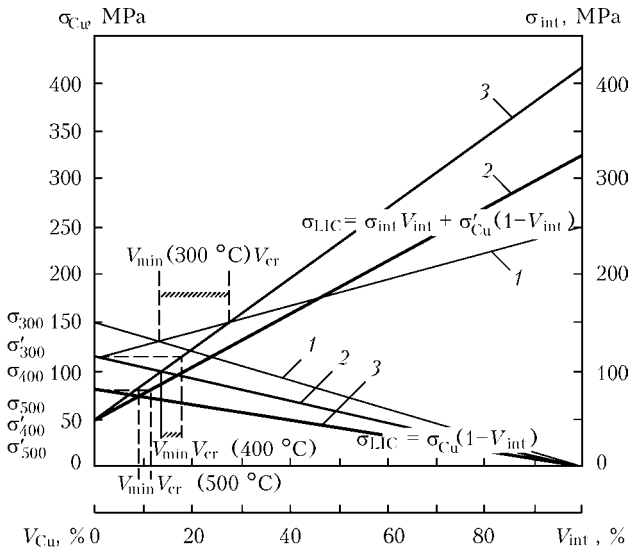

Figure 4. Theoretical dependence of strength of copper-aluminium LC on volume fraction of intermetallic interlayer at different temperature: *1* — 300, *2* — 400; *3* — 500 °C

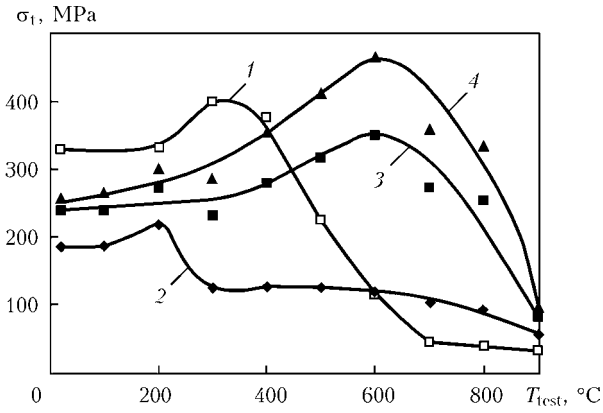

Figure 5. Experimental (*1*) and calculated (*2–5*) dependencies of tensile strength on testing temperature at tension of 08kp steel (*1*) and titanium-steel LC with V_{int} = 10 (*2*), 50 (*3*) and 70 (*4*) %

• high-temperature HT of rolled sheets to form on interlayer boundaries continuous or dispersed intermetallic interlayers of the specified thickness, the temperature-time parameters of which allow for the alloying system and «loading history» (technological conditions of EW and R);

• composite heat-protection elements (CHPE), which are two- and three-layer structures from active thermal assemblies (through-thickness channels from dissimilar metals with circulating coolant) and passive assemblies from formed on the dissimilar metal boundaries intermetallic interlayers with heat conductivity which is many times lower than that of the metals forming the CHPE. Integrated technology of CHPE manufacturing includes application of anti-welding paste by a template on the plate surfaces being joined in the areas of formation of coolant circulation channels; assembly and EW of the pack in the optimum mode; blowing of coolant circulation channels by liquid or high-pressure gas, high-temperature HT to create a diffusion intermetallic interlayer. Total thermal-protection effect of CHPE is the result of thermal processes in active and passive components [16];

• composite multichannel heat exchangers from different combinations of titanium, aluminium, cop-

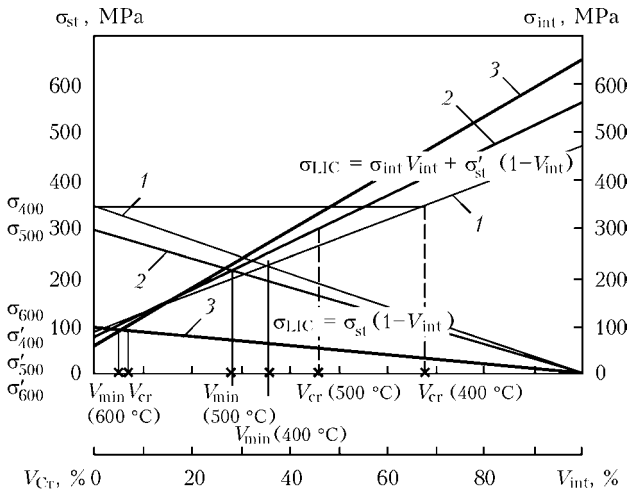

Figure 6. Theoretical dependence of strength of titanium-steel LC on volume fraction of the intermetallic interlayer at different temperature: *1* — 400; *2* — 500; *3* — 600 °C

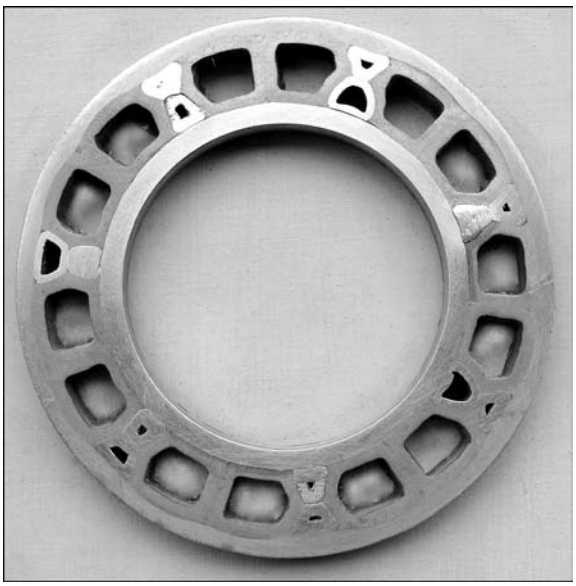

Figure 7. Appearance of a cylindrical composite multichannel heat exchanger

per, magnesium and steel (Figure 7), made by the integrated technology including pipe deformation to form the working channels of the required geometry; pouring filler into them, which prevents inadmissible deformations at EW; pre-assembly of the product from dissimilar elements capable of forming intermetallics at subsequent HT; one- and two-sided EW of the assembled structure by flat or circular explosive charges; filler removal by thermal, chemical or hydraulic methods; HT of the heat exchanger to form intermetallic interlayers with a lower coefficient of heat conductivity on the boundaries of profiled tube joints;

• fibrous intermetallic composites (FIC) in the form of multiconductor cables (Figure 8) or blanks for subsequent drawing or rolling, the integrated technology of manufacturing which envisages producing tri-, tetra- or hexahedral profiles of wire type and profiled tubes from metals and alloys capable of forming intermetallic joints; manufacturing containers, the geometry of which corresponds to the created FIC; explosive compression of containers with «filler» from

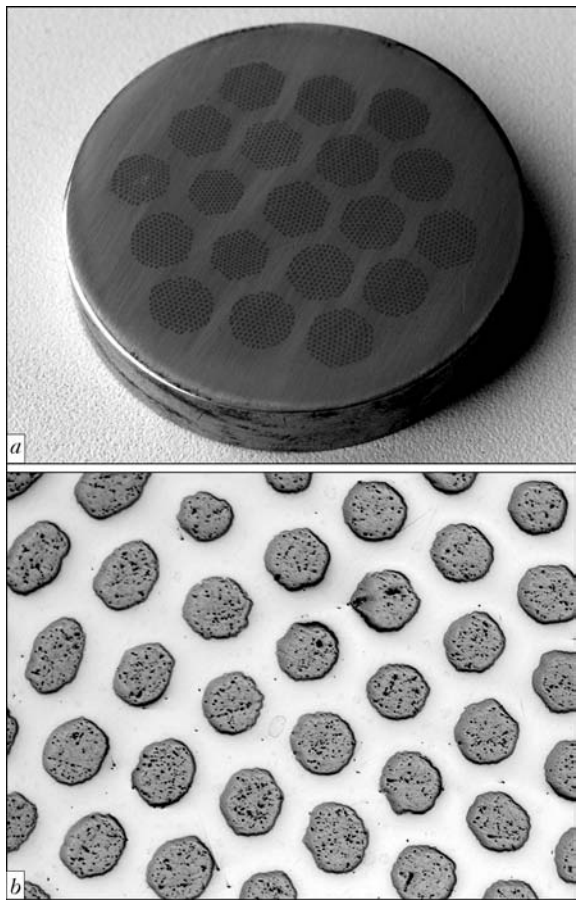

Figure 8. Appearance of a fibrous composite: *a* — template; *b* — fibre distribution in the bundle (×50)

dissimilar wire and tubular elements to realize physical contact and activate the surfaces being jointed; plastic working (broaching, drawing) to achieve the required linear dimensions and improve the strength of element adhesion; high-temperature heating of compressed blanks to create diffusion intermetallic interlyaers with the required thermophysical properties on the dissimilar element boundaries.

The advantages and applications of the developed kinds of structural and functional LIC are given in the Table.

Advantages and applications of the developed layered intermetallic composites

Composite type	Properties	Applications
Multilayered sheets	Excellent high-temperature properties due to preservation of an ordered structure of intermetallics right up to melting temperature	Flying vehicles, thermally stressed equipment, corrosion-resistant tank equipment, heavy-duty assemblies of power and cryogenic plants
Composite heat-protection elements	Realisation of heat-protection effect due to interaction of a system of channels with coolant and intermetallic interlayers with a low heat conductivity	Cryogenic, chemical and power equipment with improved service and technical-economic characteristics
Composite multichannel heat exchangers	High-strength joining of elements due to partial melting of pipe metal, many times reduction of heat transfer by intermetallic interlayers	Chemical and power plants with improved service and technical-economic characteristics, cryogenic equipment
Fibrous intermetallic composites	Excellent high-temperature properties, possibility to produce superconducting cables	Flying vehicles, thermally stressed equipment, heavy-duty assemblies of power and cryogenic plants, power transmission lines

Work was performed with the financial support of grant RFFI 08-08-00056 and project 2.1.2/573 of purpose-oriented program of Rosobrazovanie «Development of Scientific Potential of Higher Education Institutions».

1. Trykov, Yu.P., Shmorgun, V.G. (1999) *Properties and serviceability of layered composites*. Volgograd: VolgGTU.
2. Trykov, Yu.P., Shmorgun, V.G., Gurevich, L.M. (2001) *Deformation of layered composites*. Volgograd: VolgGTU.
3. Trykov, Yu.P., Gurevich, L.M., Shmorgun, V.G. (2004) *Layered composites on the base of aluminium and its alloys*. Moscow: Metallurgizdat.
4. Trykov, Yu.P., Gurevich, L.M., Arisova, V.N. (2006) *Diffusion processes in layered composites*. Volgograd: VolgGTU.
5. Shmorgun, V.G. (2001) Evaluation of energy consumption for plastic deformation in wave generation zone during explosion welding. *Svarochn. Proizvodstvo*, **3**, 25–27.
6. Trykov, Yu.P., Gurevich, L.M., Gurulev, D.N. (1999) Influence of rolling at elevated temperatures on properties of titanium-aluminium composite made by explosion welding. *Ibid*., **6**, 6–10.
7. Trykov, Yu.P., Shmorgun, V.G., Epishin, E.Yu. (2002) Study of the influence of hot and cold rolling on structure and properties of near-weld contact zone of titanium-steel bimetal made by explosion welding. *Proizvodstvo Prokata*, **8**, 35–39.
8. Trykov, Yu.P., Shmorgun, V.G., Slautin, O.V. (2003) Study of the influence of cold rolling on structure and properties of near-weld contact zone of copper-aluminium bimetal made by explosion welding. *Ibid*., **11**, 23–27.
9. Trykov, Yu.P., Gurevich, L.M., Gurulev, D.N. (2000) Diffusion processes in heating of titanium-aluminium composite produced by explosion welding. *Svarochn. Proizvodstvo*, **12**, 19–21.
10. Trykov, Yu.P., Shmorgun, V.G., Epishin, E.Yu. (2004) Diffusion processes in titanium-steel bimetal. *Fizika i Khimiya Obrab. Materialov*, **4**, 85–89.
11. Trykov, Yu.P., Shmorgun, V.G., Slautin, O.V. (2003) Kinetics of growth of diffusion interlayers in copper-aluminium bimetal produced by an integrated technology. *Perspekt. Materialy*, **3**, 83–88.
12. Trykov, Yu.P., Shmorgun, V.G., Rogozin, V.D. et al. (2003) Technology of explosion welding of magnesium-aluminium composite joints. *Svarochn. Proizvodstvo*, **3**, 38–41.
13. Gurevich, L.M., Trykov, Yu.P., Zhorov, A.N. et al. (2008) Structure formation in titanium-aluminium composites in presence of liquid phase. *Zhurnal Funktsion. Materialov*, 2(**4**), 153–157.
14. Shmorgun, V.G., Trykov, Yu.P., Abramenko, S.A. et al. (2005) Mechanical properties of layered intermetallic composites of Al–Cu system at elevated temperatures. In: *Izvestiya VolgGTU*. Series Materials science and strength of structure elements, 12(**3**), 12–16.
15. Shmorgun, V.G., Trykov, Yu.P., Slautin, O.V. et al. (2005) Layered intermetallic composites of Ti–Fe system with improved heat-resistance properties. *Ibid*., 16–21.
16. Trykov, Yu.P., Shmorgun, V.G., Pronichev, D.V. (2000) Complex technologies for manufacturing composite heat-protection elements. *Svarochn. Proizvodstvo*, **6**, 40–43.

LIST OF MAIN MONOGRAPHS ON EXPLOSION WELDING

1. Belyaev, V.I., Kovalevsky, V.I., Smirnov, G.V. et al. (1976) *High-velocity deformation of metals*. Minsk: Nauka i Tekhnika, 224 pp.
2. (2000) *Transact. on Wave Formation at Glancing Collisions*. Ed. by I.V. Yakovlev et al. Novosibirsk: SO RAN, 221 pp.
3. Gelman, A.S., Tsemakhovich, B.D., Chudnovsky, A.D. et al. (1978) *Explosion cladding of steel*. Moscow: Mashinostroenie, 191 pp.
4. Deribas, A.A. (1972) *Physics of explosion strengthening and welding*. Novosibirsk: Nauka, 188 pp.
5. Deribas, A.A. (1980) *Physics of explosion strengthening and welding*. 2nd ed. Novosibirsk: Nauka, 222 pp.
6. Dudin, A.A. (1979) *Magnetic-pulse welding*. Moscow: Metallurgiya, 206 pp.
7. Zakharenko, I.D. (1990) *Explosion welding of metals*. Minsk: Navuka i Tekhnika, 206 pp.
8. Konon, Yu.A., Pervukhin, L.B., Chudnovsky, A.D. (1987) *Explosion welding*. Ed. by V.M. Kudinov. Moscow: Mashinostroenie, 216 pp.
9. Karpenter, S. (1976) *Explosion welding of metals*. Minsk: Belarus, 43 pp.
10. Kobelev, A.G. (2006) *Materials science and technology of composites*: Manual. Moscow: Intermet Engineering, 496 pp.
11. Kriventsov, A.N. (2005) *Design and manufacturing of FCM by explosion welding*. Volgograd: Politekhnik, 184 pp.
12. Krupin, A.V., Soloviov, V.Ya., Popov, G.S. (1991) *Explosion treatment of metals*. Moscow: Metallurgiya, 495 pp.
13. Kudinov, V.M., Koroteev, A.Ya. (1978) *Explosion welding in metallurgy*. Moscow: Metallurgiya, 168 pp.
14. Kuzmin, G.E., Paj, V.V., Yakovlev, I.V. (2002) *Experimental-analytical methods in problems of dynamic loading of materials*. Novosibirsk: SO RAN, 311 pp.
15. Lysak, V.I., Kobelev, A.G. (2006) *Metal layered composites*: Encylopedia on Machine Building. Vol. III-6: Technology of manufacturing of layered metal composites and products from them. Moscow: Mashinostroenie, 576 pp.
16. Lysak, V.I., Kuzmin, S.V. (2005) *Explosion welding*. Moscow: Mashinostroenie, 544 pp.
17. Majboroda, V.P., Kravchuk, A.S., Kholin, N.N. (1986) *High-velocity deformation of structural materials*. Moscow: Mashinostroenie, 261 pp.
18. Ogolikhin, V.M., Yakovlev, I.V. (2009) *Explosion welding in electrometallurgy*. Novosibirsk: SO RAN, 160 pp.
19. Pashkov, P.O., Gelunova, Z.M. (1968) *Action of shock waves on hardened steels*. Volgograd: Nizhn.-Volzh. Knizhn. Izd-vo, 168 pp.
20. Petushkov, V.G. (2005) *Application of explosion in welding engineering*. Ed. by B.E. Paton. Kiev: Naukova Dumka, 756 pp.
21. Petushkov, V.G., Kudinov, V.M., Fadeenko, Yu.I. (1993) *Explosion treatment of metal structure welded joints*. Moscow: Metallurgiya, 161 pp.
22. Rainhart, J.S., Pearson, J. (1966) *Explosion treatment of metals*. Moscow: Mir, 392 pp.
23. Sedykh, V.S., Kazak, N.N. (1971) *Explosion welding and properties of welded joints*. Moscow: Mashinostroenie, 70 pp.
24. Simonov, V.A. (1995) *Applications of explosion welding. Main parameters and criteria*. Novosibirsk: M.A. Lavrentiev IH of SD, 61 pp.
25. Smirnov, G.V. (1999) *Effects of dynamic cumulation*. Minsk: Remiko, 160 pp.
26. Stepanov, V.G., Shavrov, I.A. (1975) *High-energy pulse methods of metal treatment*. Moscow: Mashinostroenie, 200 pp.
27. Stepanov, G.V. (1991) *Elastic-plastic deformation and fracture of materials in pulse loading*. Kiev: Naukova Dumka, 288 pp.
28. Trishin, Yu.A. (2005) *Physics of cumulative processes*. Novosibirsk: M.A. Lavrentiev IH of RAS SD, 324 pp.
29. (2002) *Physics of explosion*. Ed. by L.P. Orlenko. 3rd ed. Vol. 1. Moscow: Fizmatlit, 832 pp.
30. Kharchenko, V.V. (1999) *Modeling of high-velocity deformation of materials taking into account the viscous-plastic effects*. Kiev: IPS of NASU, 223 pp.
31. Epshtejn, G.N. (1988) *Structure of metals deformed by explosion*. Moscow: Metallurgiya, 280 pp.
32. Crossland, B. (1982) *Explosive welding of metals and its application*. Oxford: Clarendon Press, 233 pp.
33. (1983) *Explosive welding, forming and compaction*. Ed. by T.Z. Blazynski. London; New York: Appl. Sci. Publ., 276 pp.
34. Ezra, A.A. (1973) *Principles and practice of explosive metalworking*. London: Industrial Newspapers.
35. Lysak, V.I., Kuzmin, S.V. (2003) *Explosive welding of metal layered composite materials*. Ed. by B.E. Paton. Kiev: PWI of NASU, 117 pp.
36. Petushkov, V.G. (2009) *Explosion and its applications in metalworking*. New York: Nova Sci. Publ., 696 pp.
37. Petushkov, V.G., Simonov, V.F., Sedykh, V.S. et al. (1996) Explosion welding criteria. Ed. by B.E. Paton. In: *Welding and Surfacing Rev.*, Vol. 3, Pt 4. Harwood A.P., 127 pp.
38. Petushkov, V.G. (1994) Explosion treatment of welded joints. Ed. by B.E. Paton. In: *Ibid.*, Vol. 3, Pt 1. Harwood A.P., 95 pp.
39. Petushkov, V.G., Fadeenko, Yu.I. (1995) Explosion-thermal treatment of welded joints. Ed. by B.E. Paton. In: *Ibid.*, Vol. 8, Pt 2. Harwood A.P., 110 pp.
40. Petushkov, V.G., Fadeenko, Yu.I. (1999) *Welding stress relief by explosion treatment*. New York: Backbone, 179 pp.
41. Ryabov, V.R., Dobrushin, L.D., Moon, J.G. (2003) *Welding of bimetal*. Ed. by B.E. Paton. Kiev: PWI of NASU, 130 pp.

Moscow Regional Shared Use Explosion Center of the Russian Academy of Sciences (SUEC)

Technological basis of SUEC is composed of explosion chambers and units, as well as diagnostic systems, including:

1. Unique spherical explosion chamber 13Ya3 («Sfera» unit) — 12 m in diameter and 100 mm wall thickness, made from armored steel and designed for explosion of up to 1000 kg of TNT.
2. Explosion chamber VBK — double-layer cylindrical chamber with a capacity of 110 m^2, designed for explosion of up to 50 kg of TNT.
3. Special equipment for explosion experiments: six reinforced-concrete explosion domes designed for explosion of up to 10 kg of TNT; 39 reinforced-concrete boxes for dangerously explosive operations, designed for explosion of up to 5 kg of TNT; four open explosion sites with armored cells with a permitted weight up to 1000 kg of TNT; metallic explosion chamber designed for explosion of 6 kg of TNT; warehouse for storing up to 12 t of explosives with 5 room for lock box storage of 10 kg of explosives; and specialized rooms for synthesis and examinations of explosives, powders etc.
4. Shock tubes.
5. Current and voltage explosive generators.
6. Electromagnetic explosive emitters.

Activity of SUEC is based on addressing fundamental and applied problems in the following areas:

- development of explosion in combustible gas mixtures, detonation (for solving industrial facilities safety problems);
- magnetic-explosive generators for new technologies (pulse effects on natural and artificial objects);
- equations of state of structural materials in a wide (including megabar) range of parameters;
- physical-chemical properties of materials at extreme pressure and temperatures;
- chemical physics of shock and detonation waves;
- interaction of heavy flows of a directed energy with materials;
- chemical physics of non-ideal plasma;
- rheological properties of condensed media;
- explosion processes in reactive media;
- dynamic synthesis of metastable compounds;
- numerical modeling of pulse effects;
- conversion of chemical energy of combustion and explosion processes into other energy types (mechanical, kinetic, electromagnetic);
- safety in nuclear power generation and chemical engineering;
- non-ideal plasma and technical applications;
- effect of electromagnetic radiations on information channels and networks;
- hydrogen power generation.

Contact information: 13 Izhorskaya str., bldg. 2, 125412, Moscow, Russian Federation
http://www.ihed.ras.ru/ckpv/